TOWARDS THE RECONCILIATION OF THE EMPIRICAL AND RATIONAL DESIGN PROVISIONS OF CSA S304-14

A Thesis Submitted to the
College of Graduate and Postdoctoral Studies
in Partial Fulfillment of the Requirements for the Degree of
Master of Science in the Department of Civil, Geological and Environmental Engineering
University of Saskatchewan
Saskatoon

By:
Amir Rezaeivahdati

Permission to Use

In presenting this thesis in partial fulfillment of the requirements for a Postgraduate degree from the University of Saskatchewan, I agree that the Libraries of this University may make it freely available for inspection. I further agree that permission for copying of this thesis in any manner, in whole or in part, for scholarly purposes may be granted by the professor or professors who supervised my thesis work or, in their absence, by the Head of the Department or the Dean of the College in which my thesis work was done. It is understood that any copying or publication or use of this thesis or parts thereof for financial gain shall not be allowed without my written permission. It is also understood that due recognition shall be given to me and to the University of Saskatchewan in any scholarly use which may be made of any material in my thesis.

Requests for permission to copy or to make other use of material in this thesis in whole or in part should be addressed to:

Head of the Department of Civil, Geological and Environmental Engineering
University of Saskatchewan
Engineering Building
57 Campus Drive
Saskatoon, Saskatchewan, S7N 5A9, Canada

Or

Dean of the College of Graduate and Postdoctoral Studies
University of Saskatchewan
116 Thorvaldson Building, 110 Science Place
Saskatoon, Saskatchewan, S7N 5C9, Canada

Abstract

Masonry structures in Canada are designed in accordance with CSA S304-14 which includes both empirical and rational design provisions. The two design methods result in inconsistent outcomes in certain cases. This thesis investigates one such case where the empirical design provisions for unreinforced, vertically spanning, non-loadbearing, exterior concrete block walls subject to wind load result in less conservative outcomes than the rational design provisions. This discrepancy of design outcomes can indicate either the inadequate levels of safety of the empirical design method or unnecessary conservatism of the rational design method. The goal of this study is to contribute to the reconciliation of the two design methods included in CSA S304-14 for the aforementioned case.

A review of past experimental investigations suggests that parameters influencing the flexural tensile strength of walls include mortar type, support conditions, wall slenderness ratio, and the load application method. An experimental program was conducted to provide additional data in areas where test data was lacking: walls constructed using mortar cement mortar, walls with slenderness ratios equal and greater than 16, and walls with realistic support conditions. A database was compiled using test results from the past and the present experimental investigations, and was used to perform a reliability analysis for unreinforced concrete block walls subject to out-of-plane loading. The reliability analysis was conducted using a Monte Carlo simulation and the unfactored rational equation as the limit state function. Results were used to provide recommendations for the empirical provisions of CSA S304-14 assuming a minimum acceptable reliability index equal to 2.5 based on past investigations.

Walls with slenderness ratios equal to or greater than 16 consistently resulted in reliability indices lower than 2.5. Walls with a slenderness ratio equal to 12 resulted in reliability indices lower than 2.5 when subjected to a 1 in 50 years wind pressures equal to 0.53 kPa and 0.29 kPa, respectively, for the minimum and maximum values of internal pressure. Potential correlation of the different included parameters may have influenced the results and, therefore, no changes to CSA S304-14 were proposed. It was, however, recommended that the standard include a commentary to inform users of the lack of quantitative evidence supporting the safety of unreinforced masonry walls subject to wind when designed according to the empirical provisions, in particular for increasing slenderness ratios and 1 in 50 years wind pressure.

Co-Authorship

All experimental and analytical work presented herein were performed by Amir Rezaeivahdati and reviewed by Dr. Lisa R. Feldman. The literature review provided in Chapter 2 of this thesis was presented at the 13th Canadian Masonry Symposium in Halifax, Canada, in 2017, and published in the proceedings of the conference. The results for the experimental portion of this investigation and the reliability analysis were presented at the 10th International Masonry Conference in Milan, Italy, in 2018, and published in the proceedings of the conference.

Acknowledgments

I would like to express my gratitude to my supervisor, Dr. Lisa Feldman, for the valuable lessons she patiently taught through her expertise and character. I would also like to thank my committee members, Dr. Bruce Sparling, and Dr. Leon Wegner, for their guidance and advice throughout this program.

I would like to extend my appreciation to Sasha Kisin for his continuous and extensive support. I am grateful for the guidance provided by Dr. Ian MacPhedran with the reliability analysis. I greatly appreciate Dr. Han-Ping Hong from the Western University for his kind advice and for providing the wind data required for the reliability analysis. I also thank Dr. Richard Bennett from the University of Tennessee for his help with finding past research data.

I am grateful to Brennan Pokoyoway, the technician in the Structural Laboratory. The experimental program of this research would not have been possible without Brennan's immense patience and resourcefulness. I would also like to thank Roy Nicolas for constructing the wall and companion specimens. I appreciate the help and company of fellow graduate students Nipun Tissera, Umesh Poudyal, Henry Miranda, and Kien Doan throughout this program.

I gratefully acknowledge the financial and technical support provided by the Canada Masonry Design Centre and the Saskatchewan Masonry Institute. Scholarships awarded by the National Science and Engineering Research Council of Canada, the American Concrete Institute, and the University of Saskatchewan are also greatly appreciated.

Finally, I would like to thank my family whose unconditional support made the receiving of this education possible for me.

Table of Contents

Chapter 3

Chapter 4

List of Tables

List of Figures

List of Symbols

A_e	Effective cross-sectional area of masonry
C_e	Exposure factor
C_g	Gust effect factor
C_{gi}	Internal gust effect factor
C_p	External pressure coefficient
C_{pi}	Internal pressure coefficient
C_t	Topographic factor
COV_{P_f}	Coefficient of variation of the probability of failure
$\overline{COV}$	Average coefficient of variation of the probability of failure
f_t	Flexural tensile strength of masonry
$F(v)$	Cumulative distribution function of the annual maximum wind speed
$F(v)_{50}$	Cumulative distribution function of the 50-year wind speed
h	Reference height as defined by Article 4.1.7.3 of NBCC 2015
I_w	Importance factor for wind load
k	Effective length factor for walls and columns
l	Vertical span lengths of masonry walls
M	Moment due to the wind load
M_{sw}	Moment due to the self-weight of the wall
N	Total number of simulation cycles
N_f	Number of simulation cycles resulting in failure
p	Wind pressure
P_f	Probability of failure
q	Wind velocity pressure
$R_{xbottom}$	The bottom reaction force of a masonry wall in the horizontal direction
R_{xtop}	The top reaction force of a masonry wall in the horizontal direction
$R_{ybottom}$	The bottom reaction force of a masonry wall in the vertical direction
S	Elastic section modulus
t	Wall thickness

v	Annual maximum wind speed
W_{half}	Self-weight of the top half of the wall
W_{total}	Total self-weight of the wall
α	Scale parameter for a Gumbel distribution
α_D	Dead load factor
α_w	Wind load factor
β	Reliability index
μ	Location parameter for a probability distribution function
ρ	Air density
σ	Scale parameter for a Lognormal distribution
ϕ_m	Resistance factor for masonry
Φ	Standard cumulative distribution function

1.0 Introduction

Masonry structures have been constructed for thousands of years based on empirical knowledge. The first codifications for the design of masonry, however, took place in the past century. The first design code for masonry in Canada was introduced in the National Building Code (NBC) in 1941 (NBC, 1941) and included empirical design rules exclusively. Canadian design standards for masonry have developed significantly since. Rational design rules using the working stress method were introduced in the National Building Code of Canada NBCC in 1965 (NBCC, 1965). The first Canadian standard specific to masonry design, CSA S304, was published in 1977 (CSA, 1977). The working stress method was eliminated from CSA S304 in 2004 (CSA, 2004); limit states design has been the only rational design method permitted since. The current version of the standard, CSA S304 (2014), includes both rational and empirical design methods. The use of the empirical design for masonry in CSA S304 (2014) only applies to unreinforced masonry and is limited by height, seismic activity, and the wind pressure in the construction region (Laird, 2013).

The outcomes of the empirical and rational design methods for masonry are inconsistent in certain cases. One such case occurs when non-loadbearing, ungrouted, unreinforced, exterior concrete block walls are subject to wind load. The empirical design method included in CSA S304 (2014) permits such walls to have a maximum height-to-thickness ratio equal to 20 and be constructed in areas where the 1 in 50 years hourly wind pressure as prescribed by NBCC (2015) has a maximum value of 0.55 kPa. Counterintuitively, the rational design method results in more conservative values of 1 in 50 years hourly wind pressure than the empirical design method for increasing wall height-to-thickness ratios. The two design methods should be reconciled to ensure the economic efficiency and the safety of structures. Structural safety of the two design methods for walls in flexure has not been previously determined.

Work included in this thesis is aimed to provide a reconciliation of the rational and empirical design methods included in CSA S304 (2014) as related to the aforementioned case. A review of the literature as related to the flexural tensile strength of unreinforced concrete block walls subject to out-of-plane loading was conducted. An experimental program was developed to bolster the available test database. Finally, a reliability analysis was conducted to determine the

structural safety of unreinforced concrete block walls designed in accordance with the empirical design method using the database compiled from the past and the present investigations.

1.1 Objectives

The primary objective of the current investigation is to contribute to the reconciliation of the rational and empirical design methods included in CSA S304 (2014) as related to non-loadbearing, ungrouted, unreinforced, exterior concrete block walls subject to wind load. The specific objectives of this investigation are the following:

- Identify shortcomings in the available test database for the flexural tensile strength of unreinforced concrete block walls;
- Determine the structural reliability of unreinforced concrete block walls subject to out-of-plane loading using the test database; and
- If warranted, provide recommendations for changes to the empirical design method included in CSA S304 (2014) to ensure adequate levels of safety.

1.2 Scope

The work included two components: an experimental, and an analytical study. The experimental investigation was conducted to bolster the test database in areas where shortcomings were identified. The overall test database was then assembled using results reported from past and present experimental investigations. The analytical study consisted of a reliability analysis using Monte Carlo simulation to determine the safety of unreinforced concrete block walls subject to out-of-plane loading based on parameters taken from the test database.

Eighteen full-scale unreinforced concrete block walls were constructed as part of the current experimental investigation. The walls were constructed using Type S mortar cement mortar and three slenderness ratios equal to 16, 18, and 20. Walls of each geometry were tested using both realistic and ideal supports. The realistic supports attempted to simulate real construction practice while the ideal supports provided pinned-roller support conditions. All walls were subject to quasi-static, lateral, displacement-controlled, four point-loading.

Analytical work included a reliability analysis for unreinforced concrete block walls subject to wind loads in Canada. A database for the flexural tensile strength of walls was compiled and classified based on the parameters included in tests. Probabilistic information for the annual

maximum wind speeds across Canada and the wind pressure coefficients were obtained from the literature. A Monte Carlo simulation was used to determine the reliability index for each investigated parameter based on 1 in 50 years hourly wind pressures. Recommendations were made to the empirical design provisions of CSA S304 (2014) based on the results of this analysis.

1.3 Layout of Thesis

This thesis consists of five chapters as outlined below:

- Chapter 1 provides a general introduction to the present investigation followed by the objectives and the scope of the study.

- Chapter 2 describes the CSA S304 (2014) standards as related to the empirical and rational design provisions for unreinforced concrete block walls subject to wind load. A review of the relevant past experimental investigations is then provided. Finally, reliability methods suitable for the purpose of the current investigation are introduced.

- Chapter 3 provides the details for the experimental portion of the study. The properties and the construction process for the specimens are discussed followed by a description of the test setup and process.

- Chapter 4 of this thesis first presents the test results for the experimental program. The compilation of the test database including results from the current and past investigations is described. The probabilistic information for the variables used in the reliability analysis are then presented. Finally, a discussion of the reliability analysis and results is provided as related to the empirical design provisions of CSA S304 (2014).

- Chapter 5 provides the conclusions of the present study and offers recommendations for future research.

2.0 Design of Unreinforced Masonry in Canada

This chapter presents the background information and literature review as related to the design and resistance of non-loadbearing, ungrouted, unreinforced, exterior masonry (URM) walls subject to out-of-plane loading. These walls are currently designed in Canada in accordance with CSA S304 (2014). Two design methods are included in the standard: the rational, and the empirical design methods. The rational design provisions are based on principles of engineering mechanics, while the empirical design provisions are based on rules-of-thumb and acceptable past performance of masonry walls. The design outcomes of the two methods are inconsistent for the case of URM walls subject to wind load. The empirical design method can result in less conservative design outcomes than the rational design method, indicating either inadequate conservatism of the empirical design provisions or the inefficiency of the rational design provisions. The discrepancy should therefore be addressed.

This chapter provides information necessary to establish a procedure to reconcile the two design methods. A demonstration of this discrepancy between the design methods is first provided. Past investigations focusing on the strength of URM walls are then examined. The parameters impacting the flexural tensile strength of URM walls, as obtained from experimental investigations, are discussed. Finally, reliability methods that can be used to assess the structural safety of URM walls are introduced.

2.1 Empirical and Rational Design Provisions as Provided in CSA S304-14

The requirements of the empirical and rational design provisions of CSA S304 (2014), as related to URM walls subject to wind load, are outlined in this section. The provisions introduced specifically apply to non-loadbearing, ungrouted, unreinforced, exterior concrete block walls. A comparison of the outcomes of the two design methods is provided that highlights the need for the reconciliation of the two design methods.

2.1.1 Design Requirements

The empirical design method is performed according to Annex F of CSA S304 (2014). Clause F.1.1 of Annex F specifies a maximum height limit equal to 20 m above grade for non-loadbearing exterior walls. The clause additionally specifies that the maximum 1 in 50 years hourly wind pressure, referred to hereafter as the ‘50-year wind pressure’, given in Appendix C of the National Building Code of Canada (NBCC, 2015), should not exceed 0.55 kPa. Clause

3.3.1 of Annex F of CSA S304 (2014) states that the minimum thickness of nonloadbearing exterior walls shall conform to limits described in Table F.2 of the standard. Accordingly, ungrouted exterior masonry walls constructed using hollow units shall have a minimum thickness of 190 mm and a maximum slenderness ratio of 20, where the slenderness ratio is defined as the height-to-thickness ratio of the wall.

The rational design of nonloadbearing unreinforced exterior walls is performed with reference to Clause 7.2 of CSA S304 (2014), and so in accordance with Equation 2.1, using basic strength of materials concepts. Equation 2.1 limits the sum of stresses due to load effects, shown on the left-hand side of the equation, to being less than or equal to the factored flexural tensile strength, as shown on the right-hand side of the equation:

$$\frac{M - M_{sw}}{S} - \frac{W_{half}}{A_e} \leq \phi_m f_t \tag{2.1}$$

In Equation 2.1, M is the moment due to the lateral load; M_{sw} is the moment due to the self-weight of the wall; S is the elastic section modulus; W_{half} is the self-weight of the top half of the wall, the use of which is a result of the assumption that the maximum moment occurs at the mid-height of walls subject to uniform out-of-plane loading; A_e is the effective cross-sectional area of the wall; ϕ_m is the resistance factor for masonry which is equal to 0.60 according to Clause 4.3.2 of CSA S304 (2014); and f_t is the flexural tensile strength of masonry as established from Table 5 of CSA S304 (2014). The value of f_t for vertically spanning concrete block walls and Type S mortar is 0.40 MPa.

Determining the moments due to the wind load and the self-weight of walls requires knowledge of parameters such as: the support conditions of walls, and the terrain conditions in the vicinity of the building. A brief discussion regarding the calculation of M and M_{sw} is provided in the following sections to provide further insight into the process of rational design.

Moment due to the wind load, M

The wind pressure, p, needs to be determined before M can be calculated. The wind pressure is determined using Equation 2.2. The equation is based on Sentences (1) and (3) of Article 4.1.7.3 of NBCC (2015):

$$p = I_w q C_e (C_p C_g + C_{pi} C_{gi}) \tag{2.2}$$

In Equation 2.2, q is the wind velocity pressure based on Sentence (4) of Article 4.1.7.3 of the NBCC (2015). The importance factor for wind load, I_w, is based upon building use and is equal to 1.0 for buildings in the normal importance category, including typical residential buildings. The exposure factor, C_e, is a function of the reference height, h, and the terrain conditions, as described in Sentences (5) and (6) of Article 4.1.7.3 (NBCC, 2015). The prescribed value of C_e is equal to $\left(\frac{h}{10}\right)^{0.2}$ but not less than 0.9 for open terrain, and equal to $0.7\left(\frac{h}{12}\right)^{0.3}$ but not less than 0.7 for rough terrain. The external pressure coefficient and the gust effect factor are represented by C_p and C_g, respectively. The product of C_pC_g is determined from Figure 4.1.7.6-B in the NBCC (2015). The internal pressure coefficient and the internal gust effect factor are represented by C_{pi} and C_{gi}, respectively. The value of C_{gi} is required to be taken as 2.0 in the absence of detailed calculations taking into account the sizes of openings in the building envelope. The internal pressure coefficient, C_{pi}, is determined according to Table 4.1.7.7 in NBCC (2015). The table includes three cases for building openings. The present investigation focuses on the two extreme cases. In the first case, openings make up less than 0.1% of the surface area of the building. This case will be referred to as 'sealed buildings' in this work. In the second case, the building includes large openings which are likely to remain open during storms. This case will be referred to as 'buildings with significant openings' in this work. The case not considered in this work results in intermediate values of C_{pi} and corresponds to buildings containing non-significant, non-uniformly distributed openings, or significant openings which are wind resistant and remain closed during storms. The topographic factor, C_t, introduced in Article 4.1.7.4 of NBCC (2015) is equal to 1.0 for buildings on hills with a slope less than or equal to 0.1. The current study assumed buildings to be on a slope equal to zero and so the topographic factor was excluded from Equation 2.2.

The moment, M, can then be calculated assuming simple support conditions and a uniform wind pressure on the surface of the wall, using Equation 2.3, where l is the vertical span length of walls. The wind load factor, denoted by α_w in the equation, is equal to 1.4:

$$M = \frac{\alpha_w p l^2}{8} \tag{2.3}$$

Moment due to the wall self-weight, M_{sw}

The factored moment due to the self-weight of the wall, M_{sw}, is calculated using Equation 2.4, where W_{total} is the total self-weight of the wall, t is the wall thickness, and α_D is the dead load factor equal to 0.9:

$$M_{sw} = \frac{\alpha_D W_{total} t}{4} \tag{2.4}$$

The moment due to the self-weight of the wall relates to the manner in which the wall supports are assumed to behave under lateral loading. Figure 2.1 (a) shows support conditions in real construction practice, referred to hereafter as 'realistic supports'. The figure shows that a layer of mortar exists between the concrete grade beam and the first block course of the wall above. The first layer of mortar is assumed to crack when subject to wind load, resulting in the base of the wall acting as a pin support. Figure 2.2 (a) shows the free body diagram of the wall under wind pressure and after the crack has occurred. The figure shows that a lever arm equal to $\frac{t}{2}$ results between the self-weight of the wall, W_{total}, acting along the centroid of the wall thickness, and the vertical support reaction at the bottom of the wall, $R_{ybottom}$. The resulting counter-clockwise moment acts in the opposite direction to the moment caused by the wind load. The wall can resist greater out-of-plane loads as a consequence.

The design of supports for the majority of URM walls included in previous investigations differs from realistic support conditions. Wall supports in past investigations, referred to hereafter as 'ideal supports', were designed to provide pinned-roller support conditions. This is shown in Figure 2.1 (b) where roller supports allow the ends of the wall to rotate. The setup shown in the figure is in accordance with the requirements of ASTM E72 (2015) and is generally the setup used in past investigations. The position of the bottom roller, providing the vertical reaction, prevents the formation of moment due to self-weight. Figure 2.2 (b) shows that the vertical support reaction at the bottom of the wall, $R_{ybottom}$, is aligned with the line of action of the wall self-weight so that no moment results. The mitigating effect of the moment due to self-weight under lateral loading was therefore not present in the test results, resulting in an apparent reduction of the out-of-plane resistance of walls.

2.1.2 Comparison of the Outcomes of the Empirical and Rational Design Methods

Figure 2.3 presents a comparison of the design outcomes for the rational and empirical design provisions of CSA S304 (2014) for a selected set of parameters. The outcomes of the two design methods, as shown in the figure, were calculated using Equations 2.1 to 2.4. The figure provides the maximum allowable 50-year wind pressure for varying slenderness ratios, where k, as included in the calculation of the slenderness ratio plotted along the horizontal axis, is the effective length factor determined in accordance with Annex B of CSA S304 (2014). The building was assumed to have non-uniformly distributed insignificant openings or significant openings that remained closed during storms (internal pressure coefficient, C_{pi}, equal to 0.45). In addition, a wall thickness equal to 190 mm and a building use corresponding to the normal importance category were assumed. The outcome for the rational design method is demonstrated for both open and rough terrain conditions. Design outcomes, as shown in Figure 2.3, were limited to a maximum slenderness ratio equal to 20, as required by the empirical provisions, and a minimum slenderness ratio equal to 10, for practicality.

Figure 2.3 shows that the rational provisions lead to more conservative results than the empirical provisions for slenderness ratios exceeding 14 and 16 when open and rough terrain conditions are assumed, respectively. The figure shows that the empirical provisions, by definition, consistently result in an allowable 50-year wind pressure equal to 0.55 kPa, while the rational provisions result in a 50-year wind pressure equal to 0.38 kPa at a slenderness ratio equal to 20 when rough terrain conditions are assumed. The allowable 50-year wind pressure is reduced to 0.30 kPa when open terrain conditions are assumed. The difference in design outcomes implies either inadequate levels of safety associated with the empirical design provisions, or economically inefficient designs associated with the rational provisions. The discrepancy between the outcomes of the two design methods has not previously been resolved. The two design methods should, however, be reconciled to ensure the safety and the economic efficiency of all resulting structures designed in accordance with the CSA S304 standard.

Any contribution towards the reconciliation of the two design methods requires a better understanding of the flexural tensile strength of URM walls. Experimental investigations of the out-of-plane strength of unreinforced masonry date back to, at least, the early 1930's (Richart, 1932). The extensive time span over which investigations were conducted makes the study of

parameters included in the construction and testing process important. For example, different mortar types were used in the construction of walls included in past experiments, while CSA S304 (2014) does not account for the potential variation in flexural tensile strength when different mortar types are used. Additionally, no reliability analysis has been done in Canada for the flexural tensile strength of masonry (Laird, 2013). Sections 2.2 and 2.3 address such concerns.

2.2 Flexural Tensile Strength of Unreinforced Masonry Walls

Nine experimental investigations were identified in which non-loadbearing, unreinforced concrete block walls were subject to out-of-plane loads. Included parameters in each investigation were summarized and are shown in Tables 2.1 and 2.2. The development of the existing test database was intended to determine the impact of the various parameters investigated on the flexural tensile strength of masonry, and potentially lead to the inclusion of the influence of these parameters in a reliability analysis of masonry for flexural tensile strength. Table 2.1 identifies parameters elated to the material used in the construction of specimens and the properties of the included specimens. The table also provides the resulting average values for the flexural tensile strength of specimens. Table 2.2 presents the curing condition of specimens, the retempering of mortar during construction, and the load application method. A discussion of results, as related to these parameters, is provided in this section.

2.2.1 Mortar Type and Flexural Tensile Strength

Table 2.1 shows that Portland cement lime mortar (PCL), masonry cement mortar (MC), and mortar cement mortar (MrC) were used in the testing of the URM walls. The mortar types in the table are listed as they were reported in the corresponding research programs rather than based on the requirements of CSA A179 (2014). All discussions related to mortar in this study refer specifically to Type S mortar, unless otherwise stated. Laird (2013) stated that the flexural tensile strength of masonry constructed with PCL is generally greater than that constructed with masonry cement mortar, while mortar cement mortar was designed to have a flexural tensile strength similar to PCL. This cannot be deduced from results shown in Table 2.1. The use of MrC in construction resulted in a flexural tensile strength that had an average value equal to 0.120 MPa, which was the lowest of all mortar types investigated. The second lowest value

(0.136 MPa) and the second highest value (0.819 MPa) resulted when MC was used. Results when PCL was used in wall construction ranged between 0.164 MPa to 1.30 MPa.

In addition to the wide range of resulting strengths, as described, the disproportionate amount of available test data for different mortar types makes determining the impact of mortar type on the flexural tensile strength of masonry difficult. Six out of nine investigations used PCL, while three used MC, and only one used MrC mortars. Results show the need for additional test data for mortar cement and masonry cement mortars.

2.2.2 Full-Scale Wall versus Prism Tests

Table 2.1 shows the ratio of the flexural tensile strength obtained from full-scale wall tests to those obtained from prism tests. Two to five course prisms were used in tests. The average ratios of flexural tensile strengths obtained for full-scale walls to prisms ranged from 0.74 to 3.1. The inconsistency of the resulting ratios indicates that the strength of full-scale walls cannot reliably be derived from prisms. As a result, it is apparent that the study of the flexural tensile strength of URM walls, and potential reliability analyses, should include only test results for full-scale walls since values of flexural tensile strength obtained through prism tests do not appear to be representative of the strength of walls.

2.2.3 Wall Span

Table 2.1 shows that the maximum wall span used in past investigations was equal to 3.0 m. The wall thickness in the majority of cases was 190 mm, which is equal to the minimum thickness permitted in the empirical provisions of CSA S304 (2014) for exterior walls constructed using hollow units. A wall with a span length equal to 3.0 m and thickness equal to 190 mm has a slenderness ratio of 16. Therefore, no test results are available for walls with slenderness ratios exceeding 16, while the empirical provisions permit slenderness ratios of up to 20.

The flexural tensile strength of URM walls for slenderness ratios greater 16 cannot be assumed to be the same for those with ratios less than 16. It was shown previously that specimen size affects the resulting flexural tensile strength of masonry, and, that tests of full-scale walls yield different results than prism tests. In addition, NCMA (1994) reported that walls with a thickness of 90 mm result in higher flexural tensile strengths than those with thicknesses of either 190 or

290 mm when span length is constant; the latter two values for wall thickness were found to result in similar values for flexural tensile strength. Results from NCMA (1994) are not directly applicable to the current investigation since a wall thickness of 90 mm is not permitted in the empirical provisions for non-loadbearing walls constructed with hollow units. It does, however, indicate that changes in slenderness ratio can impact the flexural tensile strength of walls. Additional test data for URM walls with slenderness ratios between 16 and 20 and constructed with blocks meeting the thickness requirements of the empirical provisions are therefore needed.

2.2.4 Support Conditions

The difference in support conditions for walls with realistic and ideal supports was described in Section 2.1. The impact of this difference on the out-of-plane resistance of URM walls had not been investigated until Udey (2014) reported a 63% increase in moment resistance, due to the presence of arching action, when walls were constructed with realistic supports as compared to ideal supports. Additional test data can be helpful in determining the flexural tensile strength of URM walls with realistic supports and, possibly, in reconciling the discrepancy between the design methods of CSA S304 (2014).

2.2.5 Curing Method

Table 2.2 shows the different curing conditions as reported in each of the past investigations. Two out of the nine investigations did not report curing conditions. The remaining investigations reported wide ranges of temperature and relative humidity. The temperatures in which specimens were stored after construction varied from 21 to 33 °C, and the relative humidity ranged from 38% to 75%. In addition, NCMA (1994, 1997) reported the curing method rather than the relative humidity.

Two investigations studied the impact of curing on the flexural tensile strength of masonry directly. Copeland and Saxer (1964) reported that curing methods such as covering the specimens with plastic sheeting and spraying them with water for the first few days after construction can increase the resulting flexural tensile strength of masonry. It was also reported that improved curing is most beneficial for high strength mortars which have a compressive strength greater than 22 MPa. NCMA (1994) compared four different curing methods. The first method involved spraying the specimens with water after construction and keeping them in

polyethylene bags until two days prior to testing. The second method involved keeping the specimens in the laboratory air and spraying them at 7 and 14 days after construction. The third and fourth method involved, respectively, keeping the specimen in the open laboratory air and in the open air outside the laboratory. Results indicated an increase of the flexural tensile strength of specimens by at least a factor of three when the first two methods were used.

It is therefore observed that the curing method can have a significant impact on the flexural tensile strength of masonry. Results, however, are neither consistent nor comprehensive enough to provide a quantitative understanding of this impact. This should be considered when comparing the resulting values of flexural tensile strength in past experiments.

2.2.6 Retempering of Mortar

Retempering of mortar is permitted by Clause 6.4 of CSA A179 (2014) to restore desirable workability. However, Table 2.2 shows that some of the past investigations imposed limits on the retempering of mortar. Examining the impact of this parameter on the flexural tensile strength of masonry in past investigations should be considered in the interpretation of the resulting strengths.

Two investigations did not permit the retempering of mortar: Richart (1932) and Drysdale and Essawy (1984). NCMA (1994, 1997) permitted retempering only once during construction. Furthermore, Copeland and Saxer (1964) was the only investigation to specifically examine the impact of retempering on the strength of masonry. It was reported that adding water to the mortar more than one hour after initial mixing reduced the flexural tensile strength of one mortar mix by 30%, but did not have an effect on other mortar mixes. This suggests the possibility of higher flexural tensile strength when retempering is limited.

It is therefore suggested that data obtained for experiments in which retempering was limited be considered with caution since there is a possibility of overestimation of flexural tensile strength in such cases.

2.2.7 Load Application Method

Two load application methods were implemented in the testing of walls in past investigations: point loading and uniform loading. Point loading involved the application of two point loads at the quarter points of walls, with the exception of Richart (1932), where a single load was

applied at the mid-span of walls. Three of the nine investigations identified in Table 2.2 used point loading as the method of load application. Uniform loading was applied by increasing the air pressure in the airbag used for load application. Investigations using either load application methods were generally in compliance with the specifications of ASTM E72 (2015), with the exception of Richart (1932).

ASTM E72 (2015) recognizes that the resulting out-of-plane strength of spans may be greater if uniform loading is implemented. There are, however, no official guidelines related to the quantification of the difference in results obtained when different loading methods are used. Two investigations were found to have commented on this difference quantitatively. Monk (1955) reported walls subject to uniform loading can result in a flexural tensile strength 1.97 times greater than those subject to point loading. NCMA (1967) reported a value equal to 1.99 for this same relationship. Monk (1955) attributed this difference partially to the concentration of stress under the rollers used in the point loading of walls.

Representing the wind load by the uniform loading method includes shortcomings such as an incomplete or non-uniform filling of the airbag and potential for membrane action resulting from the use of airbags. Nonetheless, it has been assumed in past works (Monk, 1955, NCMA, 1967, Kim and Bennett, 2002) that uniform loading provides a better representation of the wind load on the surface of walls than point loading. Examination of test data obtained in past investigations should consider the potential impact of the load application method on results. Use of a correction factor should be considered for data related to walls subject to point loading if uniform loading is assumed to provide a more accurate representation of the wind load.

2.2.8 Summary of Literature Review

Experimental investigations applicable to the scope of the current work were reviewed. It was shown that parameters such as support conditions, mortar type, curing method, load application method, and slenderness ratio can impact the resulting strength. It was found that values of flexural tensile strength obtained from prism tests cannot be taken as representative of the strength of full-scale walls. It was also shown that additional test data are needed for walls with realistic supports, walls constructed with mortar cement mortar, and walls with slenderness ratios greater than 16.

The results of the literature review were used to design an experimental program to supplement the available test data for the out-of-plane strength of non-loadbearing URM walls. The results were also used to perform a reliability analysis in order to obtain a quantified estimate of the level of safety of URM walls. Section 2.3 examines common reliability techniques in order to determine the most effective method for the purpose of the current investigation.

2.3 Structural Reliability of Unreinforced Masonry for Flexural Tensile Strength

There are uncertainties in the prediction of the behavior of engineering systems. Such uncertainties include, but are not limited to: uncertainties associated with the physical characteristics of the systems, statistical uncertainties resulting from the limited available data for the system properties, and uncertainties related to the simplifying assumptions made in designing models which represent the systems. Reliability methods can be used to quantify the impact of such uncertainties on the behavior of systems and, thus, provide measures for the level of safety (Ayyub and McCuen, 2003).

Reliability in structural engineering is related to the fulfillment of specific requirements referred to as limit states. The present investigation is concerned with the 'ultimate' or 'safety' limit state. The ultimate limit state is related to the safety of a structure as opposed to its ability to perform its intended use. Methods used in structural reliability can be studied at different levels. The following is an overview of such methods at three levels as discussed by Melchers and Beck (2018):

- Level I reliability methods are generally considered to be deterministic or partially probabilistic depending on the information used in the analysis. Level I reliability methods do not result in the explicit determination of the probability of failure. Instead, characteristic values used to represent variables are associated with partial safety factors for loads and resistance to ensure the desired level of safety.
- Level II reliability methods are considered to be probabilistic methods. Variables are modeled using normal probability distributions which are represented using their means and variances. The probability of failure is calculated explicitly by determining the probability that the load effects exceed resistance. Results for Level II reliability methods are affected by the variability and uncertainties related to the load effects and resistance, as included in their respective probability distributions.

- Level III reliability methods use any types of probability distributions for variables to explicitly determine the probability of failure. Two general calculation methods are used at Level III. The first method, which is classified as a Level II method by some authors (Schueremans, 2001), requires the non-normal distributions of all variables be transformed into their equivalent normal distributions, and then represented by their means and variances as is done in Level II methods. In the second calculation method, simulation techniques such as the Monte Carlo method use the probability distributions directly and, therefore, no transformation of distributions is required. Random samples from the probability distributions of variables are used to calculate the limit state function. The repetition of this process results in the calculation of the probability of failure.

Level III reliability methods provide the most accurate estimate of the probability of failure. Schueremans (2001) recommends that Levels I and II methods, including the transformation of non-normal distributions, be calibrated using Level III methods for accuracy. Monte Carlo simulation is the simplest method available to calculate the probability of failure of structures (Laumakis and Harlow, 2016, Melchers and Beck, 2018). A traditional setback for this method has been the extensive calculation time required due to the reliance of the method on the generation of a large number of samples. However, the use of Monte Carlo simulation has become more practical with the increased availability of computers with high processing power. Accordingly, Monte Carlo simulation is considered the most appropriate reliability method for the current investigation due to its accuracy, simplicity, and flexibility with the types of probability distributions of variables included in the limit state function. An overview of this method is provided below.

2.3.1 Monte Carlo Simulation

The principle behind Monte Carlo simulation is to evaluate the behavior of a system which is represented by a model through repeated creation of artificial numerical experiments. The method produces outcomes for each simulated experiment using random sampling based on the available probabilistic information related to the parameters included in the model. The accuracy of results increases with increasing number of artificial experiments for a given set of probabilistic information and model.

Monte Carlo simulation applies to structural engineering where the behavior of a structural component under certain loading conditions is to be examined. The probabilistic information contains the uncertainties and variabilities associated with resistance and loads, and the outcome of each simulation determines whether or not the structural component fails. The steps involved in determining the reliability of a structural component using the Monte Carlo simulation follow (Ayyub and McCuen, 2003).

(1) The model describing the behavior of the structural component should first be defined. The model in the case of URM walls subject to out-of-plane loading is described by Equation 2.1. This equation is referred to as the limit state function as it defines the relationship between the relevant variables and the failure or survival of walls.
(2) Variables included in the limit state function are represented by probability distribution functions. The probability distributions are calculated using available experimental data for the variables.
(3) A random number is generated for each variable using its probability distribution. These numbers are used as input values for the limit state function.
(4) The limit state function is evaluated using the input values. The outcome is recorded as a failure or survival of the structural component.
(5) The procedure is repeated many times. The probability of failure, P_f, is then equal to the ratio of the number of times the structural component has failed, N_f, to the number of times the simulation is run, N. The number of times the simulation needs to be repeated increases with decreasing values of P_f and increasing desired accuracy of results.

2.4 Summary

This chapter identified that walls designed using the empirical or rational design methods included in CSA S304 (2014) may differ for non-loadbearing, ungrouted unreinforced exterior masonry walls subject to wind. Applicable past experimental investigations were studied with regard to the parameters affecting the flexural tensile strength of unreinforced masonry. It was shown that important parameters such as slenderness ratio, support conditions, and mortar type used in the construction of walls require further investigation. It was also shown that a formal reliability analysis for unreinforced masonry for flexural tensile strength has not been determined previously in Canada. An overview of reliability methods indicated Monte Carlo

simulation to be an efficient method, in terms of both accuracy and simplicity, to determine the structural safety of URM walls subject to out-of-plane loading. The results of the literature review were used to design an experimental program to supplement available test data. Test data obtained from past investigations and the current program were synthesized and used to conduct a reliability analysis for the flexural tensile strength of unreinforced masonry. Details for the experimental program and the reliability analysis will be introduced in Chapters 3 and 4, respectively.

Table 2.1: Material and Specimen Properties as Reported in Past Investigations

Research Program, Publication Year	Flexural Tensile Strength (MPa)	Mortar Type as Specified in the Literature[1, 2]	Wall Span[3] (m)	Ratio of Flexural Strength of Full Size Walls to Prisms	Support Type (Ideal or Realistic)
Richart (1932)	0.192	PCL	2.7	Not Reported	Ideal
Hedstrom, (1961)	0.309	PCL	2.3	1.05	Ideal
Fishburn, (1961)	0.136	MC	2.3	1.01	Ideal
Copeland & Saxer, (1964)	0.538	PCL	2.3	3.1	Ideal
Drysdale & Essawy (1988)	0.310	PCL	2.8	0.74	Ideal
Matthys (1990)	0.164 - 0.293	PCL MC	2.3	1.7-1.8	Ideal
NCMA (1994)	1.30	PCL	2.2	1.11	Ideal
NCMA (1997)	0.819	MC	2.2	1.12	Ideal
Udey (2014)	0.120	MrC	3.0	2.8	Ideal & Realistic

[1] PCL: Portland cement lime. MC: Masonry cement. MrC: Mortar cement.
[2] Type S mortar was used in all cases.
[3] Vertical span lengths of walls measured between the top and bottom support reactions.

Table 2.2: Construction and Testing of Specimens as Reported in Past Investigations

Investigation	Curing Method		Retempering of Mortar	Load Application Method (Point or Uniform Loading)
	Relative Humidity (%)	Temp. (C˚)		
Richart (1932)	50-65	21-24	Not Permitted	Point[1]
Hedstrom (1961)	38-65	23	Permitted	Uniform
Fishburn (1961)	≥50	27	Permitted	Point[2]
Copeland and Saxer (1964)	75	23	Permitted	Uniform
Drysdale and Essawy (1984)	Not Reported	Not Reported	Not Permitted	Uniform
Matthys (1990)	55	22	Permitted	Uniform
NCMA (1994)	Sprayed and sealed in bags	24 ± 9	Permitted Once	Uniform
NCMA (1997)	Sprayed and sealed in bags	24 ± 9	Permitted Once	Uniform
Udey (2014)	Not Reported	Not Reported	Permitted	Point[2]

[1] Load applied at the mid-span of walls.
[2] Loads applied at the quarter points of the span.

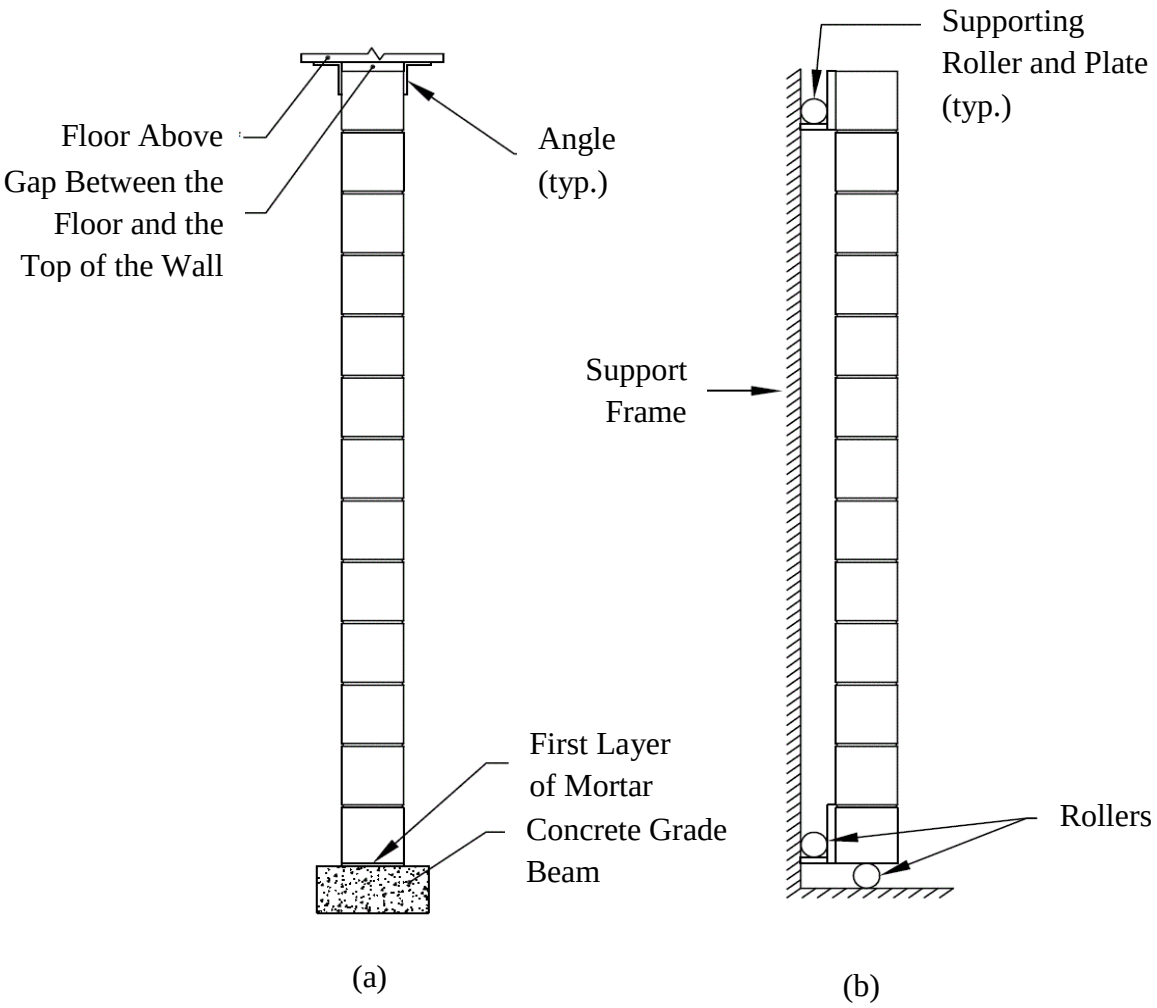

Figure 2.1: Typical Support Conditions: (a) Realistic Support Conditions, and (b) Ideal Support Conditions

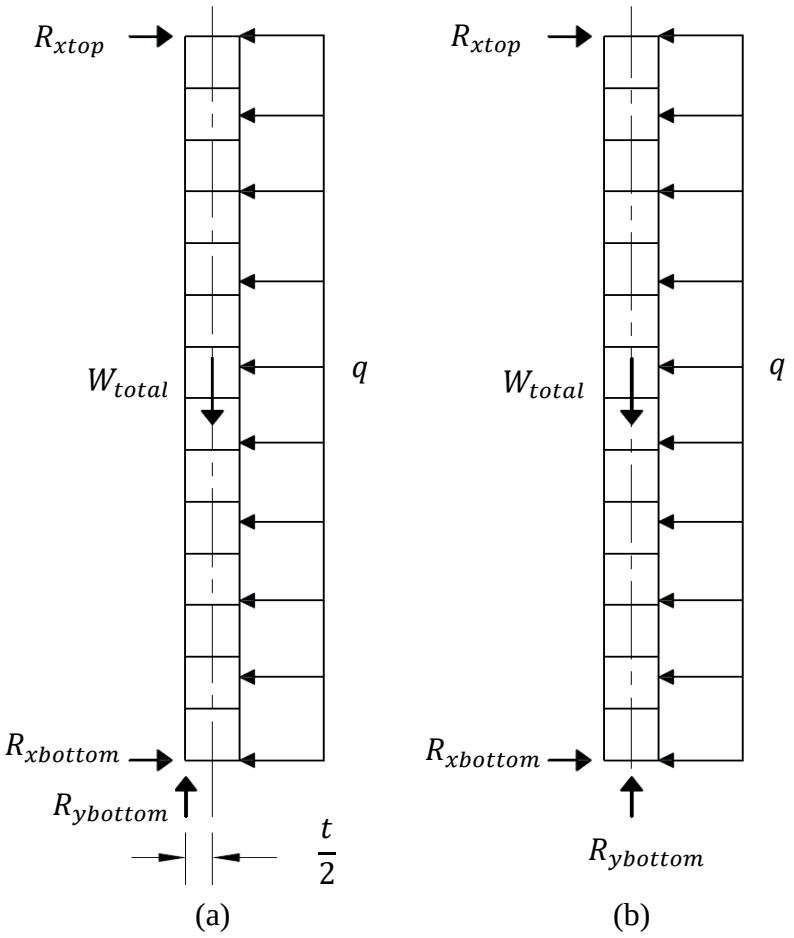

Figure 2.2: Free Body Diagrams for Walls with: (a) Realistic Supports, and (b) Ideal Supports

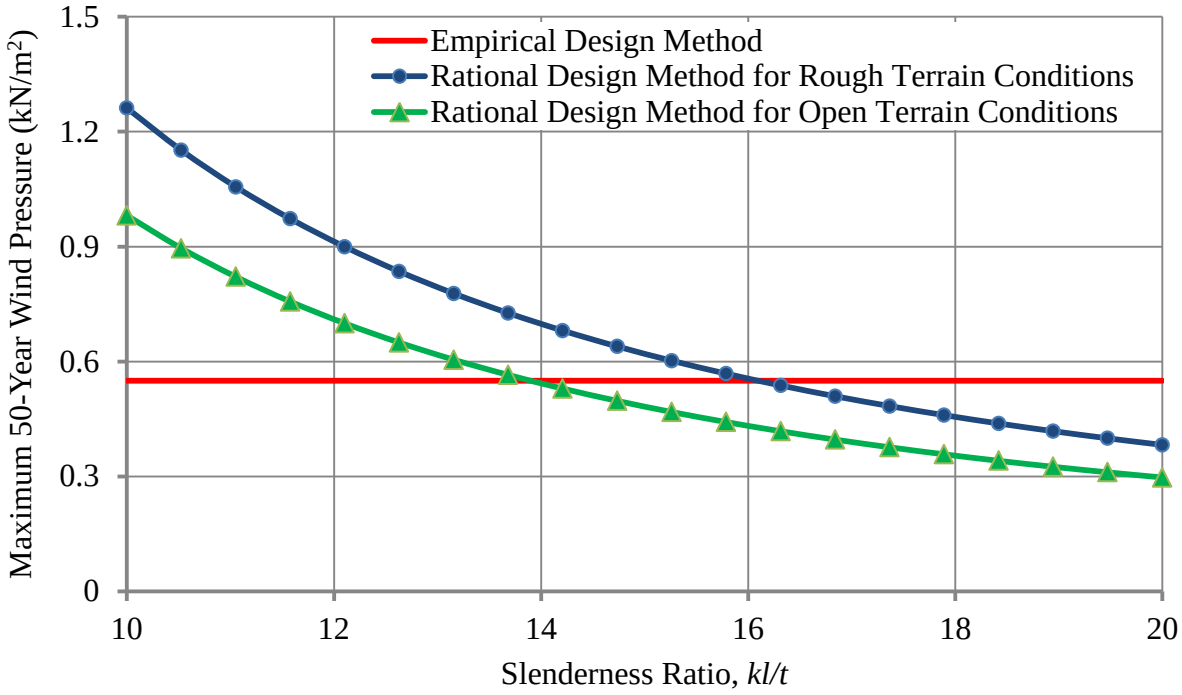

Figure 2.3: Comparison between the Rational and Empirical Design Provisions

3.0 Experimental Program

The experimental design portion of this research program is discussed in this chapter. The design of the wall and companion specimens is introduced, followed by a description of the materials used in the construction process. Finally, the construction and testing process of the wall and companion specimens is presented.

This experimental program focused on unreinforced concrete block walls subject to out-of-plane loading. The specimens were designed with the purpose of contributing towards meeting the objectives introduced in Chapter 1. The literature review presented in Chapter 2 revealed some of the areas where data are lacking, including: the flexural tensile strength of unreinforced masonry walls constructed using mortar cement mortar, walls with different support types, and walls with slenderness ratios greater than 16.

3.1 Specimen Description

The wall specimens included in the experimental program are introduced herein. Initially, the overall design of the experimental program focusing on walls is presented. The geometric and support types for walls are presented, followed by the specifics of the design of the supports used in the test setup of wall specimens.

3.1.1 Walls

Table 3.1 shows a summary of all specimens included in the experimental program. Overall, 18 unreinforced concrete block walls were constructed with three different heights using either realistic or ideal supports. This resulted in six categories (2 support types x 3 wall heights) of walls, each category containing three replicate walls. The rationale for the number of replicates selected was to satisfy Section 3.1 of ASTM E72 (2015), which requires three specimens as a minimum for tests for determining structural properties. The available space in the structural laboratory at the University of Saskatchewan was also taken into consideration when determining of the number of specimens.

Figures 3.1 (a) through (c) show the geometry and support conditions for the wall specimens. The left side of each wall shown in Figure 3.1 depicts the realistic support conditions, signified by “R”, while the right side depicts the ideal support conditions, signified by “I”. Walls were constructed in running bond with one of the following heights: 3000, 3400, or 3800 mm,

corresponding to 15, 17, and 19 courses, respectively. All walls had a constant thickness of 190 mm and a constant width of 1000 mm, corresponding to two and a half concrete blocks. Wall heights and thicknesses correspond to slenderness ratios of 16, 18, and 20, where the slenderness ratio is defined as the height to thickness ratio of walls. The selection of wall heights was based on findings from the literature review. As explained in Section 2.2.3, past research focusing on unreinforced masonry walls included slenderness ratios between 12 and 16, while the maximum slenderness ratio allowed by the empirical design provisions of CSA S304 (2014) is 20. Construction, transportation, and testing of walls based on the space and equipment available in the lab were considered in selecting the wall width.

The ideal support conditions shown in Figure 3.1 allowed for rotation both at the bottom and top of walls, imitating the assumption typically made in design. The realistic support conditions provide a degree of fixity both at the bottom and top of walls, mimicking real construction practice. With the exception of Udey (2014), all previous research programs identified have investigated the flexural strength of unreinforced concrete block walls exclusively using ideal support conditions. The inclusion of realistic supports in the current research program extends the work of Udey (2014), such that support conditions are evaluated in combination with varying slenderness ratios.

Supports

Wall supports were designed to mimic the conditions of ideal and realistic supports described in Section 2.1.1. Ideal supports were previously designed and used in experiments by Udey (2014), while bottom realistic supports were constructed as part of experiments conducted by both Udey (2014) and Miranda et al. (2016) at the University of Saskatchewan. The details of both the ideal and realistic support geometry are introduced in the following paragraphs. Top supports were similar for both ideal and realistic support types and are presented first. The bottom ideal and realistic supports are then presented.

Top Supports (Ideal and Realistic)

Top supports consisted of three main components: (a) the steel plate shown in Figure 3.2, which rested on top of the wall specimens, (2) the two steel angles shown in Figure 3.3, which clamped the two sides of the top course of the walls to the steel plate, and (3) the three 15 mm steel rods shown in Figure 3.4 (a), which connected the top steel plate to the wall support frame. Top

supports were identical in the cases of realistic and ideal supports with the exception of how the steel rods were connected to the steel plate. The connection between the steel rods and the plate determined the degree of fixity of the top supports which was the deciding factor as to whether the support was realistic or ideal.

The three lifting lugs on top of the steel plate, as shown in Figure 3.2, were used to transport the plate to the top of the walls with the aid of an overhead crane. The lifting lugs were also used to connect the plate to steel rods. Slotted holes drilled in the steel plate were used to bolt the plate to the steel angles clamping the wall specimens to the steel plate. Figure 3.3 shows the steel plate secured tightly against the wall specimen using L100x100x12 angles. The steel plate was placed on top of the wall without a gap between the two. Figure 3.4 (a) shows the use of three steel rods to connect the top steel plate to the wall support frame. Three rods were used for both ideal and realistic supports to prevent the wall from twisting about the top support during the application of lateral load. Figure 3.4 (b) shows the top steel plate pinned to supporting rods using hinges to allow for rotation and to create the ideal support conditions. Figure 3.4 (c) shows the bolted connection between the top steel plate and the steel rods as used to limit rotation for the realistic support conditions.

Bottom Ideal Support

Ideal supports located at the bottom of the wall specimens consisted of three main components: (1) the steel plate shown in Figure 3.5 upon which walls were constructed, (2) the groove plate shown in Figure 3.6 which was bolted to the steel plate, and (3) the knife edge shown in Figure 3.7 which sat underneath the groove plate. Figure 3.8 shows the assembly of the bottom ideal supports. As seen in the figures, the groove plate sits on the protruding tab on the knife edge. The tab on the knife edge was welded to two HSS 152.4x101.6x12.7 sections for stability. This mechanism allowed for the rotation of the support upon application of lateral load. Lifting lugs shown in Figure 3.5 were welded to the steel plate and used for transportation of the walls with the aid of an overhead crane. The support assembly was bolted through the strong floor using the slotted holes provided in the knife edge assembly, as shown in Figure 3.7.

Bottom Realistic Support

Figure 3.9 shows the typical grade beam used as the bottom realistic support. The grade beams shown in the figure were cast longer than the wall specimens so that they could be securely

fastened to the strong floor. Additionally, lifting lugs were included in the design of concrete grade beams to facilitate the transportation of wall specimens to the test frame using the overhead crane available in the laboratory. A layer of mortar was laid between the concrete grade beam and the underside of the first block course of the wall specimens as per typical construction practice.

3.2 Material Description

The materials used in the construction of the test specimens in the current experimental program are presented in this section. Concrete masonry blocks and mortar are introduced along with their specifications.

3.2.1 Concrete Masonry Blocks

Concrete masonry blocks were ordered and delivered to the structural laboratory by a local vendor. All blocks were normal density, 15 MPa concrete blocks that included both frog-ended and flat-ended blocks. Typical flat-ended and frog-ended blocks are depicted in Figure 3.10 (a) and (b), respectively. Both flat-ended and frog-ended blocks were used randomly in the construction of wall specimens. All blocks were 190 mm in height and width and 390 mm in length. Whole blocks were cut in half using a concrete block saw to be used in the construction of walls when needed, ensuring that all blocks originated from the same material batch.

3.2.2 Mortar

Lafarge Type S mortar cement mortar was used in the construction of wall specimens. The mortar mix was designed according to Table 4 in CSA A179 (2014). An experienced mason mixed two 17 kg bags of the mortar with approximately 0.06 m^3 of mortar sand, as available in the structural laboratory at the University of Saskatchewan. The amount of water added differed from batch to batch and varied between 19 to 25 liters, depending on the degree of dampness of the sand, as determined by the mason.

3.3 Companion Specimens Description

Four kinds of companion specimens were included in the experimental program. These specimens are described in this section, along with the purpose for their inclusion in the program.

Two sets of six full-sized concrete blocks were selected as per the requirements of ASTM C140 Standard Test Methods for Sampling and Testing Concrete Masonry Units and Related Units

(2015). Note 8 in ASTM C140 (2015) requires two distinct sets of blocks to be selected for compressive and absorption tests, assuming the net volume acquired through absorption tests is the same for the two sets of blocks. Half of the selected blocks in each set were flat-ended and the other half frog-ended. Samples of both block types were subject to compressive and absorption tests.

Six 50 mm mortar cube specimens were constructed per mortar batch, resulting in 144 mortar cubes in total. The cubes were constructed according to CSA Test Methods A3004-C2 (2008). The casting of mortar cubes started within 150 seconds after the mortar batch was mixed. A layer of freshly-mixed mortar roughly 25 mm deep was placed in each mortar mold and tamped 32 times in four rounds. A second layer was placed in the mold and the same tamping practice was followed. Excess mortar was leveled by drawing the flat side of a trowel across the top of the molds.

A single two-course tall by one-block wide stack bond pattern prism, as shown in Figure 3.11 (a), was constructed per mortar batch, resulting in 24 prisms in total. These prisms are referred to as ‘bond wrench prisms’ hereafter. A single three-course tall by one-block wide stack bond pattern prism shown in Figure 3.11 (b) was constructed alongside each wall, resulting in 18 prisms in total. These prisms are referred to as ‘three-course prisms’ hereafter. Bond wrench and three-course prisms were constructed halfway through each batch of mortar. Flat-ended and frog-ended blocks were used randomly in the construction of all prisms. All prisms were constructed on a fiber board base that provided a flat construction surface and facilitated the transportation of prisms for testing.

Companion specimens were included in the experimental design primarily for quality control purposes in order to meet the requirements of CSA S304 (2014) and CSA A179 (2014). Results obtained from concrete block tests were necessary to perform the calculations pertaining to the strength of the three-course prisms. Bond wrench prisms were included for the secondary purpose of comparing the flexural tensile strength obtained from wall tests to those obtained from the prisms. Testing of the companion specimens is discussed in Section 3.5.

Table 3.2 shows the correspondence of mortar batches to walls, bond wrench prisms, three-course prisms, and mortar cubes. Wall names begin with a number signifying the slenderness

ratio of that wall, followed by letter I (Ideal Support) or R (Realistic Support) to indicate the support type used when testing that wall, followed by a number signifying the replicate number within the test series. For example, 16I3 refers to the third replicate specimen within wall series with slenderness ratio of 16 tested using ideal supports. Three-course prisms were given the same name as the wall with which they corresponded. Bond wrench prisms were given the same identification as the mortar batch that was used in their construction. The identification of mortar batches begins with the letter B (batch of mortar) followed by the batch number. Mortar cube specimen identification followed the same system as used for the mortar batch, with the exception that mortar cube identification began with a number signifying replicate number within the test series.

3.4 Construction of Specimens

All wall specimens were built in a single construction phase over a period of three weeks by an experienced mason. Wall specimens were constructed in two lifts such that the construction of the first lift did not require scaffolding. This was done both to expedite construction and to allow the courses laid in the first lift to cure for a few days and gain strength before the weight of a second lift was placed on them.

The first seven courses of the walls with realistic supports, as well as the first eight courses of the walls with ideal supports, were constructed in the first lift. Subsequently, the second lifts of all walls were constructed. The number of courses per each lift of wall was selected based on how high the mason could safely raise the blocks. One level of scaffolding was used to construct the top portion of walls with a slenderness ratio of 16, and two levels of scaffolding were used to construct the top portion of walls with slenderness ratios of 18 and 20.

Overall, 24 batches of mortar were mixed during the 12 days of construction. The mason retempered each mortar batch several times by adding water after initial mixing to achieve the desired workability. Retempering is permitted in accordance with Clause 6.4 of CSA A179 (2014) at intervals necessary to achieve desired workability.

Walls, bond wrench prisms, and three-course prisms were cured in open laboratory air for a minimum of 28 days before being tested. Mortar cubes were cured under a plastic sheet for 48

hours after being cast. They were then removed from the molds and cured in open laboratory air for a minimum of 26 additional days.

3.5 Specimen Testing

The details of the test process and setup for wall and companion specimens are provided in this section. Section 3.5.1 describes the test setup and procedure for the wall specimens and Section 3.5.2 discusses the details of test procedure for the companion specimens.

3.5.1 Wall Testing

Figures 3.12 (a) and (b) show the front and side views, respectively, of the test setup for the case of a wall specimen with realistic supports. Figure 3.13 shows a photograph of the general test setup for the case of a wall specimen with ideal support conditions. A lateral load was applied to walls in both cases using an MTS hydraulic actuator with a capacity of 250 kN and a maximum static stroke of 264.2 mm. The hydraulic actuator was connected to a spreader beam system which applied two point loads to the wall. The height of the spreader beam system was adjusted for wall specimens of varying heights by raising the MTS hydraulic actuator on its support frame. The hydraulic actuator had to be lifted three times overall: once for each wall height used. The actuator was lifted from 1910 mm for 15-course walls to 2110 and 2310 mm for 17 and 19 course walls, respectively, measured from the top of the laboratory strong floor.

A lateral displacement-controlled static load applied at a rate of 1 mm/min was selected based on previous tests at the University of Saskatchewan. Displacement-controlled loading was deemed to be more appropriate than load-controlled loading because, in the latter case, the actuator would keep the load rate constant as the wall approached failure and, thus, would lead to a sudden collapse of the wall specimens. The sudden collapse was not desired for two reasons: (1) there was the possibility of the test setup getting damaged during the collapse, and (2) the rapid collapse could limit the number of load and displacement data points collected. Load was applied until two conditions were met: (1) a drop in the applied load, and (2) a visible crack in a mortar joint. In most cases the two conditions occurred simultaneously; however in a few cases the load application continued after a drop in the applied load until the crack became visible.

Figure 3.14 shows the details of the spreader beam system which consisted of two horizontal aluminum beams connected to a vertical beam. All three aluminum beams were 1500 mm long

and had the same cross-sectional geometry, as shown in Figure 3.14 (c). The center-to-center distance between the horizontal beams was 1200 mm. Two load cells, as shown in Figure 3.14 (a), were bolted between the horizontal beams and the vertical beam, so that each one of the two applied point loads on the wall specimens were measured and recorded. Hollow steel pipes with a 30 mm diameter, as shown in Figure 3.14 (a), were used as the contact points between the spreader beam system and the wall specimens. Figures 3.15 (a) and (b) show the locations of these steel pipes as placed on the wall specimens during testing. The pipes were not allowed to contact mortar joints during testing, in order to prevent the premature failure of walls due to a concentration of pressure on the mortar joints. Failure was expected to occur in the mortar joints due to the low bond strength between the mortar and the blocks.

Figures 3.16 (a) and (b) show how the bottom supports were bolted to the floor for the ideal and realistic supports, respectively, to prevent slippage of the wall specimens in the direction of load application. In the case of ideal supports, the knife edge component, as shown in Figures 3.16 (a), was bolted through the floor on both ends. In the case of realistic supports, shown in Figures 3.16 (b), a steel beam was placed on top of the concrete beam and bolted through the floor on both ends.

A slight modification was made to the setup of the ideal supports located at the bottom of the wall specimen as compared to the original design by Udey (2014). Figures 3.8 and 3.16 show that the ideal support assembly was raised using 180 mm tall steel beams. This was so that the ideal and realistic supports would have similar heights, to limit the number of times the actuator had to be raised on its support frame and so facilitating the testing process.

Figures 3.17 (a) and (b) show the optoNCDT laser displacement sensor used to measure the lateral displacement of walls at mid-height during testing. The applied load and the mid-height lateral displacement of walls were both measured at a rate of 100 samples per second.

3.5.2 Companion Specimen Testing

The testing procedure for all companion specimens is described in this section. Mortar cubes and three-course prisms were tested in compression for quality control. Bond wrench prisms were tested in flexure for quality control and to compare the resulting flexural tensile strength with those obtained from full-scale walls. These tests are described in the following subsections.

Mortar Cube Tests

Figure 3.18 shows a sample mortar cube tested using the Instron DX 600 Universal Testing Machine. Mortar cubes were tested within 24 hours of the testing of corresponding wall specimens. A compressive force was applied according to CSA A3004-C2 (2008), such that testing took between 20 to 80 seconds for the majority of mortar cubes. The compressive capacity of mortar was recorded using a computer connected to the testing machine.

Concrete Block Tests

Two sets of six concrete blocks were tested according to the requirements of ASTM C140 (2015). The Amsler Beam Bender testing machine was used to test the blocks. Compressive tests were conducted on the first set of blocks in accordance with Clause 7 of the ASTM C140 (2015). Each block was placed on a piece of fiber board and capped with another piece of fiber board to ensure uniform load application. The loading rate for the first half of the testing of each specimen was at a convenient rate. The remaining load was applied within one to two minutes. Absorption tests were conducted on the second set of blocks in accordance with Clause 8 of ASTM C140 (2015). Concrete blocks were immersed in water and weighed as they were suspended in water. They were removed from the water after 24 hours and weighed again to determine their saturated weights. Finally, they were dried in an oven at 110° C for 24 hours and weighed to determine their dry weights.

Three-Course Prism Compressive Tests

Three-course prisms were moved to the Amsler Beam Bender testing machine using the overhead crane in the structural laboratory. Pieces of fiber board were placed both on top and at the bottom of the prisms to ensure uniform load application. All prisms were tested within 24 hours of testing of the corresponding wall specimens. Compressive load was applied during approximately one minute as per requirements of CSA S304 Annex D (2014) until failure.

Bond Wrench Tests

The bond wrench apparatus depicted in Figure 3.19 was developed for previous research that took place at the University of Saskatchewan (Udey 2014). Bond wrench prisms were tested within 24 hours of the corresponding wall specimens. Each prism was placed in the bond wrench apparatus and the bottom block was secured in place. The top block was clamped and connected to the load cell. Load was applied manually over approximately one minute to the point of

cracking of the mortar joint between the two courses. Cracking was observed visually and corresponded to a sudden drop in applied load. The applied load was measured and recorded by the installed load cell that was connected to a computer.

3.6 Summary

The experimental design of the current research program was described in this chapter. Wall and companion specimens were described, and material used in their construction was introduced. The construction and the testing process were discussed for wall and companion specimens. Discussion and conclusions based on the analysis of test results are provided in the following chapter.

Table 3.1: Specifics of Experimental Design of Wall Specimens

Wall Height, (mm)	Number of Courses in Each Wall	Wall Slenderness Ratio	Support Conditions
3000	15	16	Ideal
			Realistic
3400	17	18	Ideal
			Realistic
3800	19	20	Ideal
			Realistic
Note: There were three wall specimens of each kind			

Table 3.2: Correspondence of Walls and Companion Specimens to Mortar Batches

Wall / Three-Course Prism	Lift Number	Mortar Batch/Bond Wrench Prism	Mortar Cube
16I1*	1	B1*	1B1 to 6B1
	2	B10	1B10 to 6B10
16I2	1	B1	1B1 to 6B1
	2	B10	1B10 to 6B10
16I3	1	B2	1B2 to 6B2
	2	B11	1B11 to 6B11
16R1*	1	B2	1B2 to 6B2
	2	B11	1B11 to 6B11
16R2	1	B3	1B3 to 6B3
	2	B12	1B12 to 6B12
16R3	1	B3	1B3 to 6B3
	2	B12	1B12 to 6B12
18I1	1	B5	1B5 to 6B5
	2	B16	1B16 to 6B16

Table 3.2 cont'd: Correspondence of Walls and Companion Specimens to Mortar Batches

Wall / Three-Course Prism	Lift Number	Mortar Batch/Bond Wrench Prism	Mortar Cube
18I2	1	B6	1B6 to 6B6
	2	B17	1B17 to 6B17
18I3	1	B6	1B6 to 6B6
	2	B18	1B18 to 6B18
18R1	1	B4	1B4 to 6B4
	2	B13	1B13 to 6B13
18R2	1	B4	1B4 to 6B4
	2	B14	1B14 to 6B14
18R3	1	B5	1B5 to 6B5
	2	B15	1B15 to 6B15
20I1	1	B7	1B7 to 6B7
	2	B19	1B19 to 6B19
20I2	1	B7	1B7 to 6B7
	2	B20	1B20 to 6B20
20I3	1	B8	1B8 to 6B8
	2	B21	1B21 to 6B21
20R1	1	B8	1B8 to 6B8
	2	B22	1B22 to 6B22
20R2	1	B9	1B9 to 6B9
	2	B23	1B23 to 6B23
20R3	1	B9	1B9 to 6B9
	2	B24	1B24 to 6B24

*Note: I: Ideal Support; R: Realistic Support; B: Batch of Mortar

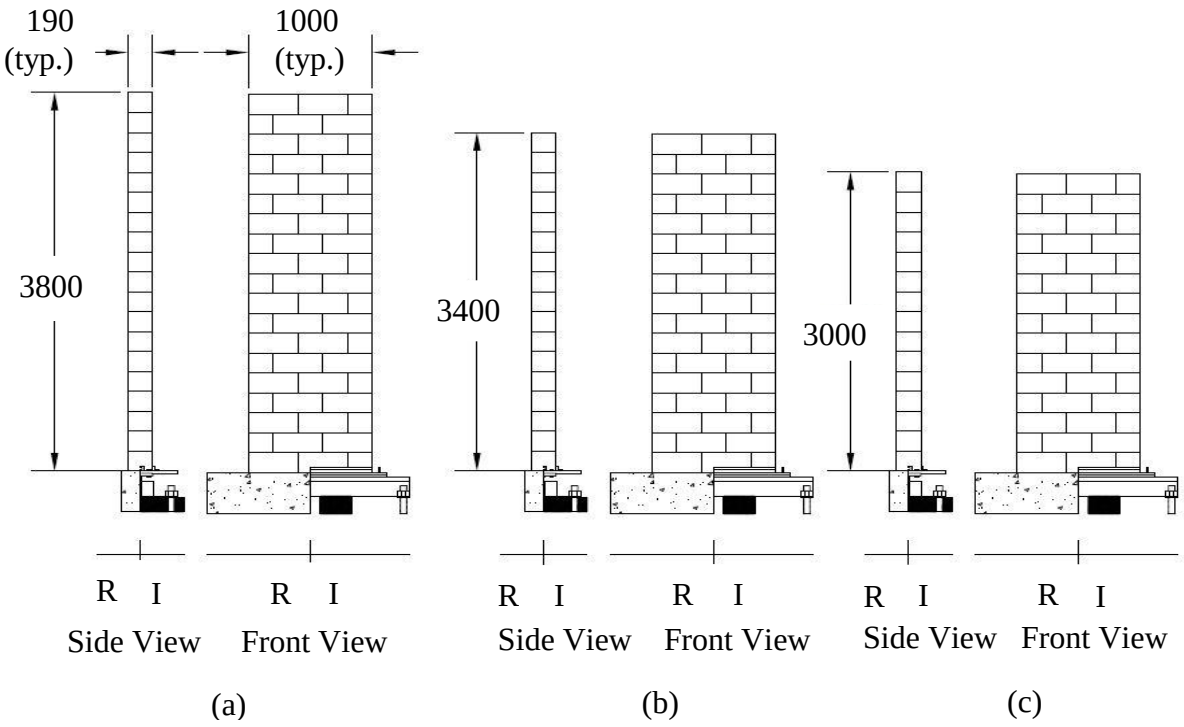

Figure 3.1: Experimental Design of Wall Specimens: (a) 19-Course Walls, (b) 17-Course Walls, and (c) 15-Course Walls (Dimensions in mm)

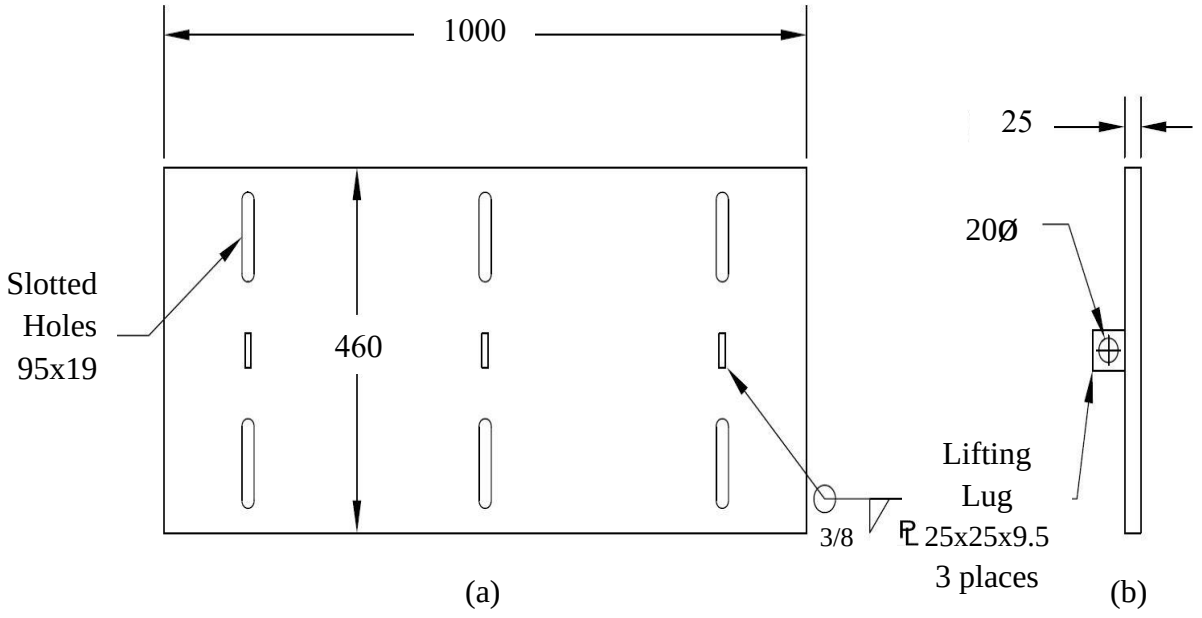

Figure 3.2: Top Support Plate: (a) Top View, and (b) Side View (Dimensions in mm)

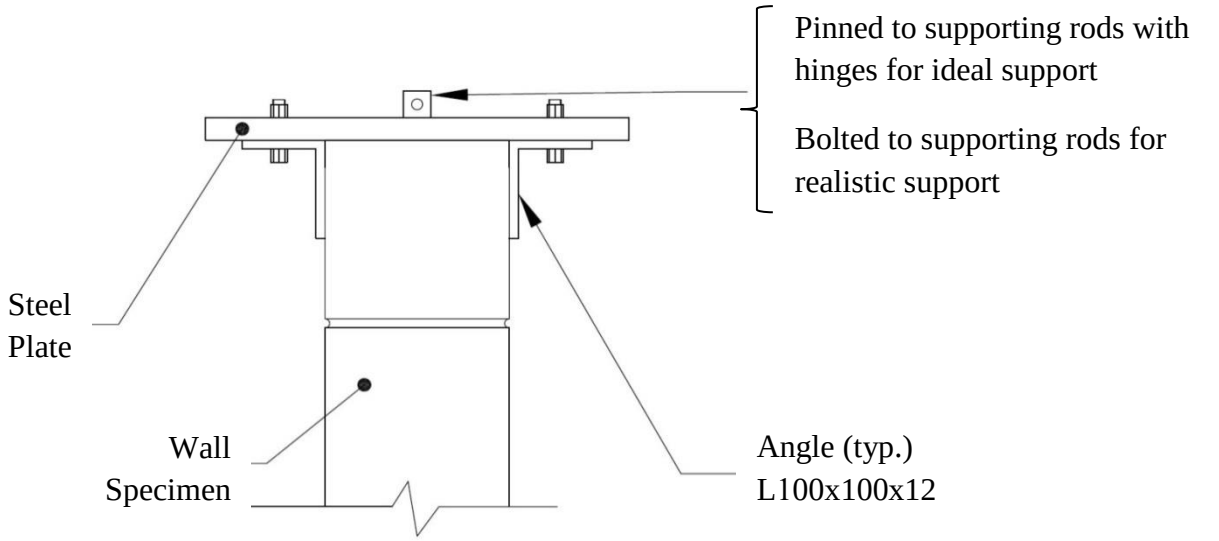

Figure 3.3: Top Support for All Wall Specimens

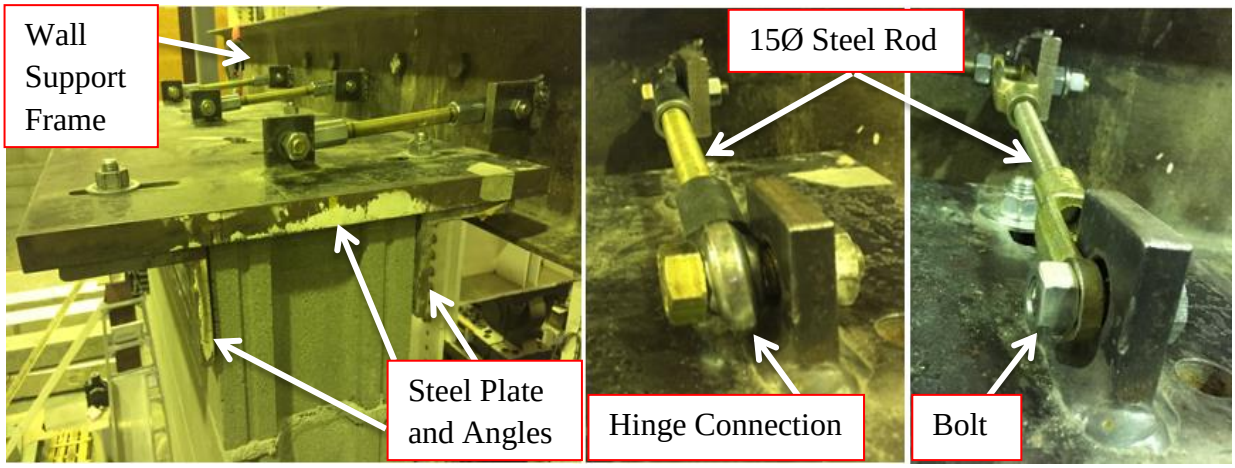

Figure 3.4: Top Support Connection to Steel Rods: (a) Overall Setup of Rods, (b) Steel Rod Pinned to Plate, and (c) Steel Rod Bolted to the Plate

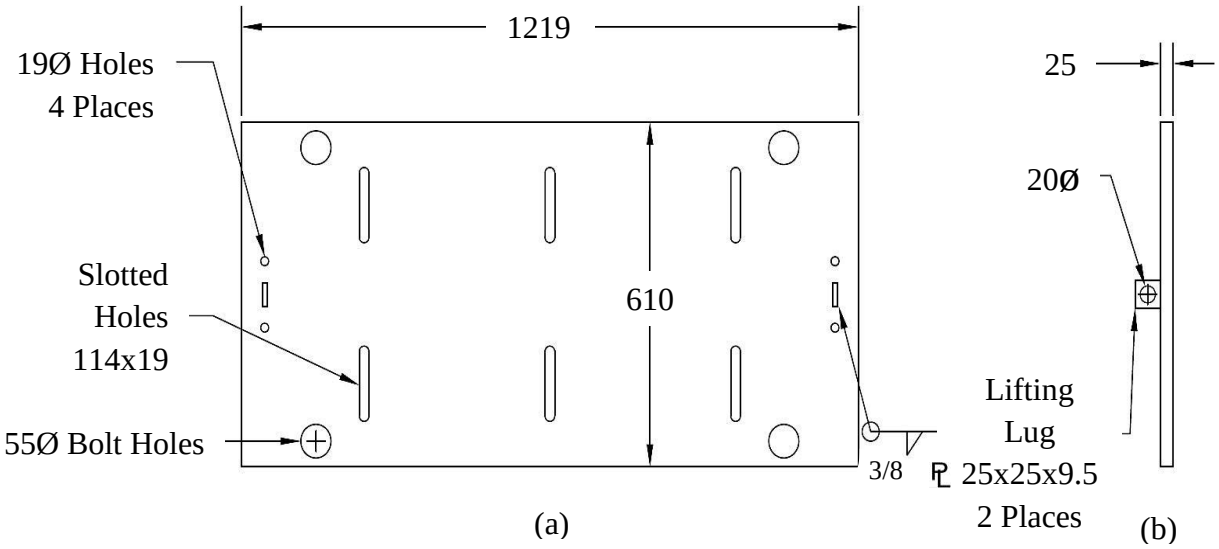

Figure 3.5: Bottom Ideal Support Steel Plate: (a) Top View, and (b) Side View (Dimensions in mm)

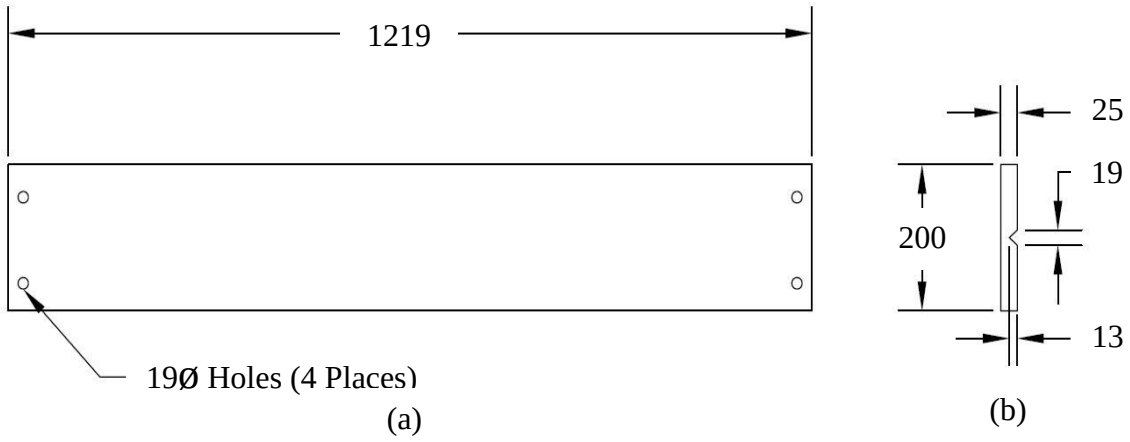

Figure 3.6: Groove Plate: (a) Top View, and (b) Side View (Dimensions in mm)

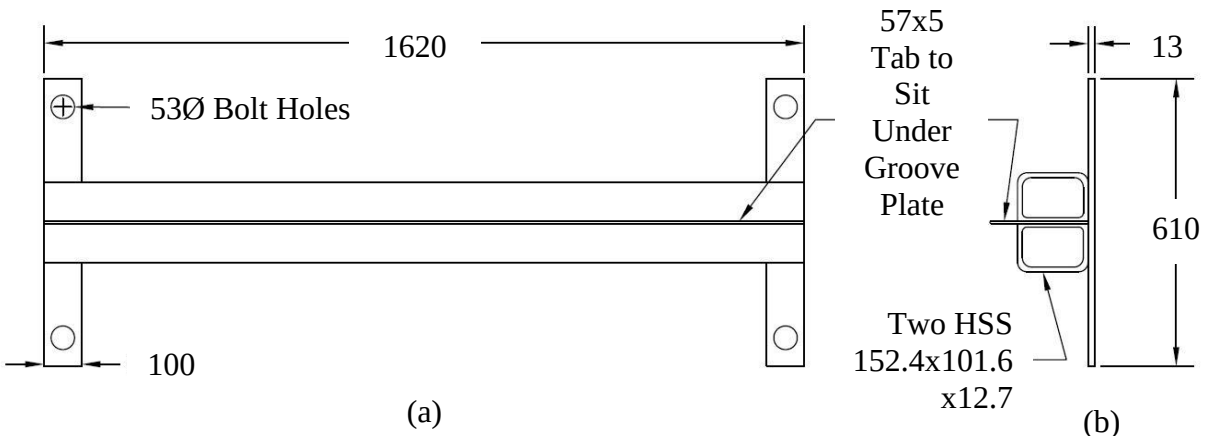

Figure 3.7: Knife Edge: (a) Top View, and (b) Side View (Dimensions in mm)

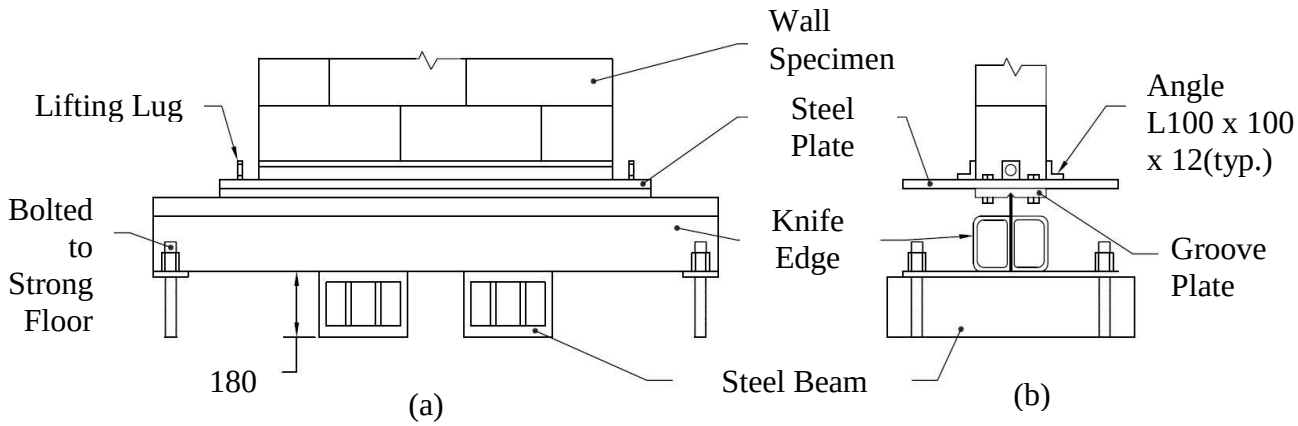

Figure 3.8: Ideal Bottom Support Setup: (a) Front View, and (b) Side View (Dimensions in mm)

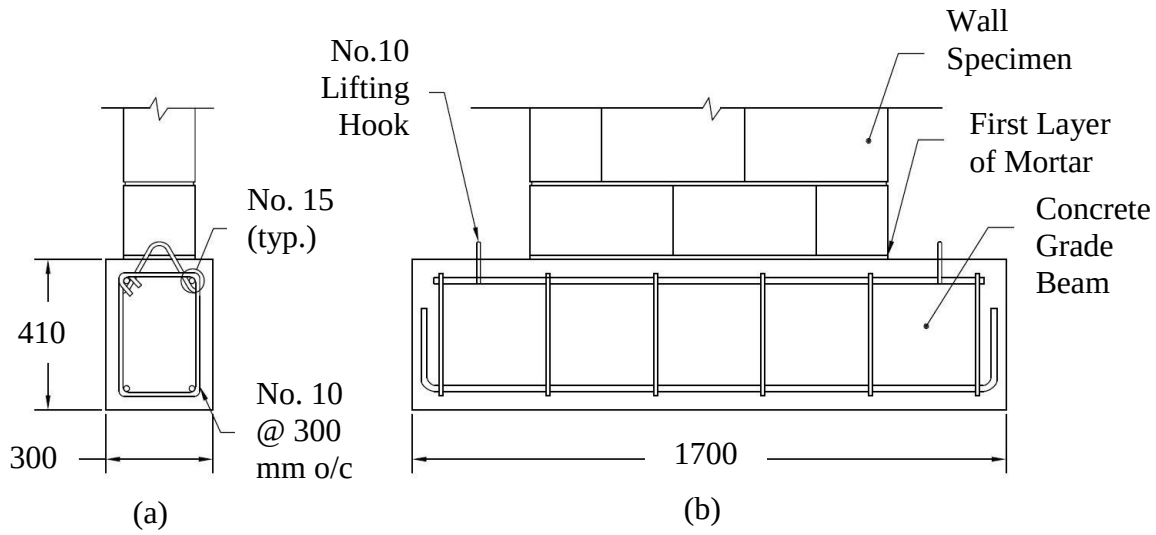

Figure 3.9: Realistic Bottom Support: (a) Side View, and (b) Front View (after Miranda et al. (2016)) (Dimensions in mm)

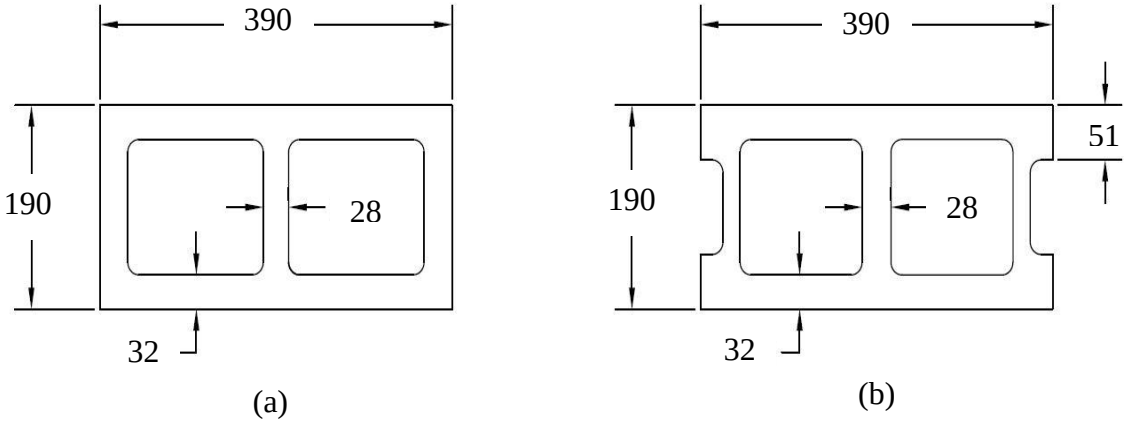

Figure 3.10: Typical Concrete Blocks Used in Construction: (a) Flat- Ended Block, and (b) Frog-Ended Blocks (Dimensions in mm)

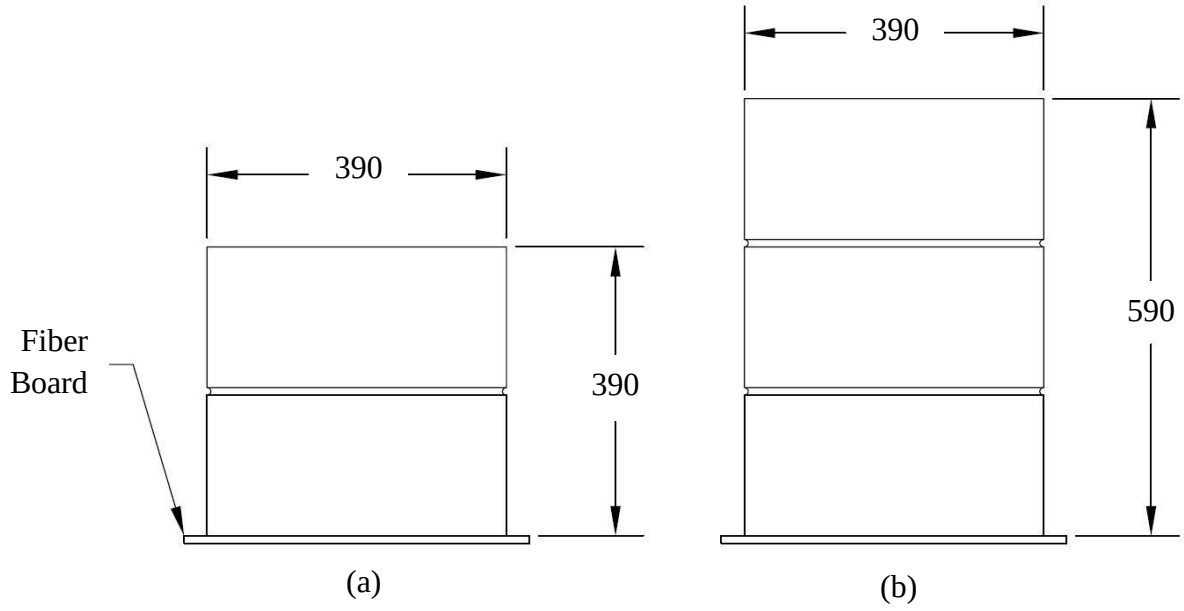

Figure 3.11: Companion Specimens: (a) Bond Wrench Prism, and (b) Three-Course Prism (Dimensions in mm)

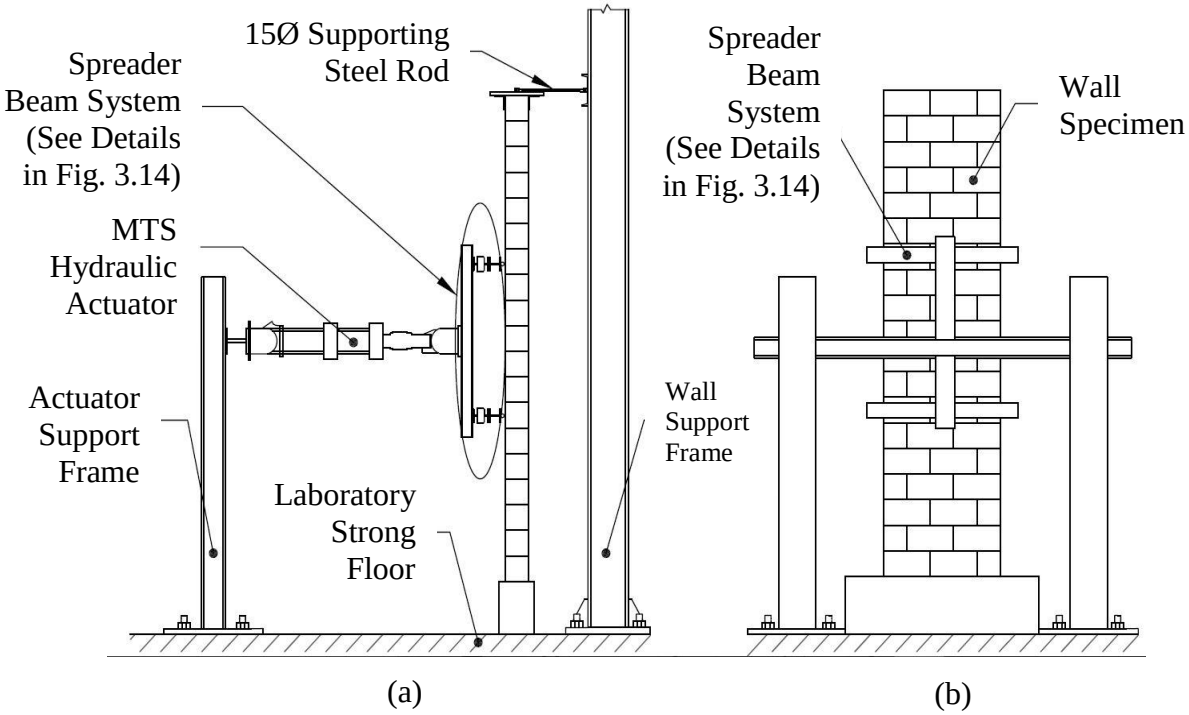

Figure 3.12: Design of Test Frame Setup for Wall Specimens: (a) Side View, and (b) Front View

Figure 3.13: Test Frame Setup for Wall Specimens

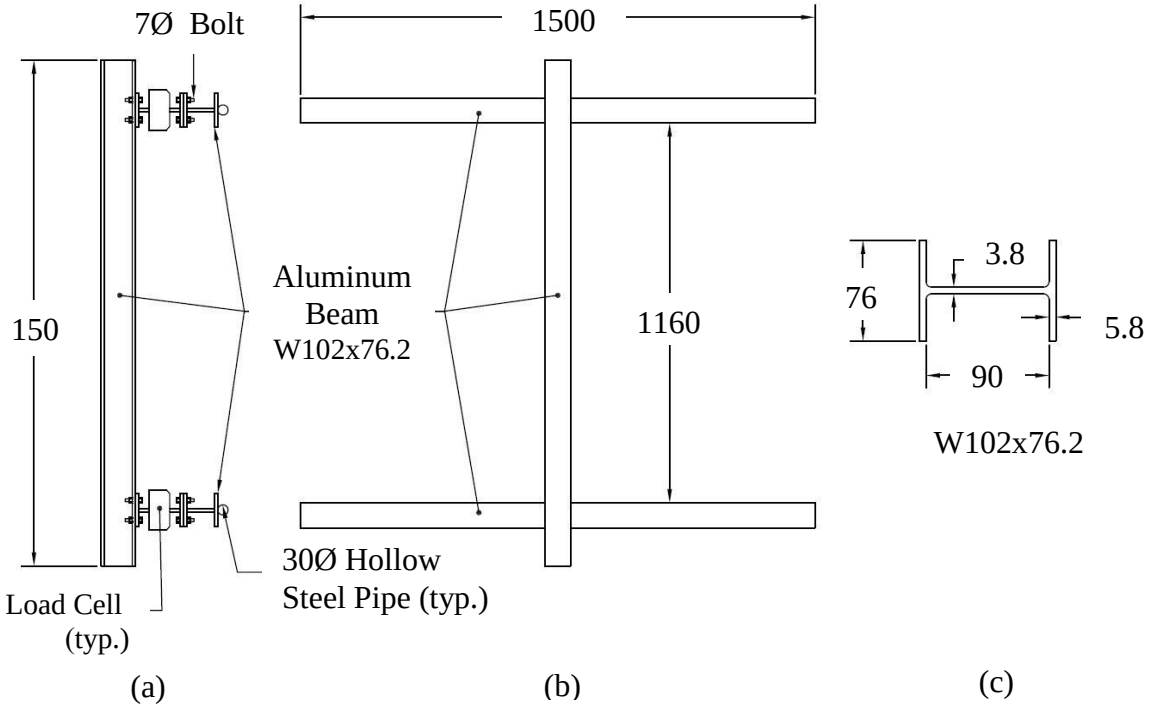

Figure 3.14: Spreader Beam System: (a) Side View, (b) Front View, and (c) Cross-Sectional Dimensions of Aluminum Beams (Not to Scale, dimensions in mm)

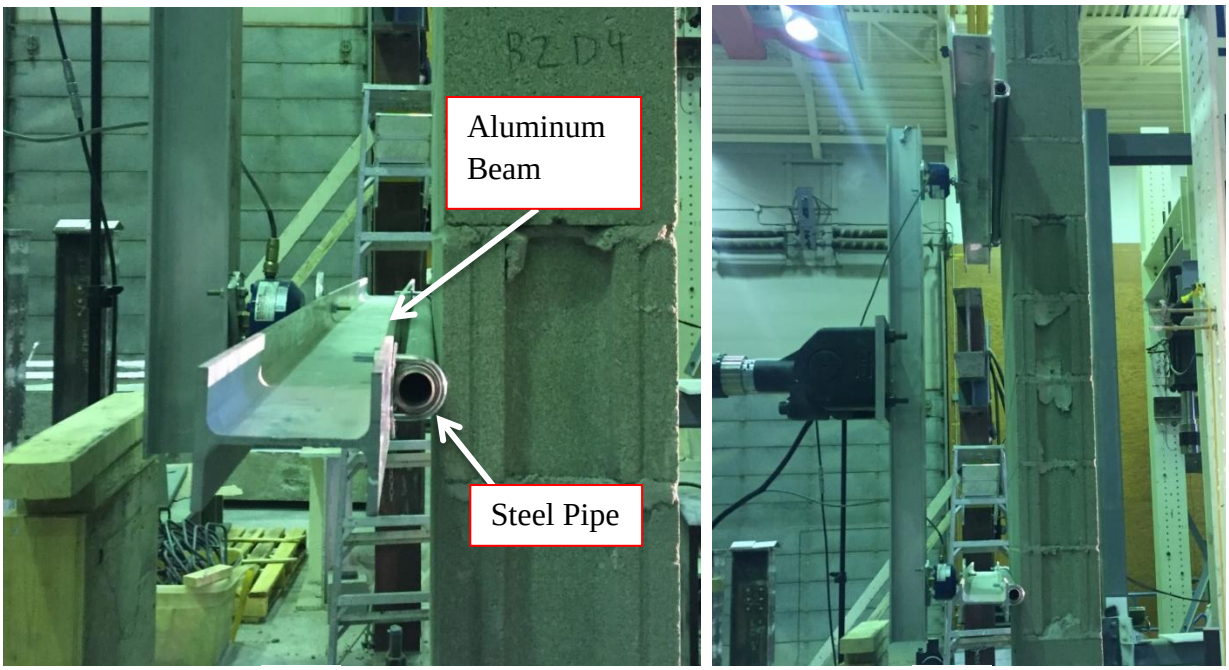

(a) (b)

Figure 3.15: Spreader Beam System Contact Point with Walls (a) Close-up View, (b) Entire Spreader Beam System in Contact with the Wall

(a) (b)

Figure 3.16: Connection of Bottom Support to the Floor for (a) Ideal Support, and (b) Realistic Support

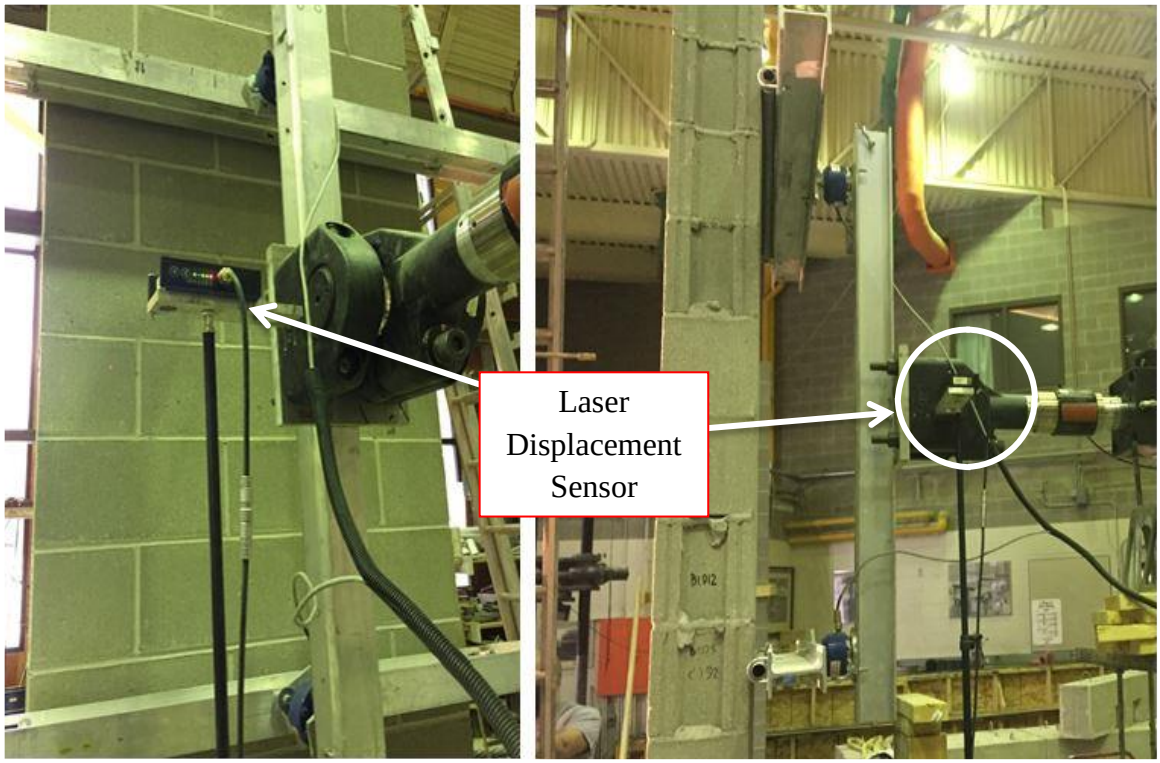

(a) (b)

Figure 3.17: optoNCDT Laser Displacement Sensor in Test Setup: (a) Front View, and (b) Side View

(a) (b)

Figure 3.18: Mortar Cube Test in Progress: (a) View of the Test Machine, and (b) Mortar Cube in Compression

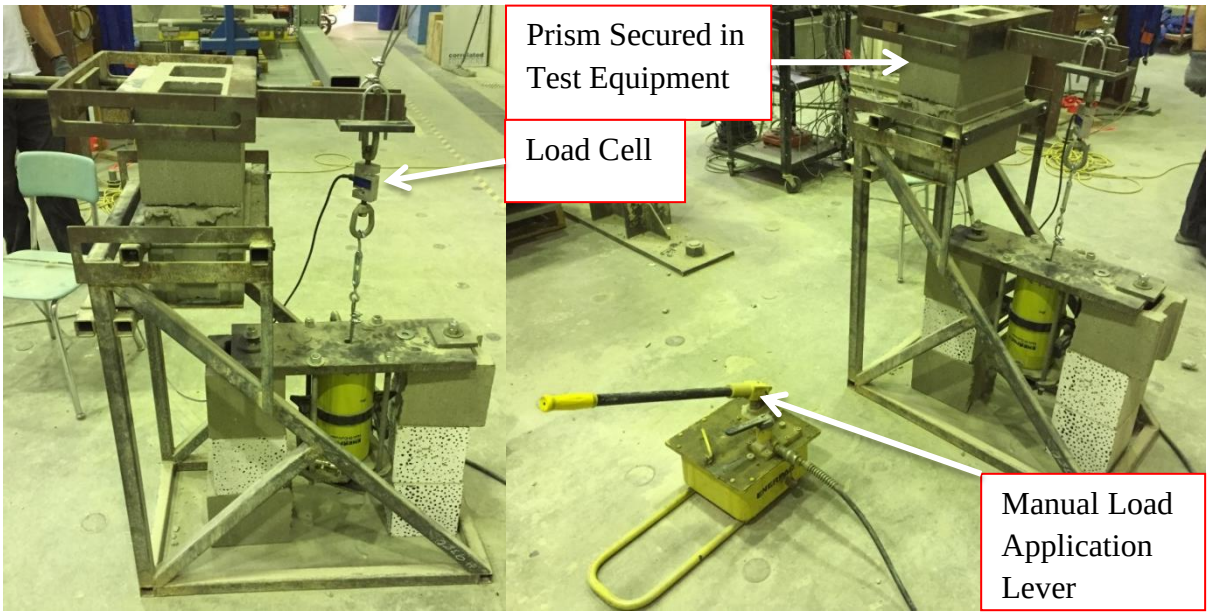

Figure 3.19: Bond Wrench Test Setup

4.0 Analysis and Results

The experimental and analytical results from the current investigation are provided in this chapter. The experimental test results are first provided for the companion specimens and subsequently for the wall specimens. Results are compared to the requirements included in applicable standards and observed trends are discussed. The test database compiled to be used in the reliability analysis is then presented. Subsequently, the reliability analysis conducted to determine the safety of current empirical provisions is described. The procedure to conduct the reliability analysis is presented, followed by the discussion of the resulting reliability indices. Finally, recommendations for changes to the empirical provisions of CSA S304 (2014) are provided based on the results of the reliability analysis.

4.1 Companion Specimens

Results for the companion specimen tests are presented in this section. Results for absorption and compressive tests of concrete masonry blocks are followed by results for compressive tests of mortar cubes, compressive tests of three-course prisms, and bond wrench tests. These tests were included to meet the requirements of CSA S304 (2014) and CSA A179 (2014).

4.1.1 Concrete Masonry Block Tests

Tables A.1 and A.2 in Appendix A show the results for absorption and compressive tests of concrete masonry blocks, respectively, conducted in accordance with ASTM C140 (2015). Table A.1 shows that the average net area of 6 concrete masonry blocks was 4.16×10^4 mm^2 with a coefficient of variation of 1.94%. Table A.2 shows that the average compressive strength of concrete masonry blocks based on the average net area was 20.7 MPa with a coefficient of variation of 14.3%, meeting the requirements of CSA S304 (2014).

4.1.2 Mortar Cube Tests

Table B.1 in Appendix B shows the results for mortar cube tests conducted in accordance with CSA A3004-C2 (2008). The average compressive strength of the 144 mortar cubes was 17.9 MPa with a coefficient of variation of 27.6%. Clause 7.2.2.4 of CSA A179 (2014) requires mortar cubes to have a minimum compressive strength of 12.5 MPa; therefore, the average result of the compressive tests met the minimum requirements. The same clause also requires no individual test result to have a strength less than 10 MPa. Results reported in Table B.1 show that 13 individual test results did not meet this requirement, with the majority belonging to the first

four mortar batches. CSA A3004-C2 (2008) Clause 5.6.2 (c) requires tamping of the mortar in preparation of the cubes to ensure uniform filling of the molds. Observation of the cubes from the first four mortar batches upon unmolding showed that molds were generally not filled uniformly. The reason that the first four batches were affected the most was that the problem of non-uniform filling of molds was identified only after the molding of these batches was completed. The tamping pressure was increased for subsequent mortar batches to correct the problem. It was therefore ensured that mortar cubes for all subsequent material batches were filled uniformly and so the resulting compressive strengths improved such that they exceeded the minimum acceptable level.

4.1.3 Three-Course Prism Compressive Tests

Table C.1 in Appendix C shows the results of the three-course prisms that were tested in compression. The average compressive strength of the 17 prisms tested was 20.5 MPa with a coefficient of variation of 18.4%. One prism cracked during transportation and, therefore, was excluded from the calculation of the average compressive strength. Provisions of Annex D in CSA S304 (2014) require the specified compressive strength of concrete block masonry normal to bed joints to be at least 10 MPa for hollow units for a specified compressive strength of 15 MPa. Clause D.3.2.3 of the same standard requires at least ten specimens to be tested should the coefficient of variation exceed 15%. Therefore, the results of test data show requirements of CSA S304 (2014) are satisfied.

4.1.4 Bond Wrench Tests

Table D.1 in Appendix D shows that the flexural tensile strength of mortar obtained from bond wrench tests of 23 joints was 0.468 MPa with a coefficient of variation of 82.4%. One specimen cracked during transportation and so was excluded from the calculation of the average value. Clauses 9.1.1 and 9.2.4 of CSA A179 (2014) require a flexural tensile strength of at least 0.20 MPa and a minimum of 15 joints to be tested, respectively. The results as reported herein meet both requirements.

Results from specimens B19 and B22, with flexural tensile strengths of 0.970 MPa and 1.97 MPa, respectively, were identified as statistical outliers using a modified Z-Score test (NIST/SEMATECH e-Handbook of Statistical Methods, 2013). The average flexural tensile strength of all specimens was reduced to 0.372 MPa and the coefficient of variation to 45.4%

after the statistical outliers were excluded from the results. Results after the exclusion of the identified outliers are still in compliance with the requirements of CSA A179 (2014).

4.2 Wall Strength

The results for the out-of-plane testing of the unreinforced masonry (URM) walls are discussed in this section. A summary of the results of the experiments is shown in Table 4.1. The table provides the failure joint number and the flexural tensile strength of each wall. The failure joint was invariably located in the maximum moment region with the exception of the specimen 20R1 where it occurred above the maximum moment region. The cause of this anomaly could be potential micro-cracking in the failure joint during the transportation of the wall specimen to the test frame. Although no physical damage was observed in any of the wall specimens prior to testing, such micro-cracking could have gone unnoticed during the inspection of the wall specimens. All failure joints occurred in the interface of the concrete blocks and the mortar. The applied loads were recorded to seven significant digits and reported to three digits for practicality. No statistical outliers were identified in the values of the flexural tensile strength as shown in Table 4.1.

Specimen 16R2 was observed to have the lowest strength. The flexural tensile strength of this specimen was 25.1% of the average value of all specimens and 57.5% of the next lowest flexural tensile strength (i.e. specimen 20R1). Table D.1 shows that mortar batch B12 was used in the failure joint of this wall specimen. The bond wrench specimen constructed with mortar batch B12 was damaged prior to testing, and so the quality of this mortar batch could not be determined from the bond wrench test results. Table B.1 shows, however, that mortar batch B12 performed satisfactorily in the mortar cube test with a resulting compressive strength of 21.7 MPa. There is therefore no evidence indicating that the low flexural tensile strength of wall specimen 16R2 was due to the quality of the mortar used.

Figure 4.1 provides a graphical representation of the flexural tensile strength of all walls versus their respective slenderness ratios. The flexural tensile strength of each wall and the average value for each wall series are presented on the figure. Lines connecting the average values are provided for a better exhibition of changes in these values with increasing slenderness ratios. A statistically significant comparison of the average values of the flexural tensile strength of walls could not be determined, due to the small number of wall specimens in each series. Figure 4.1

shows that the average flexural tensile strength of walls with ideal supports as tested in the current experimental program decreases with increasing slenderness ratio. The same pattern is observed in walls with realistic supports for slenderness ratios of 18 and 20 only. The reason for the low average flexural tensile strength of the 16R wall series is not known. Micro-cracking in the mortar joints, invisible to the unaided eye, that may have occurred during the transportation of the wall specimens could potentially have caused the lower resulting flexural tensile strength in this wall series.

Figure 4.2 shows the relationship between the capacity of walls with realistic supports to those with ideal supports in terms of the moment resistance and flexural tensile strength. The moment resistance here refers to the maximum moment due to the applied load by the actuator before cracking of the wall, as designated by M in Equation 2.1. The flexural tensile strength refers to the maximum tensile stress resisted by the bond in the interface of mortar and masonry blocks, as designated by f_t in Equation 2.1. Walls with realistic supports showed higher flexural tensile strengths than walls with ideal supports with the exception of walls with the lowest slenderness ratio. The better performance of walls with realistic supports compared to walls with ideal supports for slenderness ratios of 18 and 20 is amplified when the capacity is measured in terms of the moment resistance. Figure 4.2 shows that walls with slenderness ratios of 18 and 20 have, respectively, 51% and 44% higher moment resistance in walls with realistic supports than walls with ideal supports. These results are lower than those obtained by Udey (2014) which demonstrated a 63% increase in the moment resistance in walls with realistic supports compared to walls with ideal supports for a slenderness ratio of 16. This may be partially explained by the additional restraint against vertical translation in the upper realistic supports available in Udey's test setup as compared to the test setup in the current investigation. The mitigating effects of moment due to self-weight in walls with realistic supports contribute to the higher resistance ratio shown in Figure 4.2 when strength is measured in terms of moment capacity. A moment resulting from the specimen self-weight was not present in the case of walls with ideal supports, as discussed in Section 2.1.1.

4.3 The Test Database

Table E.1 in Appendix E presents the database comprising the values of flexural tensile strength of unreinforced masonry walls subject to out-of-plane loading. Overall, 167 data points from

nine past investigations were added to the results from the current investigation and classified according to four general parameters: mortar type, slenderness ratio, load application method, and support conditions. This database was required to conduct a reliability analysis for URM walls. The classification of data allowed the impact of each parameter on the reliability index of URM walls to be studied. A description of the composition of the test database as related to the four parameters follows:

(a) Mortar type used in the construction of walls: The mortar type used in the construction of walls included in each investigation was determined and then grouped into one of four categories, as described below. The categorization of data was performed by determining the ratio of cement and aggregate in the mortar mix used in each investigation and comparing it to Tables 3 and 4 of CSA A179 (2014). The resulting mortar type categories are:

   i. N/S PCL: Mortar made with Type N or Type S Portland, Portland limestone, or blended cement.
   ii. N/S Masonry/Mortar: Type N or Type S mortar, where it was not possible to distinguish between masonry or mortar cement mortar due to limited available information. This category was not considered when reliability indices were calculated based on mortar type, because the results would not clearly correspond to any mortar specifications included CSA A179 (2014). The test data in this category were, however, considered when reliability indices were calculated for other parameters such as support conditions or slenderness ratio.
   iii. S Masonry: Type S masonry cement mortar.
   iv. S Mortar: Type S mortar cement mortar.

(b) Average slenderness ratio of walls: Walls were grouped into three categories such that the coefficient of variation of the vertical span length for each category would be minimal to improve the accuracy of results for the reliability analysis. The average slenderness ratio in each category was calculated and used in the reliability analysis. Table E.1 in Appendix E shows both the actual slenderness ratio of each wall and the rounded average value as referred to in the reliability analysis. Only walls constructed using 190 mm thick concrete blocks were considered to eliminate the potential effects of wall thickness on the flexural tensile strength of walls. The following are the three slenderness ratio categories included in the test database:

i. Walls with an average slenderness ratio of 12: All walls in this category had a span length equal to 2.29 m resulting in a slenderness ratio equal to 12.0.
ii. Walls with an average slenderness ratio of 16: The wall span length in this category ranged between 2.8 m to 3.0 m (i.e. slenderness ratios between 14.7 to 15.8). The resulting coefficient of variation of span length was equal to 2.16%.
iii. Walls with an average slenderness ratio of 19: All data in this category were obtained from the current experimental program as shown in Section 4.2. Wall span lengths ranged from 3.4 m to 3.8 m (i.e. slenderness ratios between 17.9 to 20.0). The resulting coefficient of variation of span length was equal to 5.80 %.

(c) The load application method used in wall tests: The load application method for individual wall specimens is shown in Appendix E. Three categories of load application method were included in the test database:
i. Uniform load: The majority of walls in the past investigations were tested under uniformly distributed lateral loading which was applied using an air bag.
ii. Point load: This category includes walls that were tested under point loading. Point loads were applied at the quarter points of each wall span except for results reported by Richart (1932) in which loads were applied at the third points of the span.
iii. Corrected point load: The values of the flexural tensile strength obtained from walls subject to point loading were multiplied by a factor of 1.97 as per recommendations of Kim and Bennett (2002). This category was included to study whether the correction factor proposed by past researchers was sufficient in adjusting the reliability indices obtained from walls tested under point loading to the same levels as those tested under uniform loading.

(d) Support conditions: As shown in Appendix E, all past investigations were conducted using wall specimens with ideal support conditions with the exception of Udey (2014) and the current investigation in which walls were constructed using realistic support conditions. A description of the two support types was presented in Section 2.1.1.

4.4 Reliability Analysis

This section presents the analysis performed using a Monte Carlo simulation to determine the reliability index for the flexural tensile strength of unreinforced concrete block walls. A general summary of the method used to conduct the reliability analysis is first introduced. Random and

deterministic variables used in the analysis are then discussed. The probability distribution function (PDF) for each random variable is provided and the goodness-of-fit of the PDFs to the data in the test database is examined. Finally, a discussion of the resulting reliability indices is presented followed by recommendations for changes to the empirical provisions of CSA S304 (2014).

4.4.1 Method

This section presents the steps taken to calculate reliability indices using the Monte Carlo simulation. Equations used in the simulation are provided and the included random and deterministic variables are introduced. Methods used to calculate the probability of failure and the reliability index are presented. The equation used to evaluate the coefficient of variation of the probability of failure is then presented as a means to determine the accuracy of the simulation.

The unfactored rational design equation relating the load effects and the resistance of walls, shown as Equation 4.1, was used as the limit state function in the reliability analysis. In Equation 4.1, M is the moment due to applied load on the wall, M_{sw} is the moment due to self-weight present only in walls with realistic supports as explained in Section 2.1.1, S is the elastic section modulus, W_{half} is the self-weight of the top half portion of the wall under investigation, A_e is the effective cross-sectional area as per Clause 2.3.2 of CSA S304 (2014), and f_t is the flexural tensile strength:

$$\frac{M - M_{sw}}{S} - \frac{W_{half}}{A_e} \leq f_t \tag{4.1}$$

The applied moment, M, due to the wind pressure, p, applied uniformly on the wall span, l, was determined using Equation 4.2:

$$M = \frac{pl^2}{8} \tag{4.2}$$

The wind pressure, p, was calculated using Equation 2.2 and the variables were introduced in Section 2.1.1.

The wind velocity pressure was determined using Equation 4.3, where ρ is the air density taken as 1.2929 kg/m^3, and v is the annual maximum wind speed:

$$q = \frac{1}{2}\rho v^2 \tag{4.3}$$

The variables included in the aforementioned equations were treated as either random or deterministic based on the availability of the probability distributions of variables and their respective coefficients of variations. Variables with coefficients of variation below 5% were considered to be deterministic as per recommendation of Bartlett et al. (2003). The probability distributions of the annual maximum wind speed and the wind pressure coefficient, $C_e(C_pC_g + C_{pi}C_{gi})$, were based on the works of Hong et al. (2013) and Bartlett et al. (2003), respectively. The probability distributions of the flexural tensile strength of masonry walls were calculated in the present investigation based on the recommendations of Kim and Bennett (2002) and Ellingwood et al. (1980). A discussion of the probability distributions of the random variables is provided in Section 4.4.2. Random numbers were generated using a Matlab (Version R2017a) built-in pseudo-random-number generator from the probability distribution functions of their respective variables. The following were considered to be random variables:

a. The annual maximum wind speed, v.
b. Wind pressure coefficient, $C_e(C_pC_g + C_{pi}C_{gi})$.
c. Flexural tensile strength of wall specimens, f_t, as reported in Table E.1.

The variables listed below were treated as deterministic variables:

a. The air density, ρ, which has a coefficient of variation below 5% and, thus, would not have a significant impact on the results (Bartlett et al., 2003).
b. The variables $S, h, A_e,$ and W_{half}, which are functions of the dimensions and density of the concrete blocks. The maximum coefficients of variation of the height, length, and width of blocks are all below 2% based on the limits provided by Clause 7.1 of CSA A165.1 (2014). The coefficients of variations of the volume and density of blocks obtained from absorption tests were 1.94% and 1.72%, respectively, as shown in Appendix A.
c. The importance factor, I_w, was taken as 1.0, and so corresponded to a normal importance category.

Equation 4.1 was evaluated by inputting the random numbers generated from the probability distribution functions in the equation. If the sum of all terms on the left hand side of the equation

was larger than the value of the flexural tensile strength, f_t, as shown on the right hand side of the equation, a failure was recorded. The total number of responses, N, and the number of responses in which the system failed, N_f, were then used to determine the probability of failure, P_f, using Equation 4.4:

$$P_f = \frac{N_f}{N} \tag{4.4}$$

The reliability index, β, was calculated using Equation 4.5, where Φ is the standard normal cumulative distribution function:

$$\beta = \Phi^{-1}(1 - P_f) \tag{4.5}$$

The coefficient of variation of the probability of failure, COV_{P_f}, was estimated using Equation 4.6 (Ayyub & McCuen, 2003). The coefficient of variation was determined as a measure of the statistical accuracy of the resulting reliability indices, signifying the degree of confidence by which the results of the Monte Carlo simulation could be interpreted (Melchers and Beck, 2018):

$$COV_{P_f} = \frac{\sqrt{\left(\frac{P_f(1 - P_f)}{N}\right)}}{P_f} \tag{4.6}$$

4.4.2 Probability Distribution Functions

Probability distribution functions (PDF) for wind speed, wind pressure coefficient, and the flexural tensile strength of walls were determined based on the information available in the literature. The details of these PDFs, including their sources and the data used in developing them are presented in the following paragraphs.

Annual Maximum Wind Speed

Figure 4.3 shows the probability distribution functions for the annual maximum wind speed for 14 locations in Canada (Hong et al., 2013). At least 34 years of data for the capitals of all provinces and territories, in addition to Ottawa, were used to develop the probability distribution functions. A Gumbel distribution is the most commonly used distribution to model extreme wind speeds and, thus, was used in the current investigation (Ellingwood et al. 1980, Kim and Bennett, 2002, Bartlett et al., 2003, Hong et al., 2013). The parameters of these distributions and the 50-

year wind pressures for each location are shown in Table 4.2. It is generally observed in Figure 4.3 that the cities with the higher 50-year wind pressure, as shown in Table 4.2 (e.g. St. John's, NL and Iqaluit, NU) exhibit higher variability in the annual maximum wind speed. The annual maximum wind speeds were converted into 50-year values to meet the requirements of CSA S304 (2014) using Equation 4.7 (Melchers and Beck, 2018); where $F(v)_{50}$ refers to the cumulative distribution function (CDF) of the 50-year wind speed, and $F(v)$ corresponds to the CDF of the annual maximum wind speed:

$$F(v)_{50} = F(v)^{50} \tag{4.7}$$

Flexural Tensile Strength of Wall Specimens

Figure 4.4 shows the lognormal probability distribution functions for the flexural tensile strength of walls plotted for categories introduced in Section 4.3. Table 4.3 shows the parameters of each of the probability distributions shown in Figure 4.4. The table also shows the number of available data points for each of the investigated categories. The parameters shown in Table 4.3 were obtained by fitting a lognormal distribution to the data available in Appendix E using Matlab (Version R2017a). A lognormal distribution was selected to model the flexural tensile strength of masonry in accordance with past research (Ellingwood et al., 1980). Kim and Bennett (2002) showed that a lognormal distribution generally provides a better fit than normal and Weibull distributions for the flexural tensile strength of full-scale masonry walls. Kim and Bennett (2002) also stated that using different probability distributions could alter the resulting reliability indices significantly. They suggested, with reference to Gromala et al. (1990), that the lognormal probability distribution be used to model the resistance of masonry walls even in cases for which this distribution is not the best fit to the data. This ensures that the reliability indices obtained from different investigations can be reasonably compared.

Wind Pressure Coefficient

Figure 4.5 shows the probability distributions of the wind pressure coefficient, $C_e(C_pC_g + C_{pi}C_{gi})$. The PDFs were plotted for both buildings with significant openings and sealed buildings as explained in Section 2.1.1 The probability distributions shown in Figure 4.5 were plotted for walls with a slenderness ratio of 12 assuming a lognormal distribution, a bias factor of 0.68, and a coefficient of variation of 0.22, based on a comprehensive review of research on the wind

pressure coefficients by Bartlett et al. (2003). Probability distributions of the wind pressure coefficients corresponding to slenderness ratios other than 12 were used in the reliability analysis when required.

In calculating the overall wind pressure coefficients according to the National Building Code of Canada, NBCC (2015), C_e was taken as $\left(\frac{h}{10}\right)^{0.2} \leq 0.9$, $C_p C_g$ was conservatively taken as 1.65, assuming a maximum wall span equal to 3.8 m for a meter-wide strip of wall. The product of the internal pressure coefficient and the gust effect factor, $C_{pi}C_{gi}$, was taken as 1.4 for buildings with significant openings and zero for sealed buildings. Open terrain, as opposed to rough terrain, was assumed to maximize the value of C_e, and thus the wind pressure, p, acting on the walls.

4.4.3 Goodness of Fit

The Anderson-Darling test was selected to determine the goodness of fit of the PDFs shown in Figure 4.4. The Anderson-Darling test is a modified version of the Kolmogorov-Smirnov test, such that in the Anderson-Darling test the critical values are calculated taking into account the specific PDF under analysis (NIST/SEMATECH e-Handbook of Statistical Methods, 2013). Thus, the Anderson-Darling test is a particularly useful goodness-of-fit test method for structural reliability where different kinds of PDFs are used to model each variable (Kim and Bennett, 2002).

In the current analysis, the Anderson-Darling test was conducted using built-in functions in Matlab (Version R2017a). The results of the Anderson-Darling test are presented in Table 4.4. The second column of the table shows the Anderson-Darling test results based on the significance levels shown in the third column of the table. The null hypothesis in this test was that the values in the test database belonged to their respective lognormal distributions as presented in Table 4.3. The null hypothesis was rejected when the significance level of the data fell below 0.05, a value commonly used and recommended by Kim and Bennett (2002). Table 4.4 shows that the null hypothesis was rejected for three cases: ideal supports; point loads; and corrected point loads. The corrected point load and the point load data both result in a significance level of 0.0445: just below the 0.05 threshold. The ideal support data, however, resulted in a significance level of 0.0238.

Results from the Anderson-Darling test could be significantly affected if a small number of data points exhibit large departures from the distribution, even when the majority of the data fit well to the distribution. Probability plots were used to determine whether a few data points were causing the three categories discussed above to fail the Anderson-Darling test. Probability plots are useful tools to inspect the goodness-of-fit as they graphically demonstrate the departures of individual data points from the prescribed PDFs. The PDF under investigation is graphed as a straight line in a probability plot and the deviation of data points from the straight line signifies the degree of departure from the PDF (NIST/SEMATECH e-Handbook of Statistical Methods, 2013).

Figures 4.6 to 4.8 show the probability plots for the categories of ideal support, point load, and corrected point load. Figure 4.6 shows significant departures of data points from the lognormal PDF both at the extreme ends and the middle range of the values of flexural tensile strength. It was therefore concluded that the prescribed lognormal probability distribution did not fit well to the values of the flexural tensile strength of walls with ideal supports. Figures 4.7 and 4.8 both show that the majority of data points do follow the lognormal PDF closely except for the five data points in the lower range of the values of the flexural tensile strength. It was therefore concluded that the prescribed lognormal distributions fit well to the data for the two categories of point load and corrected point load, considering that the significance level obtained for these categories in the Anderson-Darling test were just below the threshold.

Despite the poor fit of the lognormal distribution to data in the category of ideal supports, it was decided to nonetheless continue with a lognormal PDF for this category. The reason for this was twofold:

1) As seen in Table 4.4, results from the Anderson-Darling test indicate that a lognormal distribution fits well to data for 9 out of 12 categories. A graphical examination of the probability plots of the three categories failing the Anderson-Darling test shows that two of the failing categories do follow lognormal PDF closely. A lognormal PDF, therefore, is an appropriate choice for the majority of categories in the current investigation.
2) As stated previously, past researchers (Ellingwood et al., 1980, Kim and Bennett, 2002) have used the lognormal PDF to model the flexural tensile strength of unreinforced

masonry walls. The use of a different PDF may have significant effects on the resulting reliability indices and, thus, make a comparison of results difficult.

4.4.4 Reliability Indices

Reliability indices obtained for URM walls subject to out-of-plane loading are presented in the following sections. Average reliability indices for the investigated parameters shown in Table 4.3 are presented in Section 4.4.4.1. The impact of 50-year wind pressures on the reliability indices are investigated in Section 4.4.4.2. All reliability indices were calculated for the two cases of building openings specified by NBCC (2015) and described in Section 2.1.1: sealed buildings, and buildings with significant openings. Calculations resulting in $\beta < 0$ were set equal to zero, since negative values of the reliability index are not meaningful, but result for cases where the probability of failure exceeded 50%.

4.4.4.1 Reliability Indices for Categories of Flexural Tensile Strength

Figures 4.9 to 4.12 show the reliability indices obtained for the investigated parameters as shown in Table 4.3. A reliability index of 2.5, corresponding to a probability of failure equal to 0.00621, was marked by a vertical dashed line on these figures signifying the minimum acceptable reliability index as per the recommendations of Ellingwood et al. (1980) and Kim and Bennett (2002). Figures 4.9 to 4.12 allow for the impact of different parameters included in the test database to be evaluated with the resulting reliability indices. A summary of these results and a discussion based on the results are presented in the following paragraphs.

Figure 4.9 shows the reliability indices of the flexural tensile strength of unreinforced masonry walls within the three prescribed slenderness ratio categories: 12, 16 and 19. The figure shows that only walls with a slenderness ratio of 12 in sealed buildings have a reliability index above 2.5. Walls with slenderness ratios of 16 and 19 in both sealed buildings and those with significant openings, and walls with a slenderness ratio of 12 in buildings with significant openings result in reliability indices lower than 2.5. Figure 4.9 shows that reliability indices decrease with increasing slenderness ratios for both sealed buildings and buildings with significant openings. This trend should be considered with caution: Table 4.3 shows that there were 102, 41 and 12 data points included in the reliability analysis of walls with slenderness ratios of 12, 16 and 19, respectively. Fewer data points are an indication of data originating from fewer sources. The coefficient of variation of all values of flexural tensile strength included in

Appendix E is 87.5%, indicating that any one investigation may not be a good representation of the flexural tensile strength of unreinforced masonry walls. Therefore, the database of walls with slenderness ratios of 16 and 19 should be expanded with results then re-evaluated.

Figure 4.10 shows the reliability indices for URM walls subject to out-of-plane loading for the three categories of load application method: point load, corrected point load, and uniform load. The figure shows that the resulting reliability index is higher than 2.5 for walls subject to uniform loading for both sealed buildings and buildings with significant openings. A correction factor of 1.97 applied to the flexural tensile strength of walls subject to point loading improves the reliability indices from 0.30 and 1.36 to 1.10 and 2.28 for buildings with significant openings and sealed buildings, respectively. The higher reliability indices obtained for walls subject to uniform loading compared to walls subject to point loading and the improvement of results after the application of the correction factor, as described in Section 2.2.7, are in accordance to the findings of Monk (1954) and NCMA (1967) as reported by Kim and Bennett (2002). Results shown in Figure 4.10 may be affected by other parameters included in the test database when either of the load application methods was implemented, including slenderness ratio and mortar type, and so should be interpreted accordingly.

Figure 4.11 shows the reliability index for the flexural tensile strength of unreinforced masonry walls based on the mortar type used in wall construction. The figure shows that walls constructed with all mortar types result in reliability indices higher than 2.5 with the exception of Type S mortar cement mortar and Type N PCL in buildings with significant openings. Results for Type N PCL mortar were included for comparative purposes and show that these walls have lower reliability indices than those constructed with Type S PCL mortar. As explained in Section 2.2.1, the performance of Type S PCL mortar in unreinforced masonry walls is expected to be similar to that of Type S mortar cement mortar and that they are both expected to result in higher values of flexural tensile strength than Type S masonry cement mortar (Laird, 2013). This is not, however, reflected in the reliability indices shown in Figure 4.11.

The results shown in Figure 4.11 may be affected by the composition of the test database used to perform the reliability analysis for each mortar type. Test data for walls constructed using Type S masonry cement mortar have a coefficient of variation of 41.2% with ninety one percent of the data belonging to tests performed by NCMA (1997). Results from NCMA (1994, 1997) show the

highest flexural tensile strength of all works considered. Al-Menyawi (2001) stated that the high values of the flexural tensile strength obtained by NCMA (1994, 1997) were due to the high quality control implemented in the construction of wall specimens in the two investigations. In contrast, data for Type S PCL mortar come from 5 different research programs between 1932 and 1994 and result in a coefficient of variation equal to 53.0%. An expansion of the test database as related to Type S masonry cement mortar could provide a more realistic value for the resulting reliability index. The low reliability indices obtained for walls constructed using Type S mortar cement mortar could also be explained by the composition of its database compared to other mortar types. All data for Type S mortar cement mortar result from investigations where walls were subject to point loading. Walls constructed with Type S masonry cement mortar were only tested under uniform loading and walls constructed with Type S PCL mortar were subject to both uniform and point loading. It was shown in Figure 4.10 that data from experiments implementing point loading could lead to lower values of reliability index. In addition, the average slenderness ratio of walls constructed with Type S mortar cement mortar is 17, while this value was about 12 for both Type S PCL and masonry cement mortars. It was shown in Figure 4.9 that higher slenderness ratios result in lower reliability indices.

It is therefore observed that other parameters affecting the flexural tensile strength of URM walls, such as the slenderness ratio and the load application method, differ in the database of different mortar types. It is not possible to compare the reliability indices of walls constructed using different mortar types until the database of different mortar types can be expanded. Data from additional investigations are needed specifically for the improvement of the databases of Type S mortar and masonry cement mortars.

Figure 4.12 shows the reliability index of unreinforced masonry walls subject to out-of-plane loading with either ideal or realistic supports. The figure shows that walls with both ideal and realistic supports have reliability indices lower than 2.5 for sealed buildings and buildings with significant openings. The lower reliability indices obtained for walls with realistic supports in comparison with those with ideal supports can be explained using the same reasoning as before: data for walls with realistic supports belong to only two investigations (Udey, 2014 and the current experiment) with all walls subject point loading. It was shown in Figure 4.10 that point-loaded walls generally produced conservative results. In addition, walls with realistic and ideal

supports have average slenderness ratios of 17 and 13, respectively. It was shown in Figure 4.9 that the slenderness ratio was inversely proportional to the reliability index. Therefore, a comparison of the two categories of support types is not possible until the database of walls with realistic supports is expanded.

In summary, studying the reliability indices for the flexural tensile strength of unreinforced masonry walls based on the available test database in terms of the four parameters of slenderness ratio, load application method, mortar type, and support condition resulted in the following conclusions:

- Reliability indices consistently lower than 2.5 were resulted for walls with slenderness ratios equal to or greater than 16.
- Walls subject to point loading, as opposed to uniform loading, resulted in lower values of reliability indices. Additionally, walls with realistic support conditions, as opposed to ideal support conditions, and those constructed with mortar cement mortar, as opposed to masonry and Portland cement mortars, resulted in lower values of reliability indices.
- The results of the reliability analysis should be interpreted with consideration of the limitations in the size and composition of the test database. The available test database should be expanded for the effects of the investigated parameters on the resulting reliability indices to be determined independently.

4.4.4.2 Reliability Indices vs. 50-Year Wind Pressures

Table 4.5 presents the results of the reliability analysis for the investigated parameters as related to the 50-year wind pressures. Columns two and three of the table show the reliability indices for a 50-year wind pressure of 0.55 kPa. These reliability indices show the level of safety of the current empirical provisions based on the available data for both sealed building and buildings with significant openings. The final two columns of the table show what the maximum allowable 50-year wind pressure must be if a reliability index of at least 2.5 is dictated. The terms “None” and “All” in the table indicate, respectively, that none and all of the investigated 50-year wind pressures resulted in a minimum reliability index of 2.5. The information presented in Table 4.5 is obtained from Figures 4.13 to 4.23. These figures present the reliability indices for categories of flexural tensile strength versus 50-year wind pressures. Two dashed lines on the figures are shown: a horizontal line corresponding to a reliability index of 2.5 to mark the minimum

acceptable reliability index as per the recommendations of Ellingwood et al. (1980) and Kim and Bennett (2002), and a vertical line marking a 50-year wind pressure of 0.55 kPa signifying the maximum allowable wind pressure permitted for use with the empirical provisions of CSA S304 (2014). Figures 4.13 to 4.23 also show the average reliability index and the corresponding average coefficient of variation. A summary of observations based on Table 4.5 for each one of the investigated parameters is provided in the following subsections.

Slenderness Ratio

Table 4.5 shows that walls with a slenderness ratio of 12 have reliability indices below 2.5 for a 50-year wind pressure of 0.55 kPa. Current empirical provisions result in reliability indices lower than 0.48 for walls with slenderness ratios of 16 and higher and reliability indices of 1.56 and 2.44 for walls with a slenderness ratio of 12 in buildings with significant openings and sealed buildings, respectively. Therefore, the available test database results in unacceptable levels of reliability indices for walls with slenderness ratios equal to and greater than 16. Additionally, walls with a slenderness ratio equal to 12 subject to 50-year wind pressures greater than 0.29 kPa for buildings with significant openings and 0.53 kPa for sealed buildings result in unacceptable levels of reliability indices. Among the cities considered, only Yellowknife, NT, and Fredericton, NB, have a prescribed 50-year wind pressure equal to or lower than 0.29 kPa, while all cities considered have a prescribed 50-year wind pressure equal to or lower than 0.53 kPa except Iqaluit, NU, Halifax, NS, and St. John's, NL.

Load Application Method

Table 4.5 shows that the walls subject to uniform loading result in reliability indices higher than 2.5 for 50-year wind pressures up to 0.60 kPa in the case of buildings with significant openings and for all investigated values of wind pressure in the case of sealed buildings. The reliability index for walls subject to point loading is 0.73 for sealed buildings and 0 for buildings with significant openings at a 50-year wind pressure of 0.55 kPa. A correction factor of 1.97 improved results from 0 and 0.73 to 0.54 and 1.66, respectively, for sealed buildings and buildings with significant openings. The results show that current empirical provisions result in acceptable reliability indices if test results for walls subject to uniform loading are exclusively considered.

Mortar Type

Table 4.5 shows that walls constructed with Type S masonry cement mortar result in reliability indices of at least 2.57 at a 50-year wind pressure of 0.55 kPa, while Type S mortar cement mortar results in a reliability index of zero for the same wind pressure. Walls constructed with Type S PCL mortar result in reliability indices higher than 2.5 for all 50-year wind pressures in the case of sealed buildings and for wind pressures up to 0.53 kPa in the case of buildings with significant openings. Walls constructed with Type N PCL mortar result in reliability indices higher than 2.5 for 50-year wind pressures up to 0.48 kPa and 0.25 kPa for sealed buildings and buildings with significant openings, respectively. While results indicate that the current empirical provisions lead to acceptable reliability indices for Type S masonry cement mortar and unacceptable reliability indices for Type S mortar cement mortar, it is recommended that the database of these two mortar types be bolstered for reasons stated in Section 4.4.4.1 with results re-evaluated.

Support Conditions

Table 4.5 shows that the reliability indices for walls with ideal supports are 1.91 and 1.11 at a 50-year wind pressure of 0.55 kPa for sealed buildings and buildings with significant openings, respectively; whereas results show reliability indices of 0.77 and 0 for walls with realistic supports. The current empirical provisions, therefore, produce reliability indices lower than 2.5 when evaluated in terms of support conditions. Walls with ideal and realistic supports in sealed buildings result in reliability indices equal to at least 2.5 for 50-year wind pressures up to 0.38 kPa and 0.28 kPa, respectively. Neither support types result in a minimum reliability index of 2.5 for any of the investigated 50-year wind pressures in buildings with significant openings. The test database for walls with realistic supports should be expanded and the reliability indices as shown in Table 4.5 re-evaluated.

In summary, investigating the reliability indices for the flexural tensile strength of unreinforced masonry walls in terms of the 50-year wind pressures of 14 cities across Canada result in the following conclusions:

- The available database results in reliability indices lower than 2.5 for walls with slenderness ratios equal to or greater than 16. In addition, walls with a slenderness ratio of 12 subject to 50-year wind pressures greater than 0.29 kPa for buildings with

significant openings and 0.53 kPa for sealed buildings result in reliability indices below 2.5.

- Walls subject to point loading, those constructed with realistic support conditions, and those constructed using mortar cement mortar result in lower values of reliability indices. However, the effect of these parameters cannot be determined independently due to the limits in the available test database. An expansion of the test database is recommended.

4.5 Recommendations for the Empirical Provisions of CSA S304-14

Recommendations for the empirical provisions of CSA S304 (2014) are provided in this section based on the results of the reliability analysis as discussed in Section 4.4.4. Such recommendations cannot be viewed as comprehensive and should be interpreted considering the scope of the present investigation. In particular, it should be noted that the current investigation was conducted for buildings in open terrain and a normal importance category as defined by NBCC (2015). The current investigation revealed differences in the resulting reliability indices for buildings with significant openings and sealed buildings. This difference is not accounted for in the current empirical provisions of CSA S304 (2014). It is expected that the terrain conditions and the importance category of buildings also influence the results. It is recommended that the potential impacts of such parameters on reliability indices be considered in the interpretation of results.

The current empirical provisions may be used for nonloadbearing exterior walls in areas where the 1 in 50 years hourly wind pressures are equal or less than 0.55 kPa, according to Clause F.1.1. Additionally, solid masonry of hollow units used in exterior walls shall have a maximum slenderness ratio of 20 according to Table F.2 (CSA, 2014). The results of the reliability analysis based on the available database, however, indicate potentially inadequate levels of safety for walls with higher slenderness ratios and 1 in 50 years wind pressures. It is, therefore, recommended that commentary be added to CSA S304 (2014) informing users of the lack of quantitative evidence supporting the safety of non-loadbearing, unreinforced, exterior walls constructed using solid masonry of hollow units, in particular for increasing values of slenderness ratio and 1 in 50 years hourly wind pressure.

Results of the present analysis do not warrant changes to the empirical provisions of CSA S304 (2014) due to the limits of the test database. For example, the test database for walls with

slenderness ratios greater than 16, which consistently resulted in unacceptable values of reliability indices, only included walls constructed with Type S mortar cement mortar and tested under point loading. It was not possible, therefore, to study the effect of the included parameters on the resulting reliability indices independently. An expansion of the available test database is required to ensure that any potential correlations between parameters can be quantified.

4.6 Summary

This chapter includes the results and analysis for the experimental and analytical investigation conducted to contribute towards the reconciliation of the empirical and rational provisions of CSA S304 (2014). Results from the companion specimen testing were presented first, followed by the results from the out-of-plane wall testing. The assembly of the test database and, finally, the procedure and the results of the reliability analysis were discussed. Recommendations were made to the empirical provisions of CSA S304 (2014) based on the results of the reliability analysis.

The results obtained from tests of companion specimens met the requirements of CSA A179 (2014). Results from the wall tests were provided and added to a test database comprising results from past tests of unreinforced masonry walls subject to out-of-plane loading. The data were then categorized based on the mortar type used in the construction of walls, support conditions of the tested walls, load application method used in the testing of walls, and the slenderness ratios of the tested walls.

A Monte Carlo simulation was used to determine the reliability index of non-loadbearing, exterior, unreinforced concrete masonry block walls subject to wind load as explained in Section 4.4. The probability distributions for the wind speed, flexural tensile strength of walls, and wind pressure coefficient were introduced. Resulting reliability indices showed that the current empirical provisions result in a maximum reliability index of 0.48 for walls with slenderness ratios of 16 and higher and a maximum reliability index of 2.44 for a slenderness ratio of 12. It was recommended that CSA S304 (2014) include commentary cautioning the users of the lack of quantitative proof for the safety of unreinforced concrete block walls subject to wind and designed in accordance with the empirical provisions, in particular for increasing values of slenderness ratio and 1 in 50 years hourly wind pressure. Changes to the empirical provisions of CSA S304 (2014), however, were not recommended due to the potential

correlations of the parameters included in the analysis which may have affected the resulting values of reliability indices. The test database for walls with slenderness ratios equal to or greater than 16, walls constructed with realistic supports, and those constructed with Type S mortar and masonry cement mortars should be expanded and results reassessed. An overall summary of the current research program and the results will be provided in the next Chapter.

Table 4.1: Results of the Wall Specimen Testing

Wall Specimen[1]	Failure Joint from Bottom[2]	Flexural Tensile Strength (MPa)	Mean Flexural Tensile Strength (MPa)
16I1	9	0.116	0.175
16I2	9	0.200	
16I3	10	0.210	
18I1	8	0.175	0.132
18I2	7	0.0601	
18I3	7	0.161	
20I1	9	0.117	0.112
20I2	9	0.106	
20I3	9	0.112	
16R1	7	0.122	0.085
16R2	11	0.0323	
16R3	7	0.102	
18R1	8	0.0948	0.155
18R2	12	0.227	
18R3	7	0.142	
20R1	15	0.0562	0.114
20R2	10	0.153	
20R3	10	0.132	

[1] Description of wall identification as provided in Section 3.3.
[2] First joint was considered to be between the bottom course and the support.

Table 4.2: Gumbel Distribution Parameters and 50-Year Wind Pressures (after Hong et al., 2013)

Locations for which Annual Maximum Wind Speed Distributions were Calculated*	Parameters of the Gumbel Distribution		50-year wind pressure (kPa)
	Scale Parameter, α	Location Parameter, μ (km/hr)	
Victoria, BC	0.144	57.2	0.354
Whitehorse, YT	0.141	52.5	0.321
Yellowknife, NT	0.179	48.7	0.248
Iqaluit, NU	0.083	71.8	0.703
Edmonton, AB	0.169	58.5	0.332
Regina, SK	0.146	71.9	0.485
Winnipeg MB	0.180	63.9	0.366
Ottawa, ON	0.147	62.7	0.398
Toronto, ON	0.152	73.1	0.487
Quebec, QC	0.147	64.9	0.418
Fredericton, NB	0.208	57.0	0.286
Halifax, NS	0.108	69.3	0.553
Charlottetown, PE	0.149	67.6	0.439
St. John's, NL	0.119	87.0	0.716
*All measurements made at the nearest major airport			

Table 4.3: Parameters for the Lognormal Distributions for Wall Resistance

Categories for Which the Reliability Index was Calculated Based on the Values of the Flexural Tensile Strength	Parameters of the Lognormal Distribution		Number of Available Data Points
	Location Parameter, μ	Scale Parameter, σ	
Slenderness Ratio, *kl/t* = 19	-2.13	0.411	12
Slenderness Ratio, *kl/t* = 16	-1.96	0.684	41
Slenderness Ratio, *kl/t* = 12	-0.681	0.831	102
Uniform Load	-0.253	0.576	108
Point Load	-1.94	0.563	77
Corrected Point Load	-1.27	0.569	77
Type S Masonry Cement Mortar	-0.391	0.549	33
Type S Mortar Cement Mortar	-2.19	0.663	36
Type S PCL Mortar	-0.128	0.689	55
Type N PCL Mortar	-0.972	0.688	34
Ideal Supports	-0.830	0.937	168
Realistic Supports	-2.22	0.881	17

Table 4.4: Anderson-Darling Goodness-of-Fit Test Results

Investigated Parameter	Belongs to Lognormal PDF at 5% significance?	Significance Level
N PCL	Yes	0.294
S PCL	Yes	0.185
S Masonry	Yes	0.174
S Mortar	Yes	0.0578
Slend. Ratio = 12	Yes	0.0591
Slend. Ratio = 16	Yes	0.0686
Slend. Ratio = 19	Yes	0.932
Point Load	No	0.0445
Uniform Load	Yes	0.582
Corrected Point Load	No	0.0445
Realistic Supports	Yes	0.190
Ideal Supports	No	0.0238

Table 4.5: Summary of Results for the Reliability Analysis

Investigated Parameters	Reliability index at 50-year wind pressure of 0.55 kPa		Max. 50-year wind pressure (kPa) for $\beta = 2.5$	
	Sealed Buildings	Buildings with Significant Opening	Sealed Buildings	Buildings with Significant Opening
Slenderness Ratio, *kl/t* = 19	0	0	None	None
Slenderness Ratio, *kl/t* = 16	0.48	0	None	None
Slenderness Ratio, *kl/t* = 12	2.44	1.56	0.53	0.29
Uniform Load	3.68	2.65	All	0.60
Point Load	0.73	0	0.25	None
Corrected Point Load	1.66	0.54	0.38	None
Type S Masonry Cement Mortar	3.62	2.57	All	0.57
Type S Mortar Cement Mortar	0	0	None	None
Type S PCL Mortar	3.37	2.42	All	0.53
Type N PCL Mortar	2.16	1.17	0.48	0.25
Ideal Supports	1.91	1.11	0.38	None
Realistic Supports	0.77	0	0.28	None

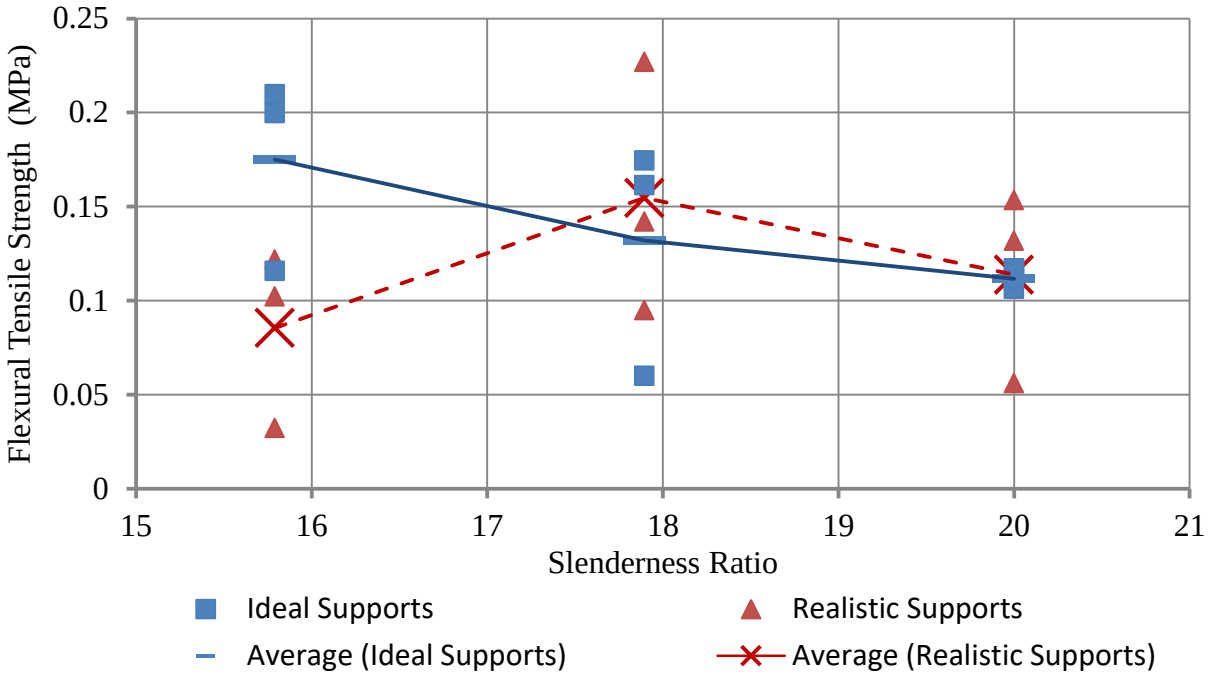

Figure 4.1: Flexural Tensile Strength of Wall Specimens

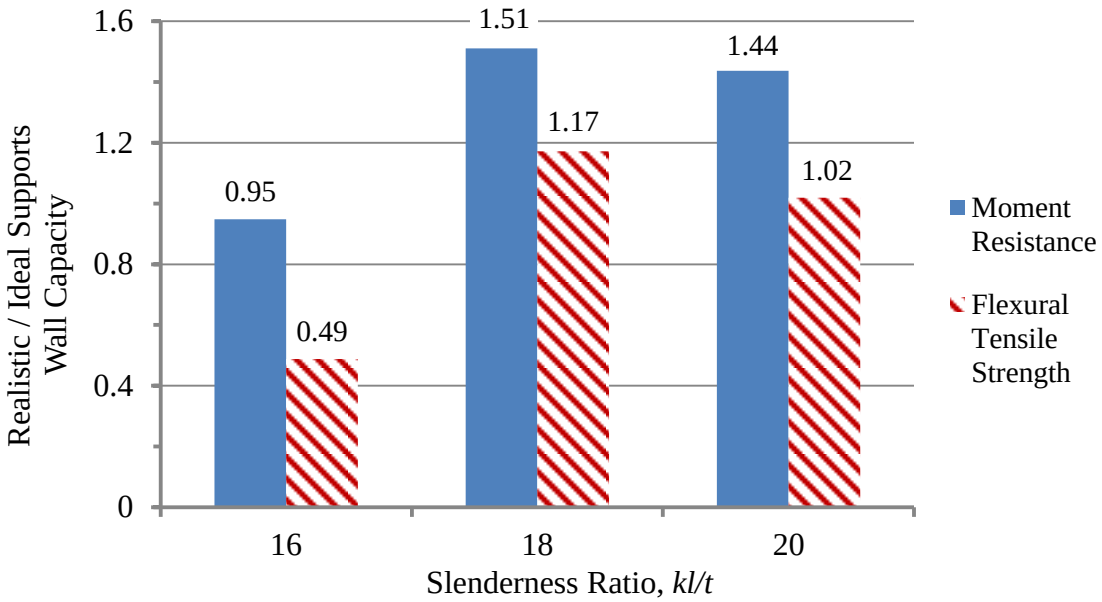

Figure 4.2: Capacity of Realistically Supported to Ideally Supported Walls

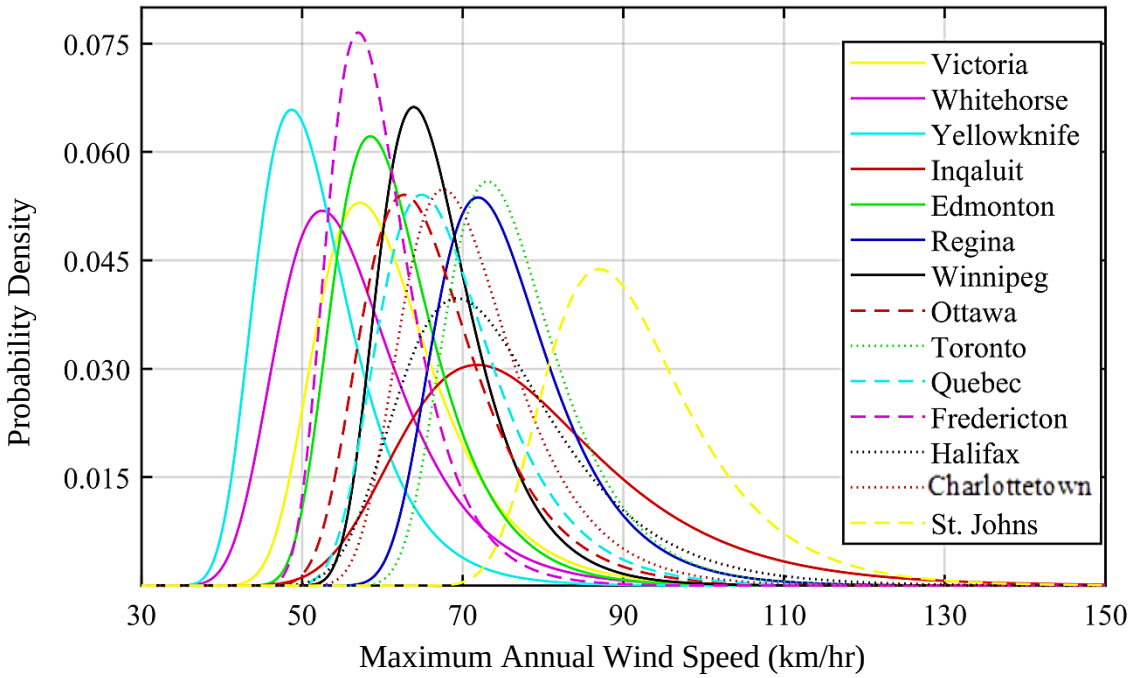

Figure 4.3: Probability Distributions for Wind Speed (Based on Hong et al., 2013)

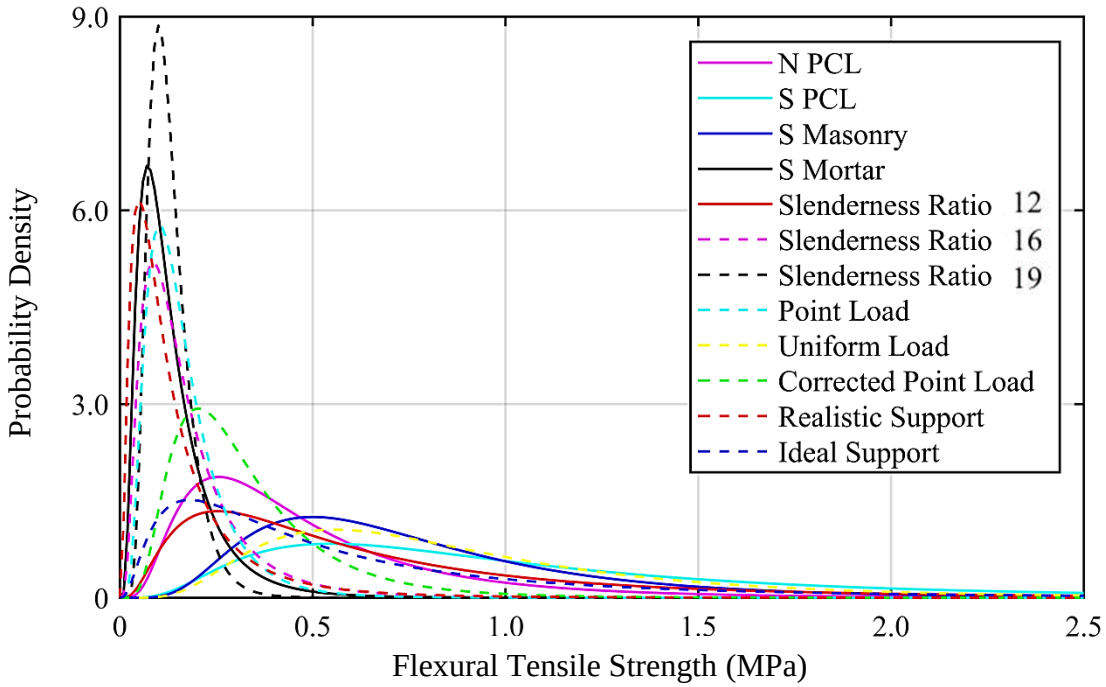

Figure 4.4: Probability Distributions for Categories of Wall Strength

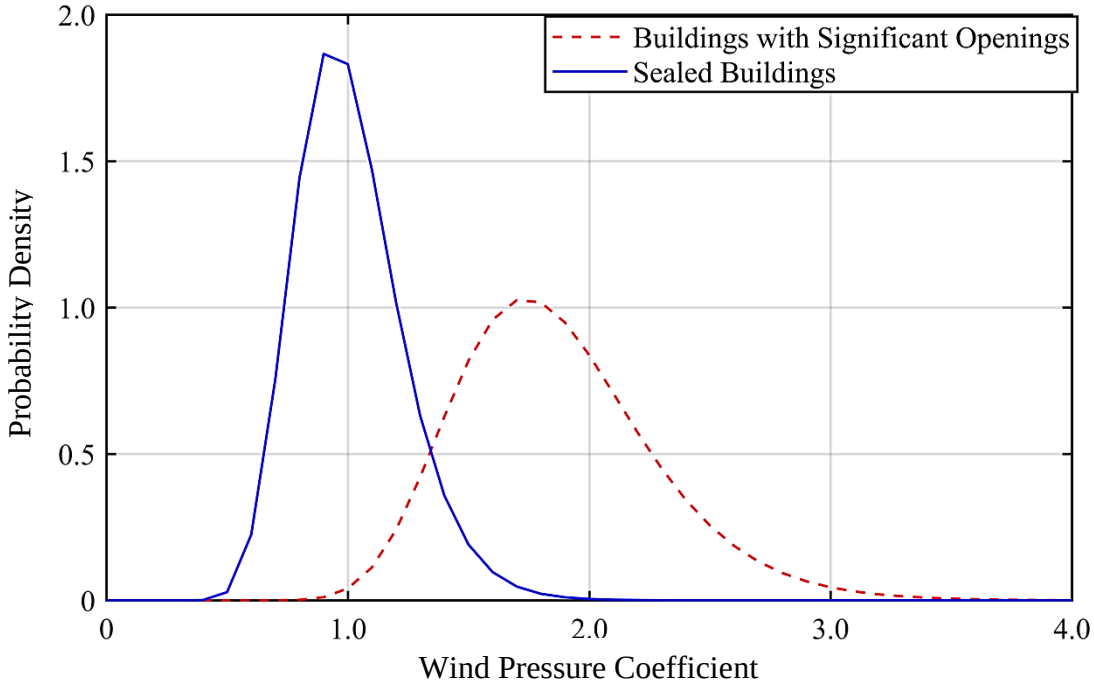

Figure 4.5: Probability Distributions for the Wind Pressure Coefficient

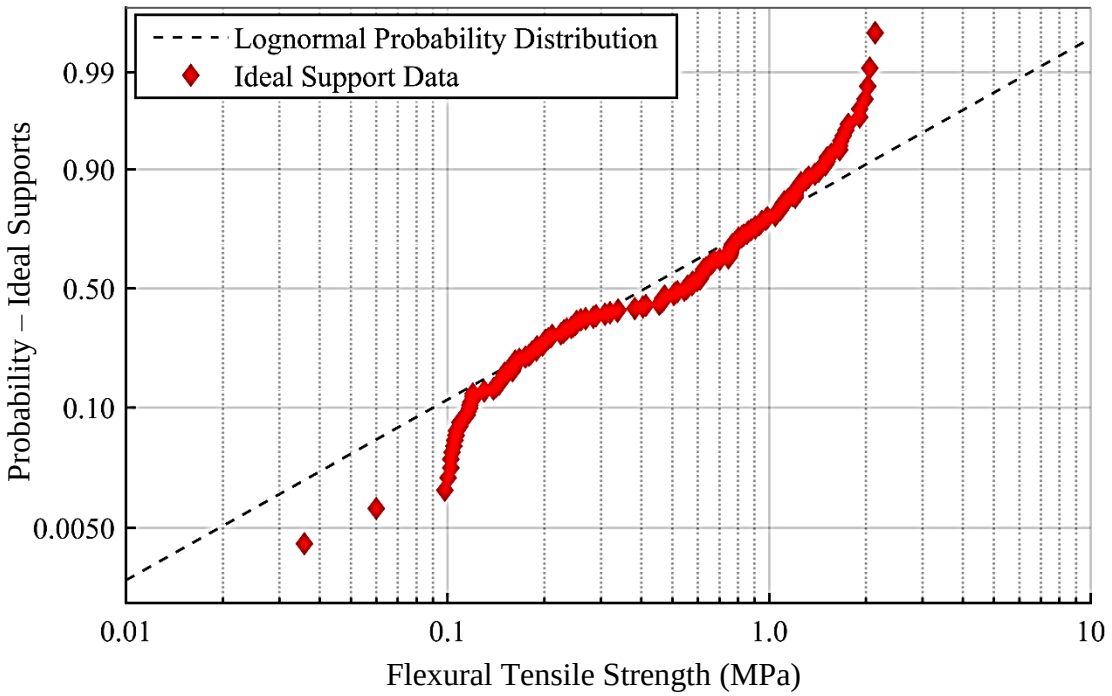

Figure 4.6: Probability Plot for Walls with Ideal Support

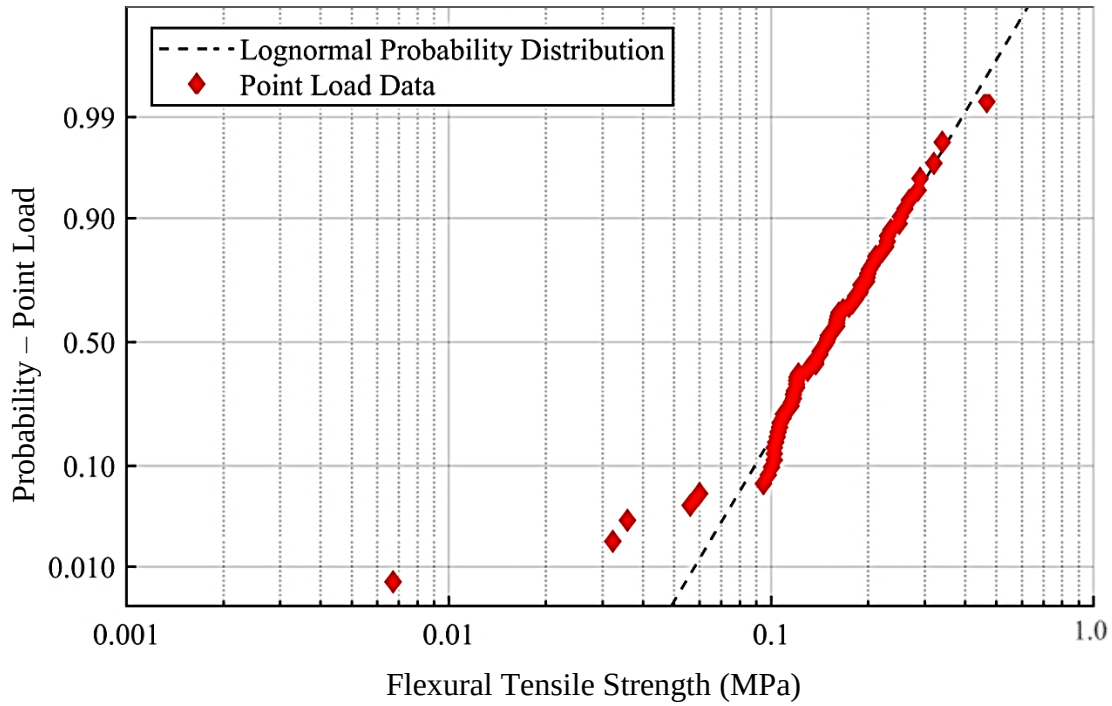

Figure 4.7: Probability Plot for Walls Subject to Point Load

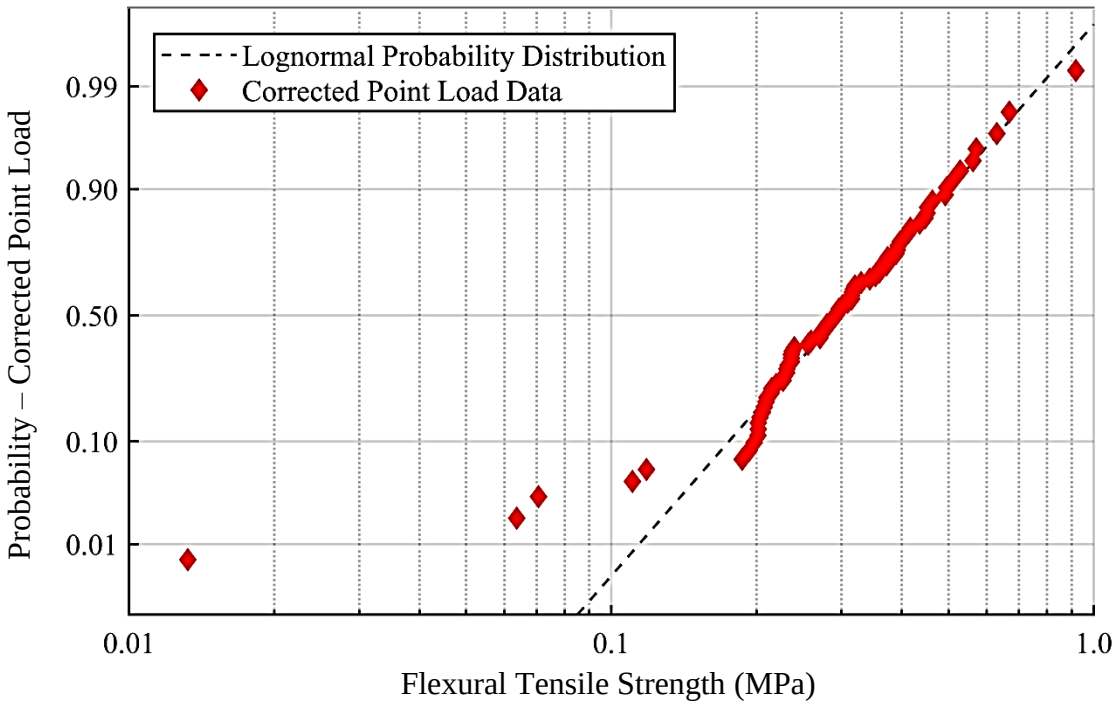

Figure 4.8: Probability Plot for the Corrected Point Load Data

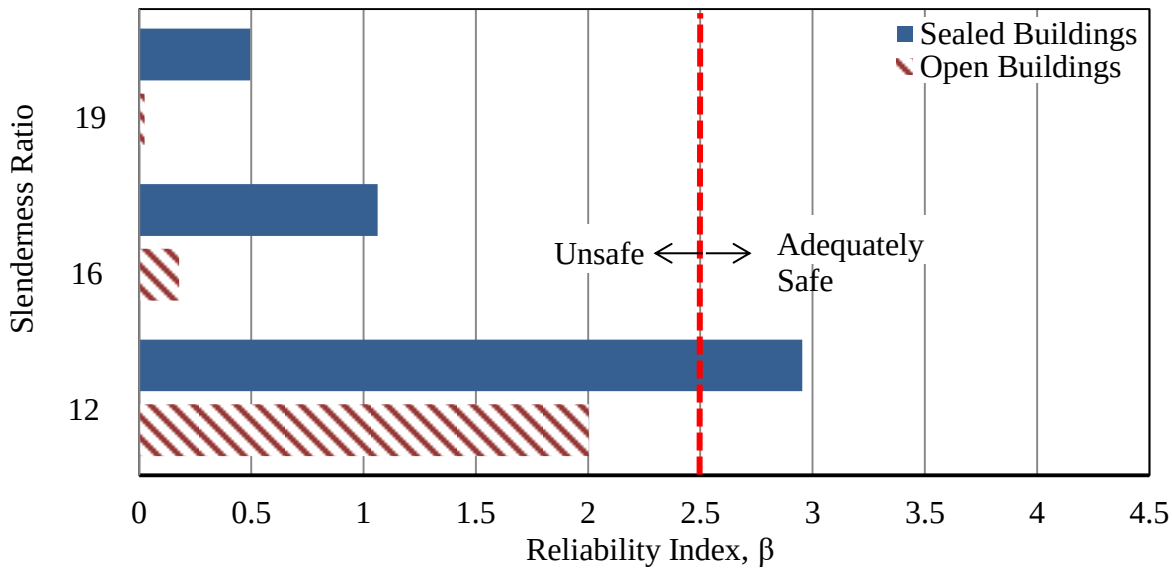

Figure 4.9: Reliability Index Based on Slenderness Ratio

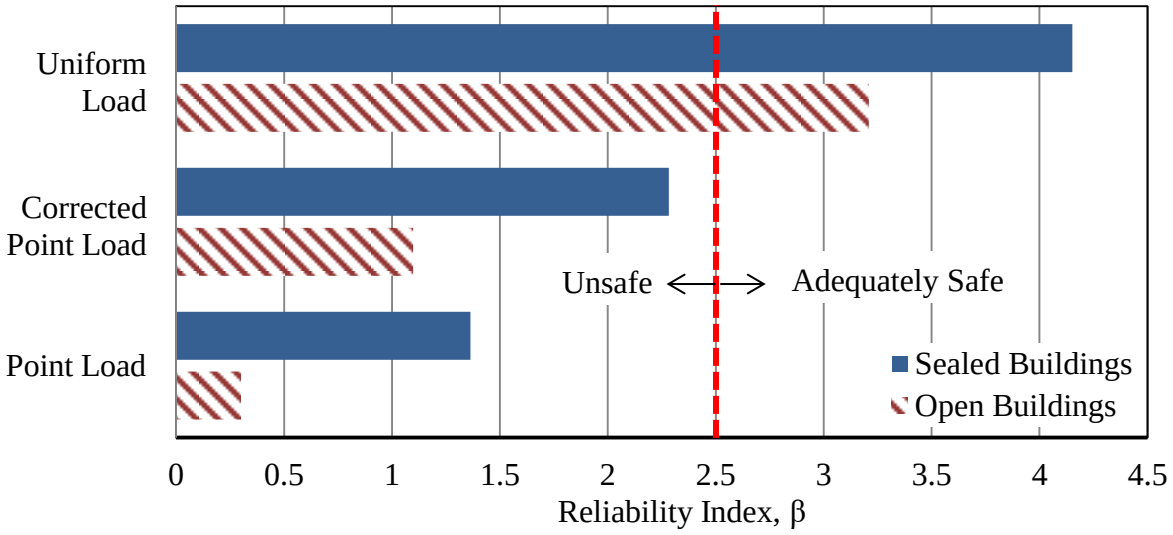

Figure 4.10: Reliability Index Based on Load Application Method

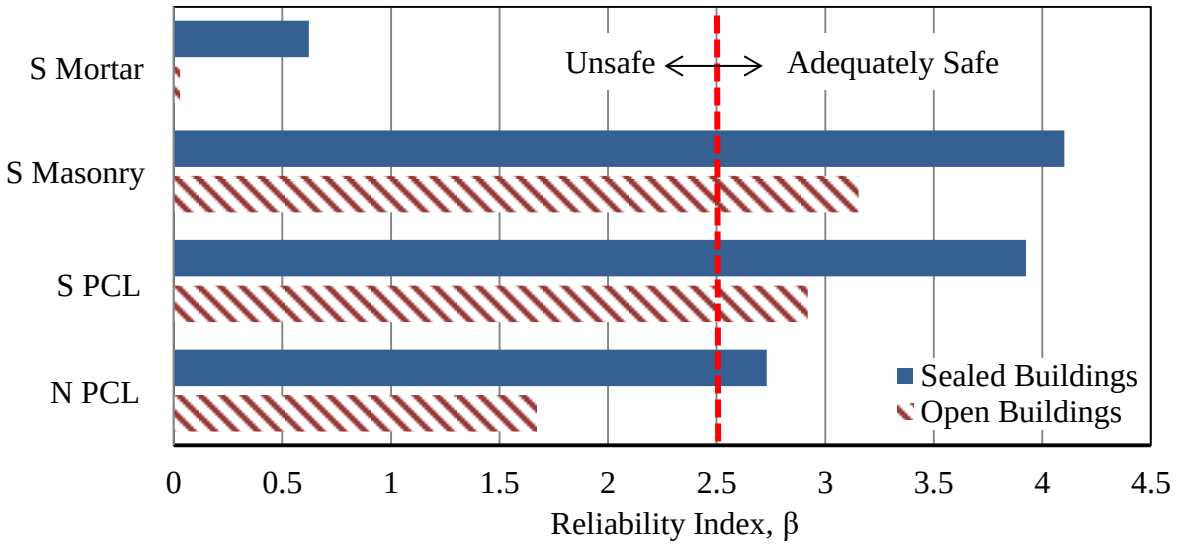

Figure 4.11: Reliability Index Based on Mortar Type

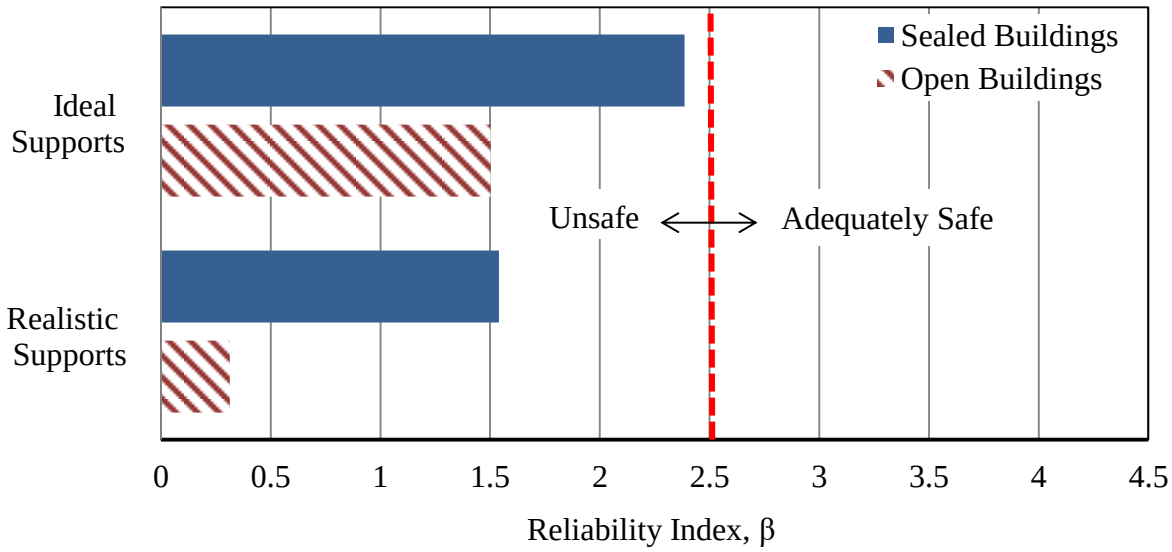

Figure 4.12: Reliability Index Based on Support Type

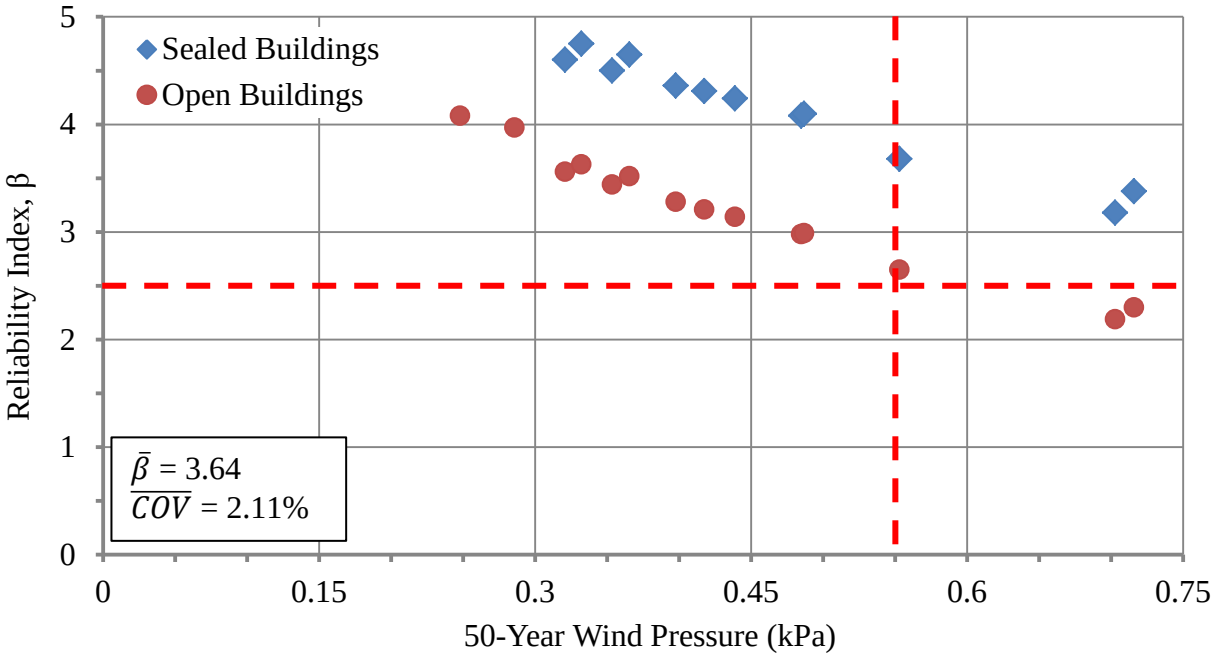

Figure 4.13: Reliability Index vs. 50-Year Wind Pressure for Uniform Load Application

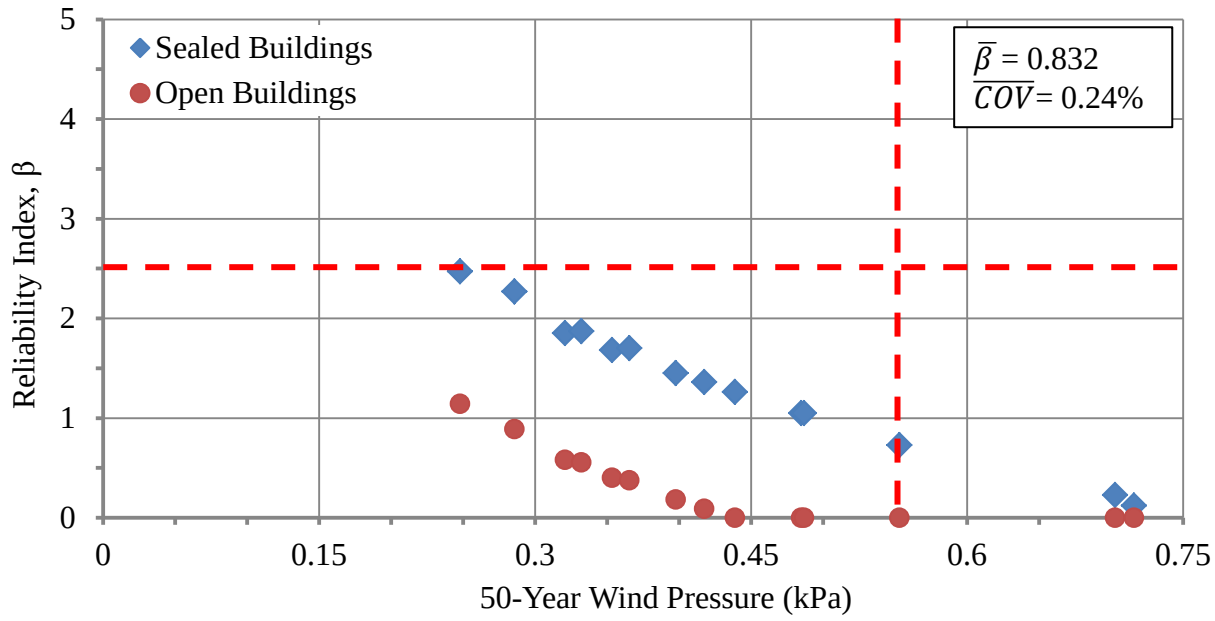

Figure 4.14: Reliability Index vs. 50-Year Wind Pressure for Point Load Application

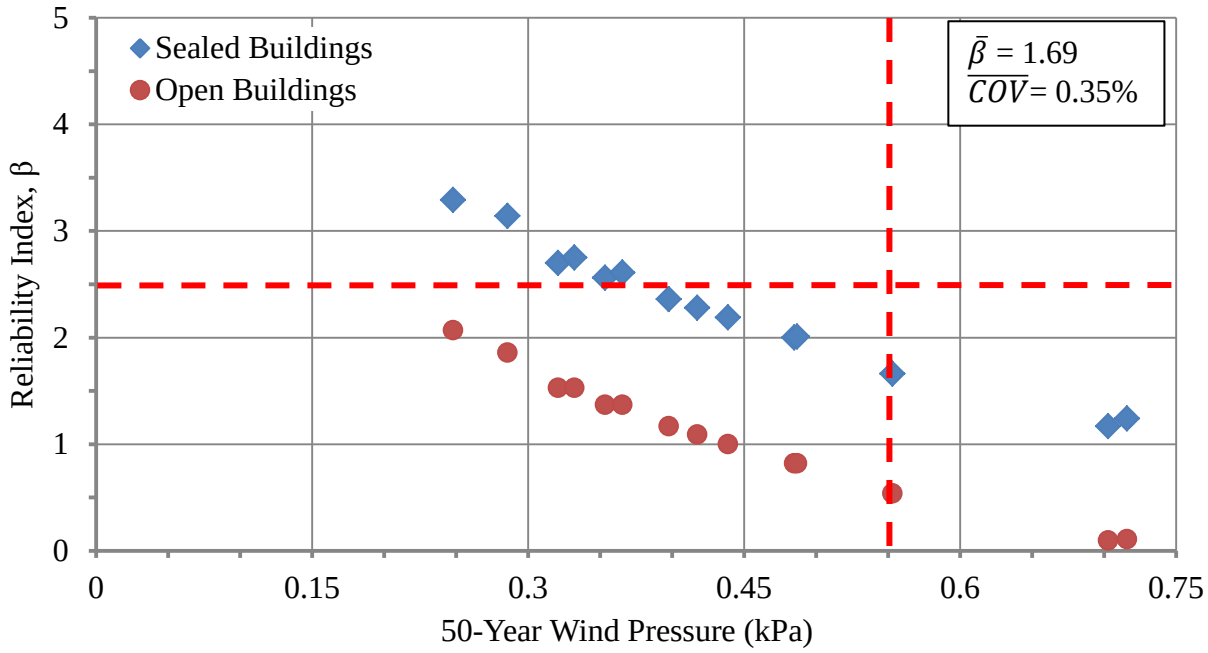

Figure 4.15: Reliability Index vs. 50-Year Wind Pressure for the Corrected Point Load Data

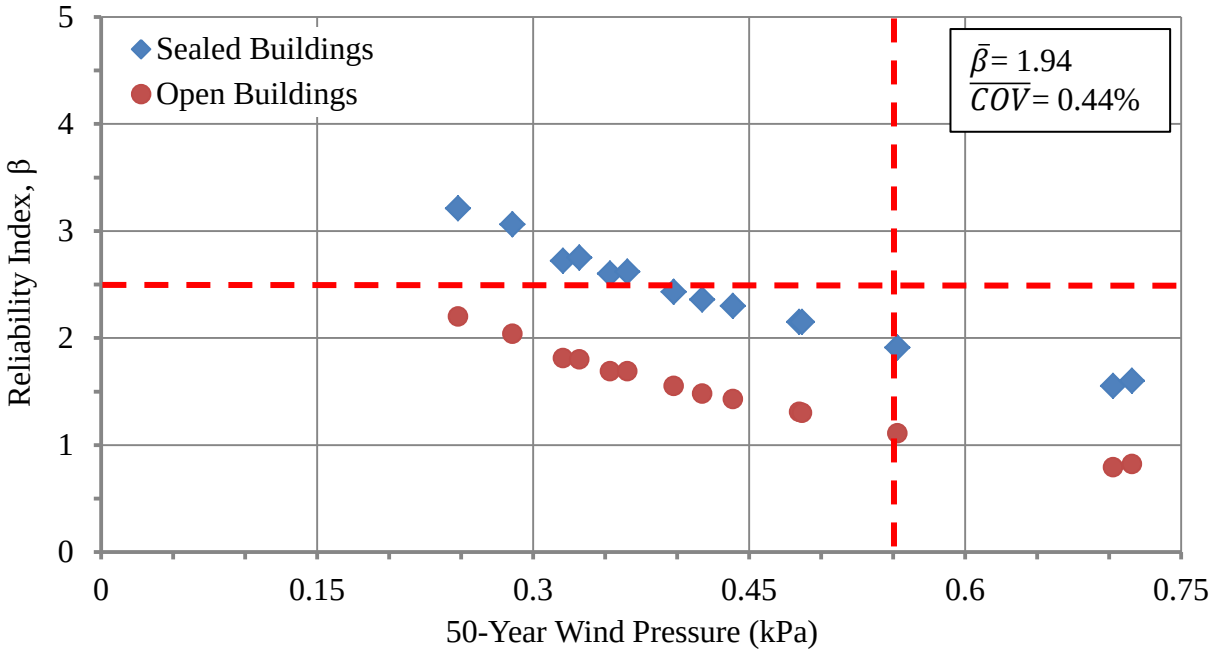

Figure 4.16: Reliability Index vs. 50-Year Wind Pressure for Walls with Ideal Supports

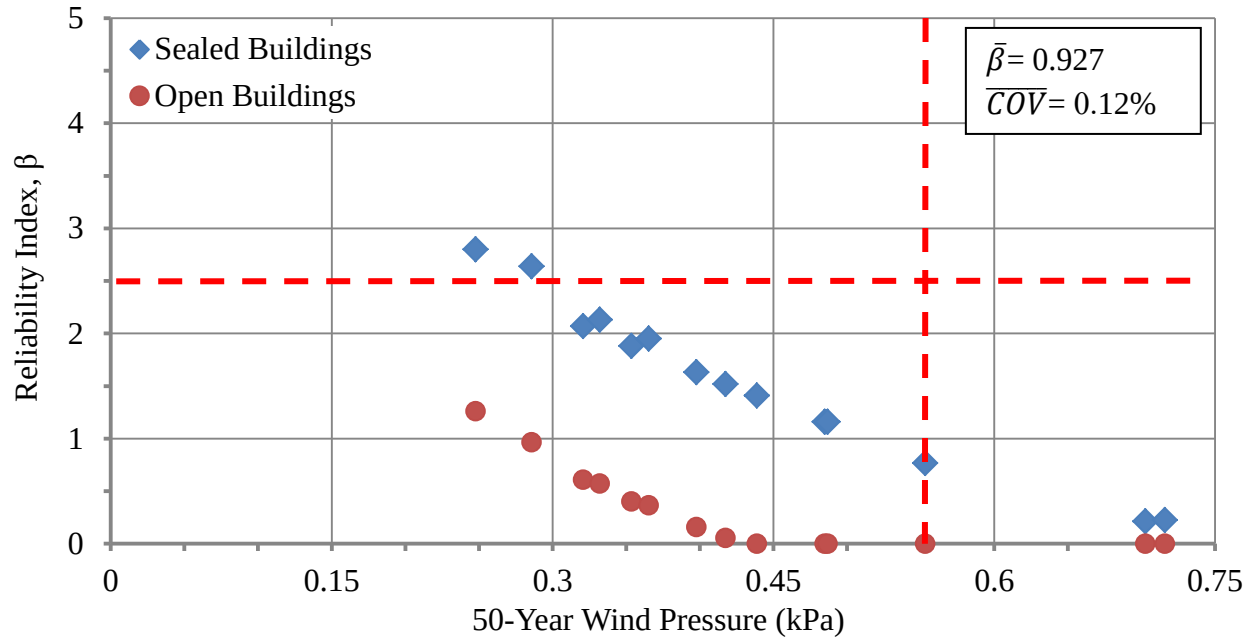

Figure 4.17: Reliability Index vs. 50-Year Wind Pressure for Walls with Realistic Supports

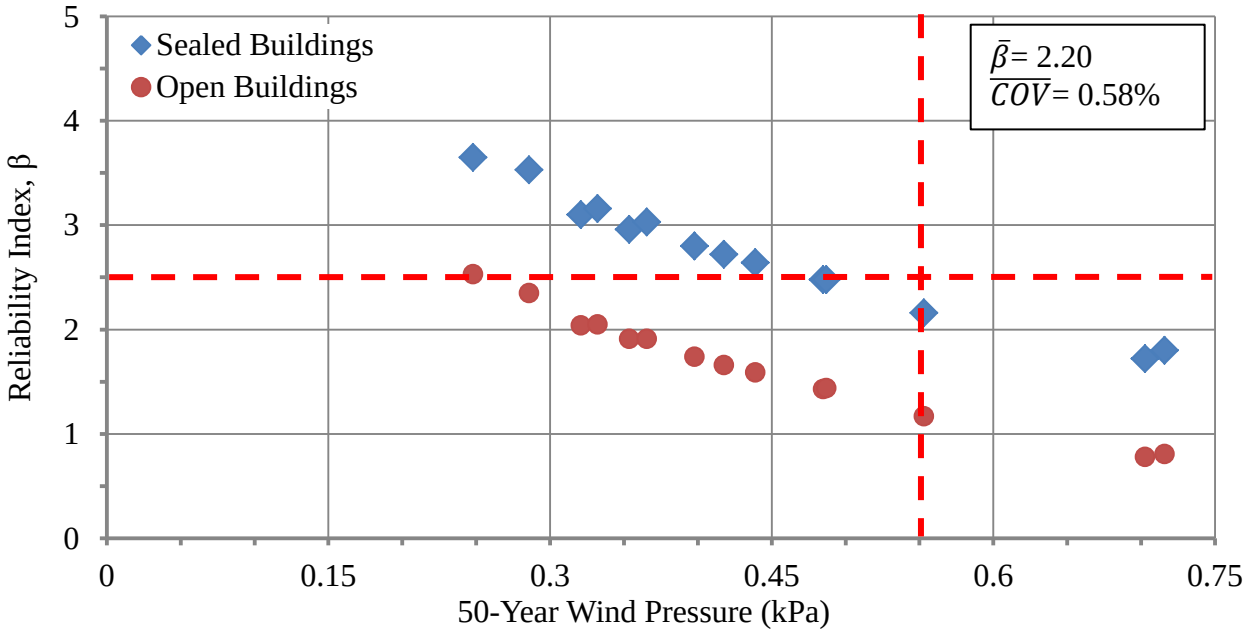

Figure 4.18: Reliability Index vs. 50-Year Wind Pressure for Type N PCL Mortar

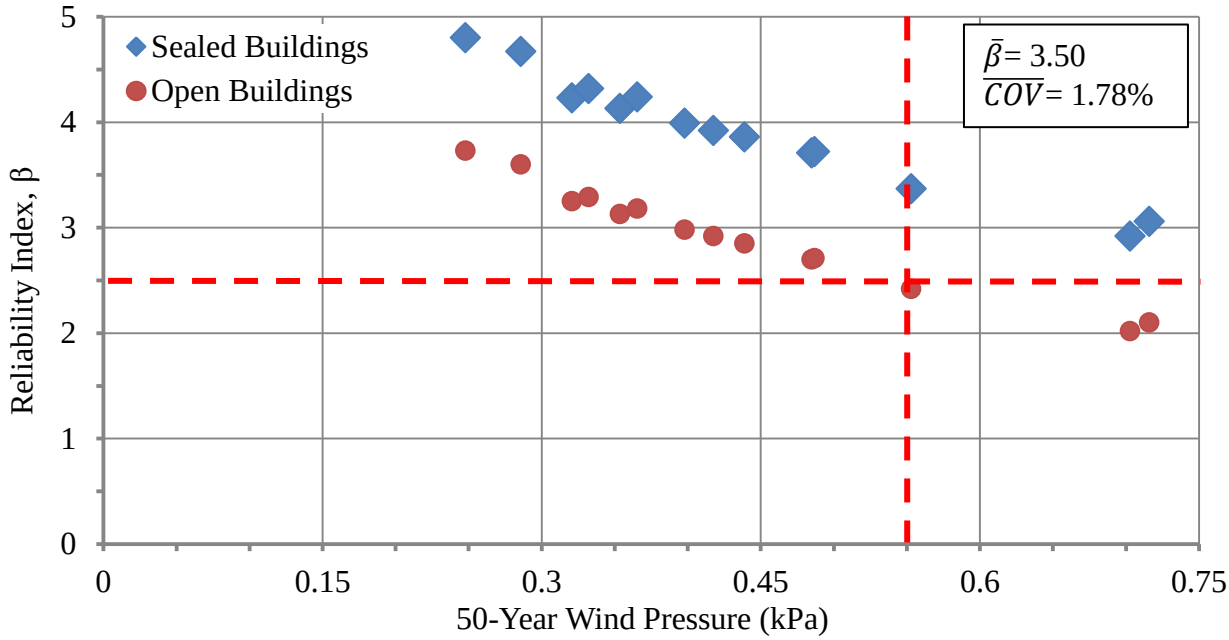

Figure 4.19: Reliability Index vs. 50-Year Wind Pressure for Type S PCL Mortar

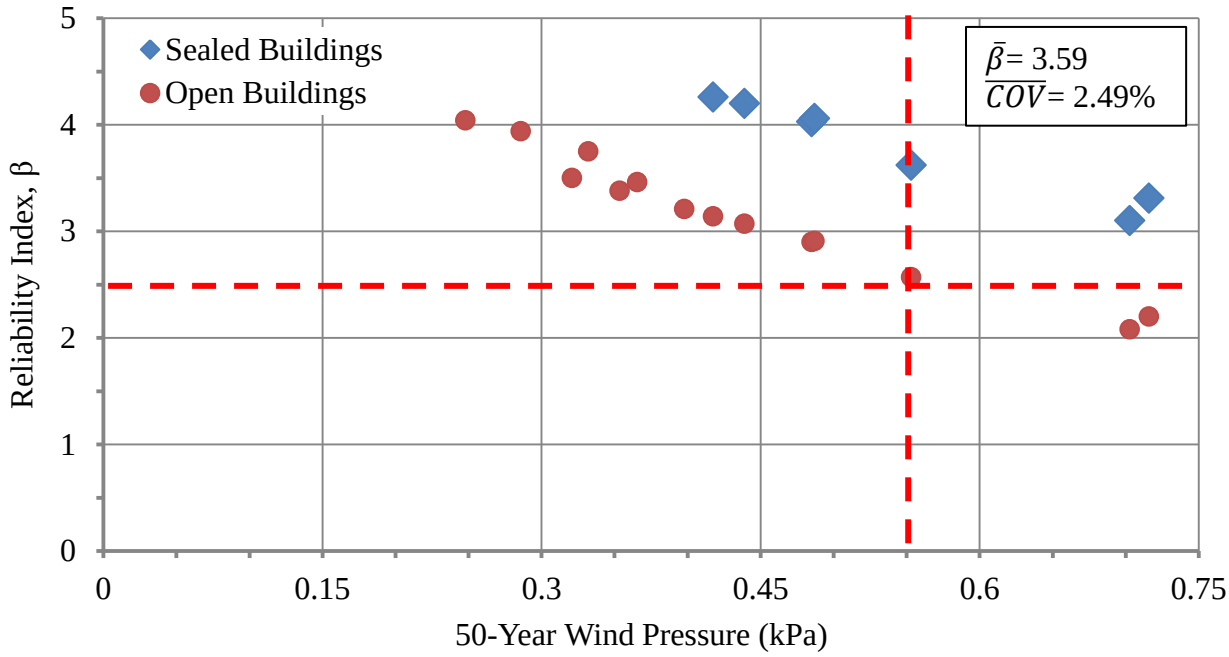

Figure 4.20: Reliability Index vs. 50-Year Wind Pressure for Type S Masonry Cement Mortar

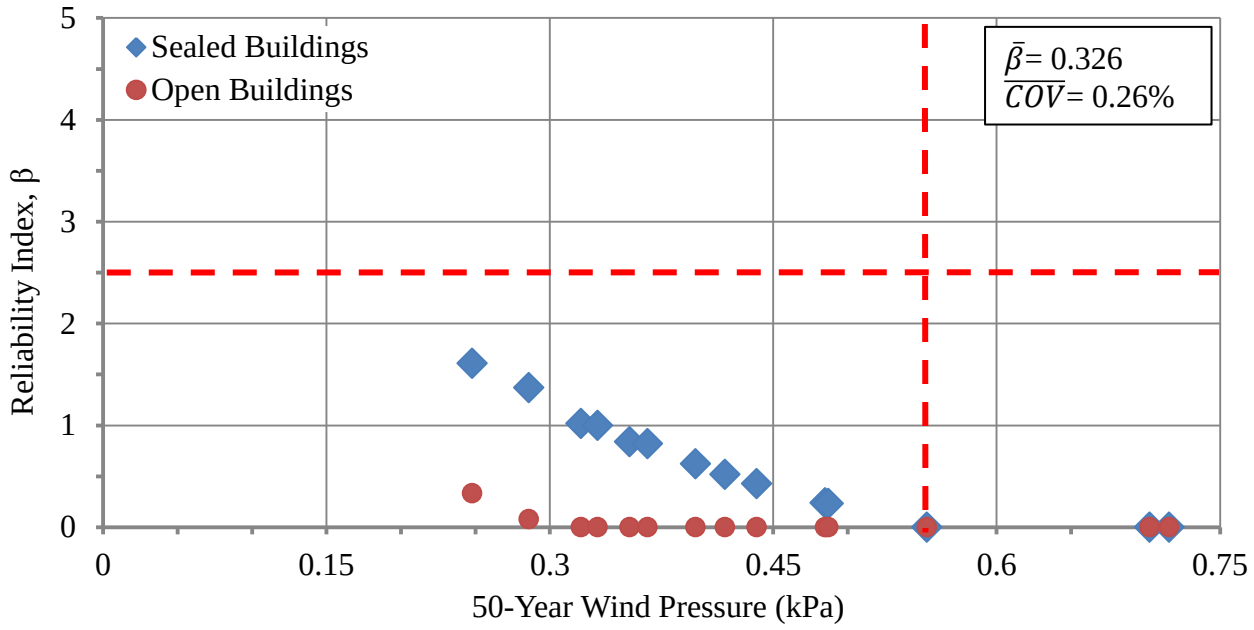

Figure 4.21: Reliability Index vs. 50-Year Wind Pressure for Type S Mortar Cement Mortar

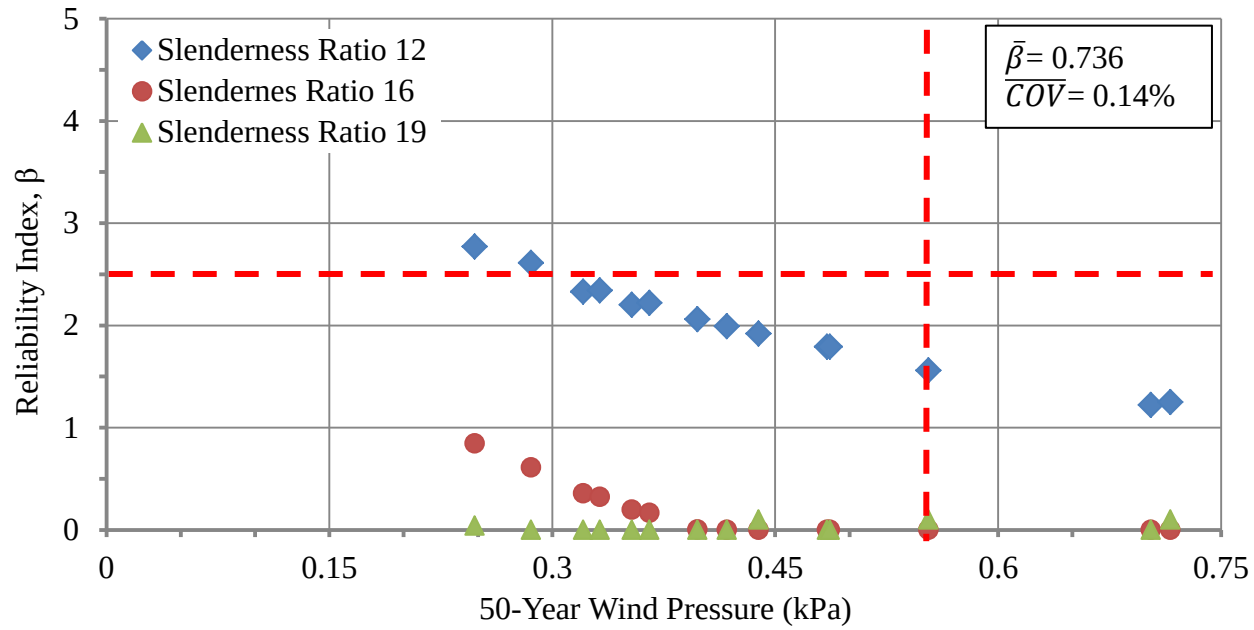

Figure 4.22: Reliability Index vs. 50-Year Wind Pressure for Buildings with Significant Openings

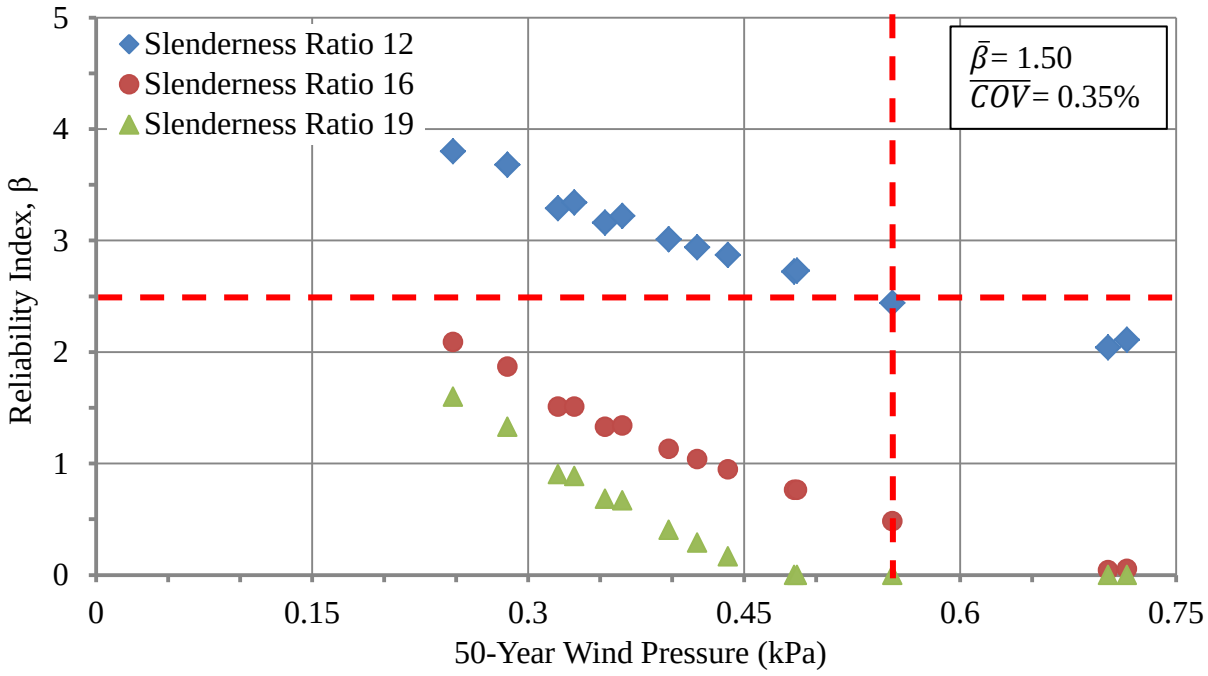

Figure 4.23: Reliability Index vs. 50-Year Wind Pressure for Sealed Buildings

5.0 Conclusions

An investigation was conducted to contribute to the reconciliation of the rational and empirical design provisions of CSA S304-14 as related to non-loadbearing, ungrouted, unreinforced, exterior concrete block walls subject to wind load. A comparison of the outcomes of the two design methods showed that the empirical design provisions can result in less conservative values of the allowable 1 in 50 years hourly wind pressure for increasing slenderness ratios. The reconciliation of the two design methods required an understanding of the resistance of walls in question. Therefore, a literature review was conducted to study the available experimental data related to the flexural tensile strength of unreinforced concrete block walls subject to out-of-plane loading. A database was compiled using test results reported in past experimental works. The test data were classified according to the included test parameters. An experimental program was designed to bolster the test database for parameters for which there was a scarcity of data.

The parameters investigated in the experimental program were slenderness ratio, mortar type, and support conditions. Overall, 18 unreinforced concrete block walls were constructed with slenderness ratios equal to 16, 18 and 20, where slenderness ratio was defined as the wall height-to-thickness ratio. Replicate walls of each slenderness ratio were tested using both ideal and realistic support conditions. All walls were constructed using mortar cement mortar. Walls were tested using lateral, displacement-controlled, four-point loading, and the resulting values of flexural tensile strength were determined. The test results of these specimens were then added to the overall test database.

A reliability analysis was conducted using the updated test database. The reliability indices of walls were determined for various parameters included in the experimental investigations and a range of 1 in 50 years hourly wind pressures corresponding to 14 locations across Canada. Recommendations were made for changes to the empirical provisions of CSA S304-14 assuming a reliability index equal to 2.5 to be the minimum acceptable value, as per recommendations made by past researchers.

A summary of findings for this investigation and recommendations for future research are presented in the following sections.

5.1 Summary of Findings

A summary of the findings of the current investigation are presented in this section and include the shortcomings of the available test database based on the literature review, the results of the reliability analysis, and recommendations for the empirical provisions of CSA S304-14.

Shortcomings of the Available Test Database

Three areas were identified where the test database, as compiled from past experimental investigations, was limited. These areas are as follows:

- The database was limited for walls constructed using mortar and masonry cement mortars. Only one work included an investigation of the flexural tensile strength of unreinforced masonry walls constructed using Type S mortar cement mortar. In addition, only three works reported the use of masonry cement mortar with the majority of data belonging to one study.
- The test database was limited for walls with higher slenderness ratios. No work was identified that investigated the flexural tensile strength of walls with slenderness ratios greater than 16, while the empirical provisions included in CSA S304-14 permit a maximum slenderness ratio equal to 20.
- The test database was also limited for walls constructed and tested using realistic support conditions. Only one study investigated the impact of realistic support conditions on the resulting flexural tensile strength of unreinforced concrete block walls.

Results of the Reliability Analysis

Reliability indices were calculated for unreinforced concrete block walls subject to various values of 1 in 50 years hourly wind pressures. Different cases of load application methods, mortar types, support conditions, and slenderness ratios were considered in the reliability analysis. In addition, reliability indices were calculated for two cases of building openings: sealed buildings (with an internal pressure coefficient equal to zero), and buildings with significant openings (with an internal pressure coefficient equal to 0.7). Results are summarized below assuming a target reliability index of 2.5 is required. Unless otherwise stated, reported values of reliability index correspond to a 1 in 50 years hourly wind pressure equal to 0.55 kPa, as permitted by the empirical provisions of CSA S304-14.

- Walls subject to uniform loading resulted in reliability indices greater than 2.5 for both sealed buildings and buildings with significant openings. Walls subject to point loading resulted in reliability indices lower than 2.5 regardless of the case of building openings. A correction factor equal to 1.97 applied to the values of flexural tensile strength for walls subject to point loading, as recommended by past researchers, did not increase the reliability indices to acceptable levels.
- Walls constructed using Type S masonry cement mortar resulted in reliability indices greater than 2.5 regardless of the case of building openings. Walls constructed using Type S mortar cement mortar resulted in reliability indices lower than 2.5 regardless of the case of building openings. Walls constructed using Type S Portland cement mortar resulted in reliability indices greater than 2.5 for sealed buildings and a reliability index equal to 2.42 for buildings with significant openings.
- Walls with ideal support conditions resulted in greater values of reliability indices than those with realistic support conditions. The resulting reliability indices were, however, lower than 2.5 for both ideal and realistic support conditions regardless of building openings.
- A maximum reliability index equal to 0.48 resulted for walls with slenderness ratios equal to 16 and 19 regardless of building openings. Walls with a slenderness ratio equal to 12 resulted in reliability indices equal to 2.44 and 1.56 for sealed buildings and buildings with significant openings, respectively.

Recommendations for the Empirical Provisions of CSA S304-14

Results of the reliability analysis were compared with the current empirical provisions of CSA S304-14. It was emphasized that the current investigation was conducted for buildings in open terrain and a normal importance category. In addition, two extreme cases of buildings openings relating to the minimum and maximum internal pressure coefficients were included in the analysis. It was determined that, when designed in accordance with the empirical provisions, unreinforced masonry walls may result in unacceptable levels of safety. Limits of the available test database, however, did not permit the effects of the investigated parameters on the resulting reliability indices to be determined independently. Therefore, results of the analysis did not warrant changes to the empirical provisions of CSA S304-14.

It was recommended that CSA S304-14 provide commentary informing users that there is lack of evidence for the safety of non-loadbearing, unreinforced, exterior, hollow concrete block walls when designed in accordance with the empirical provisions. It was recommended that users be particularly cautioned when the empirical provisions are used to design walls with increasing values of slenderness ratio and 1 in 50 years wind pressure.

5.2 Recommendations for Future Research

The current investigation was conducted to contribute to the reconciliation of the empirical and rational design provisions included in CSA S304-14. The recommendations made for changes to the empirical provisions were based on the results of a reliability analysis using the unfactored rational equation as the limit states function. Results indicate inadequate levels of safety in certain cases for the empirical provisions should a reliability index of 2.5 be considered as the minimum acceptable value. However, there has been no record of failure for unreinforced concrete block walls when designed to standards in Canada. There are two potential reasons for the absence of recorded failures:

1- It is possible that the conditions in which walls designed in accordance with the empirical method are not adequately safe have not occurred yet. Results of the current investigation show that the empirical method leads to less conservative design outcomes for higher slenderness ratios, open terrain conditions, buildings with significant openings, and increasing values of wind speed. It is not known whether the combination of building, terrain, and weather conditions required for a failure to occur for the walls in question have happened in the past. It is also unclear to what extent, if at all, climate change has affected the frequency and the intensity of maximum wind speeds. It is possible that climate change in select locations may increase the likelihood of the occurrence of maximum wind speeds.

2- Another explanation for the successful performance of walls designed according to the empirical provisions can be the discrepancy between the on-site resistance of walls and those obtained in ideal laboratory conditions. The lateral load-carrying capacity of on-site walls may be greater than those constructed and tested in the laboratory due to the additional rigidity provided by the realistic supports and the surrounding confining elements. Non-structural components such as partitions may also contribute to the additional resistance of on-site walls as compared to those constructed in the laboratory.

In addition, historical construction practice of unreinforced concrete block walls involved building the wall such that it is in direct contact with the structure above. This practice resulted in a compressive force at the top of the wall which improved the out-of-plane resistance. The impact of on-site curing on the lateral resistance of walls has also not been determined. Finally, the simulation of wind load as point loading in the laboratory likely results in an underestimation of the flexural tensile strength of walls.

With consideration to the aforementioned information, the following recommendations are made for future research to further advance the ultimate goal of reconciling the two design methods:

- The test database for the flexural tensile strength of unreinforced concrete block walls subject to out-of-plane loading should be expanded. Additional test data is required for walls with higher slenderness ratios, in particular slenderness ratios between 16 and 20. Additional test data are also required for walls constructed with mortar and masonry cement mortars and realistic support conditions.
- The expanded test database should be used to establish a relationship between results for different support types and load application methods. Relationships should be established between the flexural tensile strength of walls with ideal and realistic support conditions, and those subject to uniform loading and point loading. Test results for walls with ideal support conditions and those subject to point loading should then be corrected to represent realistic support conditions and uniform loading for a better estimation of on-site conditions.
- A reliability analysis should be conducted using the expanded database to determine the structural safety of walls as designed in accordance with the rational design method included in CSA S304-14.

References

Al-Menyawi, Y. M. (2001). “Concrete Block Masonry Construction to Resist Severe Wind.” (Doctoral Dissertation). Retrieved on February 21, 2016 from the Texas Tech University Library https://ttuir.tdl.org/ttuir/bitstream/handle/2346/22265/31295017220350.pdf;sequence=1.

ASTM. (2015). “C140/C140M – 15a Standard Test Methods for Sampling and Testing Concrete Masonry Units and Related Units.” West Conshohocken, PA: ASTM International.

ASTM. (2015). “E72-15 Standard Test Methods of Conducting Strength Tests of Panels for Building Construction.” West Conshohocken, PA: ASTM International.

Ayyub, B. M., & McCuen, R. H. (2003). “Probability, Statistics and Reliability for Engineers and Scientists.” Boca Raton, Fla.: CRC Press.

Bartlett, F. M., Hong, H. P., & Zhou, W. (2003). “Load Factor Calibration for the Proposed 2005 Edition of the National Building Code of Canada: Statistics of Loads and Load Effects.” Canadian Journal of Civil Engineering Can. J. Civ. Eng., 30(2), 429-439.

Chock, G., Yu, G., Thio, H. K., & Lynett, P. J. (2016). “Target Structural Reliability Analysis for Tsunami Hydrodynamic Loads of the ASCE 7 Standard.” Journal of Structural Engineering,142(11), 04016092-1-04016092-12. doi:10.1061/(asce)st.1943-541x.0001499.

Copeland, R. E., and Saxer, E. L. (1964). “Tests of Structural Bond of Masonry Mortars to Concrete Block.” J. American Concrete Institute, 61(11), 1411-1452.

CSA. (2014). ”A165.1-14 Concrete Block Masonry Units.” Mississauga, ON, Canada: Canadian Standards Association.

CSA. (2014). ”A179-14 Mortar and Grout for Unit Masonry.” Mississauga, ON, Canada: Canadian Standards Association.

CSA. (2008). “A3004-C2 Test Method for the Determination of Compressive Strengths.” Mississauga, ON, Canada: Canadian Standards Association.

CSA. (2014). “S304-14 - Design of Masonry Structures.” Mississauga, ON, Canada: Canadian Standards Association.

Drysdale, R. G., and Essawy, A. S. (1988). “Out-of-Plane Bending of Concrete Block Walls.” J. Struct. Eng., 114(1), 121-133.

Ellingwood, B., Galambos, T. V., MacGregor, J. G., Cornell, C. A. (1980). “Development of a Probability Based Load Criterion for American National Standards A58: Building Code Requirements for Minimum Design Loads in Buildings and Other Structures.” Vol. 13. US Department of Commerce, National Bureau of Standards.

Fishburn, C. C. (1961). “Effect of Mortar Properties on Strength of Masonry.” Washington D.C: U.S Dept. of Commerce, National Bureau of Standards.

Gromala, D.S., Sharp, D.J., Pollock, D.G., and Goodman, J.R., (1990). “Load and Resistance Factor Design for Wood: the New U.S. Wood Design Specification.” International Timber Engineering Conference, Tokyo, Japan, pp. 311- 318.

Hedstrom, R. O. (1961) “Load Test of Patterned Concrete Masonry Walls.” Journal of the American Concrete Institute, 57(4), 1265-1286 Detroit, MI.

Hong, H., Li, S., & Mara, T. (2013). “Performance of the Generalized Least-Squares Method for the Gumbel Distribution and its Application to Annual Maximum Wind Speeds.” Journal of Wind Engineering and Industrial Aerodynamics, 119, 121-132. doi:10.1016/j.jweia.2013.05.012.

Hong, H. P., Mara, T. G., Morris, R., Li, S. H., and Ye, W. (2014). “Basis for Recommending an Update of Wind Velocity Pressures in Canadian Design Codes.” Can. J. Civ. Eng., 41(3), 206-221.

Kim, Y. S., and Bennett, M. (2002). “Flexural Tension in Unreinforced Masonry: Evaluation of Current Specifications.” J. The Masonry Society, 20(1), 23-30.

Laumakis, P. J., & Harlow, G. (2002). “Structural Reliability and Monte Carlo Simulation.” International Journal of Mathematical Education in Science and Technology, 33(3), 377-387. doi:10.1080/00207390210125729.

Matthys, J. (1990). “Concrete Masonry Flexural Bond Strength Prisms versus Wall Tests.” Proc., 5th North American Masonry Conference, Vol. 2. Urbana-Champaign: University of Illinois, 677-685.

Melchers, R. E., & Beck, A. T. (2018). “Structural Reliability Analysis and Prediction.” Hoboken, NJ: John Wiley & Sons.

Miranda, H. Feldman, L. R. Sparling, B. F. (2016). “Feasibility of Using Unbonded Reinforcement in Concrete Block Walls.” Proc., 2016 CSCE Annual Conference, STR-815, 1-11, London, ON, Canada.

Monk, C.B. Jr. (1955). “Transverse Strength of Masonry Walls.” ASTM International, STP 166-EB.

NBCC. (2015) “National Building Code of Canada.” National Research Council of Canada, Ottawa, Ont. Canada.

NCMA (1967). “Research Data and Comments in Support of: Recommended Building Code Requirements for Engineered Concrete Masonry.” Prepared for American Standards Association. National Concrete Masonry Association, Arlington, Virginia, USA.

NCMA (1994). “Research Evaluation of the Flexural Tensile Strength of Concrete Masonry.” Proj. No. 93-172, Order No. MR 10. Herndon, Virginia, USA. Retrieved on Nov. 20, 2016 from http://ncma-br.org/pdfs/masterlibrary/MR10.pdf.

NCMA (1997). "Research Evaluation of the Flexural Tensile Strength of Concrete Masonry Constructed with Type S Masonry Cement Mortar.” Proj. No. 93-255, Herndon, Virginia, USA.

NIST/SEMATECH e-Handbook of Statistical Methods (2013). National Institute of Standards and Technology, US Department of Commerce. Retrieved from on March 12, 2017 from http://www.itl.nist.gov/div898/handbook/index.htm

Richart, F. E. (1932). "The Structural Performance of Concrete Masonry Walls." J. American Concrete Institute, 28(2), 363-385.

Schueremans, L. (2001). "Probabilistic Evaluation of Structural Unreinforced Masonry" (Doctoral Dissertation) Retrieved from the website of the Katholieke Universiteit Leuven at https://bwk.kuleuven.be/mat/publications/phdthesis/2001-schueremans-ph-d.pdf.

TMS (2011). "402-11/ACI 530-11/ASCE 5-11 Building Code Requirements for Masonry Structures." Masonry Standards Joint Committee, The Masonry Society, Longmont, CO, USA.

Udey, A. (2014). "Realistic Wind Loads on Unreinforced Masonry Walls." (Master's Thesis.) University of Saskatchewan, Saskatoon, SK, Canada.

Appendix A - Results for the Absorption and Compressive Tests

This appendix presents the results of the absorption and compressive tests of concrete blocks as explained in Section 4.1.1. Table A.1 shows the results for the absorption, oven dry density, net volume, and the net area of six block specimens labeled 'A1' to 'A6'. Table A.2 presents the results of compressive tests on six blocks labeled 'C1' to 'C6'. The compressive strengths shown in Table A.2 were calculated based on the average net area obtained from the absorption tests. All absorption and compressive tests were conducted in accordance with ASTM C140 (2015). The instrumentation allowed measurements to be made to five significant digits while results as shown in the table were recorded to three significant digits for practicality.

Table A.1: Results for Absorption Tests of Concrete Masonry Blocks

Block Specimen	Absorption %	Oven Dry Density (kg/m^3) ($x10^3$)	Net Volume (cm^3) ($x10^3$)	Net Area (mm^2) ($x10^4$)
A1	8.76	1.72	7.98	4.20
A2	8.95	1.73	7.89	4.15
A3	8.52	1.71	8.02	4.22
A4	9.43	1.69	8.10	4.26
A5	9.35	1.74	7.80	4.11
A6	8.00	1.78	7.68	4.04
Average	**9.00**	**1.73**	**7.91**	**4.16**
COV %	**3.82**	**1.72**	**1.93**	**1.94**

Table A.2: Results for Compressive Tests of Concrete Masonry Blocks

Block Specimen	Compressive Strength[1] (MPa)
C1	24.3
C2	16.6
C3	22.0
C4	19.7
C5	23.2
C6	18.4
Average	**20.7**
COV %	**14.3**

[1] Based on the average net area as discussed in Section 4.1.1 .

Appendix B – Results for the Compressive Tests of Mortar Cubes

This appendix presents the results for the compressive tests of mortar cubes as explained in Section 4.1.2. Six mortar cubes were tested for each of the 24 batches of mortar mixed and used in the construction of walls. Table B.1 shows the compressive strength of each mortar cube tested and the average compressive strength of mortar cubes for each batch. The Instron DX 600 Universal Testing Machine was used to measure the ultimate stress of cubes to four significant digits while results as shown in the table were recorded to three significant digits. The cubes are identified in the format xBy, where x represents the individual mortar cube tested within each batch, B stands for the word batch, and y is used to represent the batch number.

Table B.1: Mortar Cube Compressive Test Results

Batch Designation	Compressive Strength (MPa)	Batch Designation	Compressive Strength (MPa)	Batch Designation	Compressive Strength (MPa)
1B1	9.44	1B9	20.7	1B17	19.3
2B1	10.6	2 B9	18.5	2 B17	16.5
3B1	9.93	3 B9	21.2	3 B17	21.2
4 B1	12.4	4 B9	17.4	4 B17	20.9
5B1	9.84	5 B9	16.0	5 B17	21.4
6B1	12.5	6 B9	19.4	6 B17	17.8
Average	**10.8**	**Average**	**18.8**	**Average**	**19.5**
1B2	7.03	1B10	14.4	1B18	17.5
2B2	7.47	2 B10	14.5	2 B18	20.0
3B2	7.73	3 B10	16.9	3 B18	24.0
4B2	13.3	4 B10	21.3	4 B18	19.8
5B2	13.7	5 B10	14.3	5 B18	23.1
6B2	10.1	6 B10	13.2	6 B18	19.9
Average	**9.90**	**Average**	**15.8**	**Average**	**20.7**
1B3	10.7	1B11	18.9	1B19	23.3
2B3	14.6	2B11	21.2	2 B19	14.5
3B3	11.8	3B11	22.1	3 B19	21.5
4B3	13.4	4B11	22.2	4 B19	26.9
5B3	16.0	5B11	17.2	5 B19	21.1
6B3	15.2	6B11	22.6	6 B19	23.5
Average	**13.6**	**Average**	**20.7**	**Average**	**21.8**
1B4	7.72	1B12	21.1	1B20	22.9
2B4	8.41	2B12	19.3	2 B20	21.1
3B4	10	3B12	21.8	3 B20	20.7
4B4	12.4	4B12	20.7	4 B20	19.5
5B4	10.6	5B12	25.1	5 B20	21.4

Table B.1 cont'd: Mortar Cube Compressive Test Results

Batch Designation	Compressive Strength (MPa)	Batch Designation	Compressive Strength (MPa)	Batch Designation	Compressive Strength (MPa)
6B4	8.39	6B12	22.5	6 B20	21.1
Average	**9.60**	**Average**	**21.7**	**Average**	**21.1**
1B5	13.3	1B13	22.6	1B21	21.1
2B5	14.6	2B13	24.6	2 B21	21.1
3 B5	18.5	3B13	18.4	3 B21	17.4
4 B5	20.1	4B13	24.4	4 B21	19.5
5 B5	21.7	5B13	23.8	5 B21	20.3
6 B5	17.0	6B13	20.6	6 B21	20.5
Average	**17.5**	**Average**	**22.4**	**Average**	**20.0**
1B6	14.1	1B14	18.8	1B22	20.8
2 B6	14.7	2B14	24.2	2 B22	24.7
3 B6	21.2	3B14	28.8	3 B22	26.6
4 B6	9.4	4B14	17.2	4 B22	26.7
5 B6	17.2	5B14	24.4	5 B22	26.2
6 B6	12.3	6B14	18.4	6 B22	23.0
Average	**14.8**	**Average**	**22.0**	**Average**	**24.7**
1B7	16.0	1B15	22.3	1 B23	5.82
2 B7	14.6	2 B15	18.7	2 B23	12.8
3 B7	13.9	3 B15	20.7	3 B23	16.9
4 B7	9.19	4 B15	20.8	4 B23	16.0
5 B7	Damaged[1]	5 B15	20.7	5 B23	19.3
6 B7	Damaged[1]	6 B15	21.3	6 B23	Damaged[1]
Average	**13.4**	**Average**	**20.8**	**Average**	**14.2**
1B8	19.0	1B16	19.9	1B24	19.9
2 B8	16.0	2 B16	22.7	2 B24	15.5
3 B8	16.2	3 B16	26.2	3 B24	17.8
4 B8	9.29	4 B16	18.6	4 B24	15.6
5 B8	19.5	5 B16	19.2	5 B24	18.0
6 B8	11.5	6 B16	20.9	6 B24	15.4
Average	**15.2**	**Average**	**21.2**	**Average**	**17.0**
Overall Average		**17.9**			
COV (%)		**27.6**			

[1] Specimen was damaged during unmolding

Appendix C – Results for the Compressive Tests of Three-Course Prisms

This apendix presents the results for the three-course prisms tested in compression as described in Section 4.1.3. Table C.1 shows the compressive strength obtained for each of the three-course prisms tested. One prism was tested in compression for each wall. The Amsler Beam Bender provided the applied load on each prism to six significant digits and results were recorded to three significant digits for practicality. Prism designations are the same as the corresponding wall specimens as described in Section 3.3.

Table C.1: Masonry Prism Compressive Test Results

Prism Designation	Compressive Strength (MPa)	Prism Designation	Compressive Strength (MPa)
16R1	19.0	18I1	12.9
16R2	25.3	18I2	25.1
16R3	22.7	18I3	22.3
16I1	17.7	20R1	22.3
16I2	13.4	20R2	21.5
16I3	23.4	20R3	20.2
18R1	20.8	20I1	15.0
18R2	23.9	20I2	22.4
18R3	21.4	20I3	N/A[1]
Overall Average	**20.5**		
COV (%)	**18.4**		

[1] Identified as a physical outlier due to cracking when transported to the testing machine.

Appendix D – Results for the Bond Wrench Tests

This appendix includes the results of the bond wrench tests of masonry prisms as explained in Section 4.1.4. Table D.1 presents the results of the bond wrench tests. The bond wrench specimens were labeled according to the mortar batch used in the prism construction. The mortar batches used in the construction of each wall were shown in Section 3.3. The mortar batch corresponding to the material used in the failure joint of each wall was noted after the testing of the walls. The third and sixth columns in Table D.1 show which of the wall specimens included the corresponding mortar batch in the identified failure joints. The applied load on each specimen was measured and recorded using the bond wrench apparatus to three significant digits.

Table D.1: The Bond Wrench Test Results

Specimen/ Mortar Batch	Flexural Tensile Strength (MPa)	Corresponding Wall Specimen	Specimen/ Mortar Batch	Flexural Tensile Strength (MPa)	Corresponding Wall Specimen
B1	0.386		B12	N/A[1]	16R2
B2	0.311	16R1	B13	0.759	18R1
B3	0.697	16R3	B14	0.300	18R2
B4	0.329		B15	0.310	
B5	0.385	18R3	B16	0.193	
		18I1	B17	0.418	
B6	0.136	18I2	B18	0.328	
		18I3	B19	0.970[2]	20I1
B7	0.553		B20	0.165	20I2
B8	0.300		B21	0.242	20I3
B9	0.281		B22	1.97[2]	20R1
B10	0.254	16I1	B23	0.337	20R2
		16I2	B24	0.494	20R3
B11	0.642	16I3			
Average Flexural Tensile Strength (MPa)				**0.372**[3]	
COV%				**45.4**[3]	

[1] Physical outlier: damaged during transportation.
[2] Identified as statistical outlier
[3] Result exclude outliers

Appendix E – The Test Database

This appendix presents the test database used in the reliability analysis to assess the safety of unreinforced masonry walls subject to out-of-plane loading. Table E.1 shows the values of the flexural tensile strength for each wall specimen. A description of the test database as related to mortar type, slenderness ratio, load application method, and support type is available in Section 4.3. Only walls with a thickness of 190 mm were considered when reliability indices were calculated based on slenderness ratios. Walls marked as 'N/A' in fourth column of Table E.1 had a thickness of 290 mm and were, thus, excluded from the reliability analysis when slenderness ratio was the parameter being investigated.

Table E.1: The Database Used in the Reliability Analysis

Research Program	Flexural Tensile Strength (MPa)	Mortar Type	Actual *kl/t* (*kl/t* as referred to in Reliability Analysis)	Load Application Method	Support Type
Richart (1932)	0.23	N PCL	15.3 (16)	Point	Ideal
	0.29	N PCL	15.3 (16)	Point	Ideal
	0.32	N PCL	15.3 (16)	Point	Ideal
	0.19	N PCL	15.3 (16)	Point	Ideal
	0.13	N PCL	15.3 (16)	Point	Ideal
	0.16	N PCL	15.3 (16)	Point	Ideal
	0.12	N PCL	15.3 (16)	Point	Ideal
	0.19	N PCL	15.3 (16)	Point	Ideal
	0.12	N PCL	15.3 (16)	Point	Ideal
	0.12	N PCL	15.3 (16)	Point	Ideal
	0.26	N PCL	15.3 (16)	Point	Ideal
	0.15	S PCL	15.3 (16)	Point	Ideal
	0.16	S PCL	15.3 (16)	Point	Ideal
	0.25	S PCL	15.3 (16)	Point	Ideal
Hedstrom (1961)	0.456	N PCL	12.0 (12)	Uniform	Ideal
	0.246	N PCL	12.0 (12)	Uniform	Ideal
	0.225	N PCL	12.0 (12)	Uniform	Ideal
Fishburn (1961)	0.167	N Masonry/Mortar	12.0 (12)	Point	Ideal
	0.118	N Masonry/Mortar	12.0 (12)	Point	Ideal
	0.151	N Masonry/Mortar	12.0 (12)	Point	Ideal
	0.109	N Masonry/Mortar	12.0 (12)	Point	Ideal
	0.102	N Masonry/Mortar	12.0 (12)	Point	Ideal
	0.103	N Masonry/Mortar	12.0 (12)	Point	Ideal

Table E.1 cont'd: The Database Used in the Reliability Analysis

Research Program	Flexural Tensile Strength (MPa)	Mortar Type	Actual *kl/t* (*kl/t* as referred to in Reliability Analysis)	Load Application Method	Support Type
Fishburn (1961)	0.105	N Masonry/Mortar	12.0 (12)	Point	Ideal
	0.100	N Masonry/Mortar	12.0 (12)	Point	Ideal
	0.149	N Masonry/Mortar	12.0 (12)	Point	Ideal
	0.145	N Masonry/Mortar	12.0 (12)	Point	Ideal
	0.183	N Masonry/Mortar	12.0 (12)	Point	Ideal
	0.229	N Masonry/Mortar	12.0 (12)	Point	Ideal
	0.212	N Masonry/Mortar	12.0 (12)	Point	Ideal
	0.252	N Masonry/Mortar	12.0 (12)	Point	Ideal
	0.142	S Masonry/Mortar	12.0 (12)	Point	Ideal
	0.147	S Masonry/Mortar	12.0 (12)	Point	Ideal
	0.189	S Masonry/Mortar	12.0 (12)	Point	Ideal
	0.179	S Masonry/Mortar	12.0 (12)	Point	Ideal
	0.199	S Masonry/Mortar	12.0 (12)	Point	Ideal
	0.162	S Masonry/Mortar	12.0 (12)	Point	Ideal
	0.206	S Masonry/Mortar	12.0 (12)	Point	Ideal
	0.340	S Masonry/Mortar	12.0 (12)	Point	Ideal
	0.198	S Masonry/Mortar	12.0 (12)	Point	Ideal
	0.202	S Masonry/Mortar	12.0 (12)	Point	Ideal
	0.235	S Masonry/Mortar	12.0 (12)	Point	Ideal
	0.269	S Masonry/Mortar	12.0 (12)	Point	Ideal
	0.467	S Masonry/Mortar	12.0 (12)	Point	Ideal
Copeland and Saxer (1964)	0.758	S PCL	12.0 (12)	Uniform	Ideal
	0.669	S PCL	12.0 (12)	Uniform	Ideal
	0.703	S PCL	12.0 (12)	Uniform	Ideal
	0.559	S PCL	12.0 (12)	Uniform	Ideal
	0.579	S PCL	12.0 (12)	Uniform	Ideal
	0.414	S PCL	12.0 (12)	Uniform	Ideal
Drysdale & Essawy (1988)	0.284	S PCL	14.7 (16)	Uniform	Ideal
	0.338	S PCL	14.7 (16)	Uniform	Ideal
	0.309	S PCL	14.7 (16)	Uniform	Ideal
Matthys (1990)	0.383	S PCL	12.0 (12)	Uniform	Ideal
	0.243	S PCL	12.0 (12)	Uniform	Ideal
	0.252	S PCL	12.0 (12)	Uniform	Ideal
	0.182	S Masonry	12.0 (12)	Uniform	Ideal
	0.159	S Masonry	12.0 (12)	Uniform	Ideal
	0.150	S Masonry	12.0 (12)	Uniform	Ideal
NCMA (1994)	1.52	S PCL	12.0 (12)	Uniform	Ideal
	2.14	S PCL	12.0 (12)	Uniform	Ideal

Table E.1 cont'd: The Database Used in the Reliability Analysis

Research Program	Flexural Tensile Strength (MPa)	Mortar Type	Actual *kl/t* (*kl/t* as referred to in Reliability Analysis)	Load Application Method	Support Type
NCMA (1994)	1.26	S PCL	12.0 (12)	Uniform	Ideal
	1.66	S PCL	12.0 (12)	Uniform	Ideal
	1.52	S PCL	12.0 (12)	Uniform	Ideal
	1.39	S PCL	12.0 (12)	Uniform	Ideal
	2.03	S PCL	12.0 (12)	Uniform	Ideal
	1.10	S PCL	12.0 (12)	Uniform	Ideal
	1.23	S PCL	12.0 (12)	Uniform	Ideal
	1.04	S PCL	12.0 (12)	Uniform	Ideal
	0.977	S PCL	12.0 (12)	Uniform	Ideal
	0.765	S PCL	12.0 (12)	Uniform	Ideal
	0.765	S PCL	12.0 (12)	Uniform	Ideal
	0.783	S PCL	12.0 (12)	Uniform	Ideal
	1.09	S PCL	12.0 (12)	Uniform	Ideal
	1.10	S PCL	12.0 (12)	Uniform	Ideal
	1.74	S PCL	12.0 (12)	Uniform	Ideal
	1.66	S PCL	12.0 (12)	Uniform	Ideal
	0.823	S PCL	12.0 (12)	Uniform	Ideal
	1.50	S PCL	12.0 (12)	Uniform	Ideal
	0.767	N PCL	12.0 (12)	Uniform	Ideal
	0.880	N PCL	12.0 (12)	Uniform	Ideal
	0.611	N PCL	12.0 (12)	Uniform	Ideal
	0.802	N PCL	12.0 (12)	Uniform	Ideal
	0.652	N PCL	12.0 (12)	Uniform	Ideal
	0.511	N PCL	12.0 (12)	Uniform	Ideal
	0.627	N PCL	12.0 (12)	Uniform	Ideal
	0.472	N PCL	12.0 (12)	Uniform	Ideal
	0.862	N PCL	12.0 (12)	Uniform	Ideal
	1.43	N PCL	12.0 (12)	Uniform	Ideal
	1.08	S PCL	7.93 (N/A)[1]	Uniform	Ideal
	1.76	S PCL	7.93 (N/A)[1]	Uniform	Ideal
	1.70	S PCL	7.93 (N/A)[1]	Uniform	Ideal
	1.91	S PCL	7.93 (N/A)[1]	Uniform	Ideal
	1.67	S PCL	7.93 (N/A)[1]	Uniform	Ideal
	1.56	S PCL	7.93 (N/A)[1]	Uniform	Ideal
	1.45	S PCL	7.93 (N/A)[1]	Uniform	Ideal
	1.99	S PCL	7.93 (N/A)[1]	Uniform	Ideal
	1.91	S PCL	7.93 (N/A)[1]	Uniform	Ideal
	2.06	S PCL	7.93 (N/A)[1]	Uniform	Ideal

Table E.1 cont'd: The Database Used in the Reliability Analysis

Research Program	Flexural Tensile Strength (MPa)	Mortar Type	Actual *kl/t* (*kl/t* as referred to in Reliability Analysis)	Load Application Method	Support Type
NCMA (1994)	0.989	S PCL	7.93 (N/A)[1]	Uniform	Ideal
	1.21	S PCL	7.93 (N/A)[1]	Uniform	Ideal
	0.834	S PCL	7.93 (N/A)[1]	Uniform	Ideal
	1.12	S PCL	7.93 (N/A)[1]	Uniform	Ideal
	0.636	S PCL	7.93 (N/A)[1]	Uniform	Ideal
	0.751	S PCL	7.93 (N/A)[1]	Uniform	Ideal
	1.25	S PCL	7.93 (N/A)[1]	Uniform	Ideal
	0.461	S PCL	7.93 (N/A)[1]	Uniform	Ideal
	1.05	S PCL	7.93 (N/A)[1]	Uniform	Ideal
	0.945	S PCL	7.93 (N/A)[1]	Uniform	Ideal
	0.577	N PCL	7.93 (N/A)[1]	Uniform	Ideal
	0.466	N PCL	7.93 (N/A)[1]	Uniform	Ideal
	0.505	N PCL	7.93 (N/A)[1]	Uniform	Ideal
	0.675	N PCL	7.93 (N/A)[1]	Uniform	Ideal
	0.619	N PCL	7.93 (N/A)[1]	Uniform	Ideal
	0.662	N PCL	7.93 (N/A)[1]	Uniform	Ideal
	0.627	N PCL	7.93 (N/A)[1]	Uniform	Ideal
	0.624	N PCL	7.93 (N/A)[1]	Uniform	Ideal
	0.558	N PCL	7.93 (N/A)[1]	Uniform	Ideal
	0.467	N PCL	7.93 (N/A)[1]	Uniform	Ideal
NCMA (1997)	1.21	S Masonry	12.0 (12)	Uniform	Ideal
	0.932	S Masonry	12.0 (12)	Uniform	Ideal
	0.949	S Masonry	12.0 (12)	Uniform	Ideal
	0.756	S Masonry	12.0 (12)	Uniform	Ideal
	1.21	S Masonry	12.0 (12)	Uniform	Ideal
	1.06	S Masonry	12.0 (12)	Uniform	Ideal
	0.794	S Masonry	12.0 (12)	Uniform	Ideal
	0.614	S Masonry	12.0 (12)	Uniform	Ideal
	0.803	S Masonry	12.0 (12)	Uniform	Ideal
	1.30	S Masonry	12.0 (12)	Uniform	Ideal
	0.747	S Masonry	12.0 (12)	Uniform	Ideal
	0.769	S Masonry	12.0 (12)	Uniform	Ideal
	0.473	S Masonry	12.0 (12)	Uniform	Ideal
	0.648	S Masonry	12.0 (12)	Uniform	Ideal
	0.519	S Masonry	12.0 (12)	Uniform	Ideal
	0.614	S Masonry	12.0 (12)	Uniform	Ideal
	0.576	S Masonry	12.0 (12)	Uniform	Ideal
	0.545	S Masonry	12.0 (12)	Uniform	Ideal

Table E.1 cont'd: The Database Used in the Reliability Analysis

Research Program	Flexural Tensile Strength (MPa)	Mortar Type	Actual *kl/t* (*kl/t* as referred to in Reliability Analysis)	Load Application Method	Support Type
NCMA (1997)	0.598	S Masonry	12.0 (12)	Uniform	Ideal
	0.405	S Masonry	12.0 (12)	Uniform	Ideal
	0.758	S Masonry	12.0 (12)	Uniform	Ideal
	1.33	S Masonry	12.0 (12)	Uniform	Ideal
	0.757	S Masonry	12.0 (12)	Uniform	Ideal
	0.623	S Masonry	12.0 (12)	Uniform	Ideal
	0.854	S Masonry	12.0 (12)	Uniform	Ideal
	1.14	S Masonry	12.0 (12)	Uniform	Ideal
	0.905	S Masonry	12.0 (12)	Uniform	Ideal
	0.906	S Masonry	12.0 (12)	Uniform	Ideal
	0.553	S Masonry	12.0 (12)	Uniform	Ideal
	1.21	S Masonry	12.0 (12)	Uniform	Ideal
Udey (2014)	0.120	S Mortar	15.8 (16)	Point	Realistic
	0.221	S Mortar	15.8 (16)	Point	Realistic
	0.286	S Mortar	15.8 (16)	Point	Realistic
	0.0981	S Mortar	15.8 (16)	Point	Ideal
	0.160	S Mortar	15.8 (16)	Point	Ideal
	0.109	S Mortar	15.8 (16)	Point	Ideal
	0.107	S Mortar	15.8 (16)	Point	Ideal
	0.102	S Mortar	15.8 (16)	Point	Ideal
	0.138	S Mortar	15.8 (16)	Point	Realistic
	0.00672	S Mortar	15.8 (16)	Point	Realistic
	0.183	S Mortar	15.8 (16)	Point	Realistic
	0.138	S Mortar	15.8 (16)	Point	Realistic
	0.157	S Mortar	15.8 (16)	Point	Realistic
	0.115	S Mortar	15.8 (16)	Point	Ideal
	0.117	S Mortar	15.8 (16)	Point	Ideal
	0.0359	S Mortar	15.8 (16)	Point	Ideal
	0.105	S Mortar	15.8 (16)	Point	Ideal
	0.139	S Mortar	15.8 (16)	Point	Ideal
Current Investigation	0.116	S Mortar	15.8 (16)	Point	Ideal
	0.200	S Mortar	15.8 (16)	Point	Ideal
	0.210	S Mortar	15.8 (16)	Point	Ideal
	0.122	S Mortar	15.8 (16)	Point	Realistic
	0.0323	S Mortar	15.8 (16)	Point	Realistic
	0.102	S Mortar	15.8 (16)	Point	Realistic
	0.175	S Mortar	17.9 (19)	Point	Ideal
	0.0601	S Mortar	17.9 (19)	Point	Ideal

Table E.1 cont'd: The Database Used in the Reliability Analysis

Research Program	Flexural Tensile Strength (MPa)	Mortar Type	Actual *kl/t* (*kl/t* as referred to in Reliability Analysis)	Load Application Method	Support Type
Current Experiment	0.161	S Mortar	17.9 (19)	Point	Ideal
	0.0948	S Mortar	17.9 (19)	Point	Realistic
	0.227	S Mortar	17.9 (19)	Point	Realistic
	0.142	S Mortar	17.9 (19)	Point	Realistic
	0.117	S Mortar	20 (19)	Point	Ideal
	0.106	S Mortar	20 (19)	Point	Ideal
	0.112	S Mortar	20 (19)	Point	Ideal
	0.0562	S Mortar	20 (19)	Point	Realistic
	0.153	S Mortar	20 (19)	Point	Realistic
	0.132	S Mortar	20 (19)	Point	Realistic

[1] Data point was excluded from the reliability analysis when slenderness ratio was the parameter being investigated.